Soil Organic Carbon Stability, Storage and Response to Heat Wave Events in Agroforestry Systems in Central Alberta, Canada

by

Zhengfeng An

A thesis submitted in partial fulfillment of the requirements for the degree of

Doctor of Philosophy

in

Soil Science

Department of Renewable Resources
University of Alberta

Abstract

Agroforestry systems are a common land-use type in western Canada and play an essential role in mitigating greenhouse gas (GHG) emissions and soil organic carbon (SOC) sequestration. The stability of SOC within agroforestry systems is critical to achieving the long-term goal of C sequestration in agroecosystems. Increasing extreme climate events (e.g., summer heat waves) may reduce the potential of agroforestry systems to mitigate GHG emissions. Information on past C losses, current C storage, and future potential for C sequestration in agroforestry systems on a regional scale is critical to understand better the full biological and economic impact of agroforestry systems. This thesis research investigated SOC structural, thermal and biological stability and the influence of heat wave events and their frequencies on GHG emissions and soil labile C in the forest and cropland components (or land-uses) of common agroforestry systems (hedgerow and/or shelterbelt). This thesis also evaluated the current regional C storage (in hedgerow, shelterbelt and silvopasture systems), historical C loss (in hedgerow and silvopasture) and the future potential for forest land-uses to sequester C (in shelterbelts).

In the hedgerow system, cropland SOC was of a lower quality, which led to higher structural and thermal stabilities than SOC in the forest land-use ($p < 0.05$). Both SOC structural and thermal stabilities increased with soil depth regardless of the land-use type ($p < 0.01$), while SOC quality decreased with soil depth ($p < 0.01$). The SOC in the hedgerow system had higher biological stability than that in the shelterbelt system ($p < 0.1$), and the biological stability of SOC was higher in the cropland than in the forest land-use ($p < 0.01$). The thermal stability of SOC was affected by the interaction between the agroforestry system and land-use type.

Heat wave events increased CO_2 and N_2O emissions from both cropland and forest soils within the hedgerow system ($p < 0.01$), and more frequent heat wave events led to higher cumulative N_2O emissions. Forest soils consistently had higher CO_2 and N_2O emissions than cropland soils, regardless of the heat wave treatment ($p < 0.02$). Emissions of CO_2 and N_2O fell quickly after the heat wave treatment ended, and the heat wave treatment did not significantly decrease soil labile C (Permanganate oxidizable C, microbial biomass C and hot-water extractable organic C).

The forest land-use in the three agroforestry systems (hedgerow, shelterbelt and silvopasture) stored 699.9 Mt C in a 9.5 M ha area across central Alberta, corresponding to a value of $102.7 billion based on a C tax rate of $40 ton^{-1} CO_2 equivalent in Alberta, Canada, in 2021. The forest land-use in the silvopasture system had the highest C stocks (645 Mt C) in central Alberta, storing 14.2 and 67.2 times the C held in the forest land-use in the hedgerow and shelterbelt systems, respectively. Projected increases in C stocks with the expansion of shelterbelt systems in this region, to include all roadside-cropland interfaces, are estimated to be 21.8 Mt C in total, or 2.3 times the C stocks in current shelterbelt forests (9.6 Mt C). The coverage of forest land-use in hedgerow and silvopasture systems in the 9.5 M ha agricultural land area in central Alberta declined at an average rate of 2425 ha yr^{-1} from 2001 to 2020, corresponding to a decline of 8.5 Mt of C in the past twenty years.

Overall, incorporating trees to form agroforestry systems altered the quality and stability of SOC, and SOC stability in forests was not as stable as croplands within agroforestry systems despite having more C, likely as a result of the large labile C content in the forest land-use. In addition, maintaining hedgerow systems can increase the abundance of stable C more than planted shelterbelts. Particular attention should be paid to addressing the influence of extreme

climate events on agroforestry systems, which may turn agroforestry systems into GHG sources. Maintaining existing hedgerow, shelterbelt and silvopasture systems and establishing new shelterbelt forests are critical for increasing C sequestration in western Canada.

Preface

The current thesis is an original work by Zhengfeng An. Chapter 2 of this thesis has been published as An, Z.F., Bernard, G.M., Ma, Z. L., Plante, A.F., Michaelis, V.K., Bork, E.W., Carlyle, C.N., Baah-Acheamfour, M. and Chang, S.X. "Forest land-use increases soil organic carbon quality but not its structural or thermal stability in a hedgerow system," *Agriculture, Ecosystems & Environment*, vol. 321, p.107617 (2021). and Chapter 3 has been submitted to the *Science of the Total Environment*. My primary tasks are sample collection, data analysis, and manuscript writing. Drs. Scott X. Chang, Edward W. Bork, and Cameron N. Carlyle contributed significantly to the editing and submission of manuscripts.

Zhengfeng An

Acknowledgments

I am grateful to my supervisor, Dr. Scott X. Chang. He has contributed significantly to this work, and I would not be able to finish this work without his active involvement and generous help. Besides scientific guidance, his suggestions and guidance in structuring this dissertation are critical. Many thanks to my supervisory committee members, Drs. Edward Bork and David Olefeldt, for their contributions to my thesis research throughout my Ph.D. degree program. I also thank Drs. Marney Isaac and Dani Degenhardt for spending their time reading my thesis and offering comments and editorial corrections that will improve my thesis.

I acknowledge and express my gratitude to the landowners who enabled the fieldwork to occur. Thank you to Drs. Zilong Ma, Jin-Hyeob Kwak, Christopher Nzediegwu, Xiaoqiang Gong, and Jinbiao Li for their assistance in fieldwork, and Prem Pokharel and Cole Gross in laboratory training and assistance in sample analysis. I want to thank Drs. Vladimir Michaelis and Guy Bernard for their help in solid-state NMR spectroscopy training, sample analysis and manuscript editing. I would also like to thank Dr. Alain Plante for his help in sponsoring my study visit to the Department of Earth and Environmental Science, University of Pennsylvania, and Dr. Elizabeth Williams for training me on thermal analysis.

I am thankful for the financial support from the China Scholarship Council, funded by the China Ministry of Education; the Agricultural Greenhouse Gases Program (AGGP), financed by Agriculture and Agri-Food Canada (AAFC); and a Globalink Travel Award from Mitacs. Special thanks to the Faculty of Graduate Studies and Research of the University of Alberta for the tuition fee scholarship and the financial support for conference attendance.

Table of Contents

CHAPTER 1. Introduction 1

1 Background of the research 1

2. Objectives of the research 5

3. Structure of the thesis 6

References 8

CHAPTER 2. Forest land-use increases soil organic carbon quality but not structural or thermal stability in a hedgerow system 14

1. Introduction 14

2. Material and methods 17

2.1. Study area 17

2.2. Sampling design 18

2.3. Soil physical and chemical analysis 18

2.4. The ^{13}C CPMAS NMR analysis 19

2.5. Thermal analysis 21

2.6. Statistical analysis 22

3. Results 23

3.1 Characterization of SOC by ^{13}C NMR spectroscopy 23

3.2. SOC thermal stability 24

3.3 Relations of basic soil properties with SOC structural and thermal stability 25

4. Discussion 26

4.1. Effects of soil depth on SOC structural and thermal stability 27

4.2. Effects of land-use on SOC structural and thermal stability 28

5. Conclusions 31

References 39

CHAPTER 3. Biological but not thermal stability of soil organic carbon differs between two agroforestry systems and their component land-uses in western Canada 49

1. Introduction 49

2. Materials and methods 52

2.1 Study area and sampling design 52

2.2 Laboratory incubation to determine SOC biological stability 54

2.3 The thermal stability of SOC 55

2.4 Statistical analyses 57

3. Results 58

3.1 Effects of agroforestry system and land-use on SOC biological stability 58

3.2 Effects of agroforestry system and land-use on SOC thermal stability 59

3.3 Relationships among basic soil properties, SOC thermal and biological stabilities 60

4. Discussion 61

4.1 Biological stability of SOC in agroforestry systems and their component land-uses 61

4.2 Thermal stability of SOC in different agroforestry systems and land-uses 64

5. Conclusions 65

References 76

CHAPTER 4. Heat waves increase soil CO_2 and N_2O emissions from both cropland and forestland of an agroforestry system 84

1. Introduction 84

2. Material and methods 86

2.1 Soil properties 86

2.2 Laboratory incubation 87

2.3 Analysis of soil POXC, HWEOC and MBC 89

2.4 Statistical analysis 91

3. Results 92

3.1 Soil CO_2 and N_2O emissions 92

3.2 Changes of soil labile carbon 93

3.3 Relations of basic soil properties with soil CO_2 and N_2O emissions 94

4. Discussion 95

4.1 Influence of land-use type and heat wave treatment on soil CO_2 and N_2O emissions 95

4.2 Influence of land-use type and heat wave treatment on soil labile carbon 96

4.3 Limitations and implications of the current study 97

5. Conclusion 100

References 1099

CHAPTER 5. Quantifying the past, current, and projected carbon stocks of forests associated with three agroforestry systems in central Alberta, Canada 1177

1. Introduction 1177

2. Materials and methods **119**

2.1. Study area and dataset 119

2.2. Carbon density in different agroforestry systems 121

2.3 Calculation methods 122

3. Results **123**

3.1 Carbon stocks and their valuation of current agroforestry systems 123

3.2 Loss of forest land-use in agroforestry systems between 2001 and 2020 124

3.3 Future C stock increment with shelterbelt expansion 124

4. Discussion **125**

4.1. Past, current, and future carbon stocks in central Alberta 125

4.2 Valuation of forests associated with agroforestry systems 126

4.3 Limitations and future recommendations 127

5. Conclusions **129**

References **136**

CHAPTER 6. Conclusions and implications for future research **143**

1. Overview of the study objectives **143**

2. Research result summary and implications to management **144**

3. Recommendations and future research needs **146**

References **148**

Bibliography **150**

Appendices **178**

Appendix 2-1. Locations of the six hedgerow sites sampled for this study in Alberta, Canada. 178

Appendix 2-2. Select soil properties (mean ± standard deviation) for the paired cropland and forested land-uses examined within the hedgerow agroforestry system (based on data in Baah-Acheamfour et al., 2014). 179

Appendix 2-3. Pearson correlation coefficients of basic soil properties, soil organic carbon structural and thermal indices (n=6). 180

Appendix 2-4. Pearson correlation coefficients of soil texture (sand clay and silt), soil organic carbon structural and thermal indices (n=6)..... 182

Appendix 3-1. Soil organic carbon, total N, microbial biomass carbon (MBC) and nitrogen (MBN) (mean ± standard error, n=12) in the 0–10 cm soil layer as affected by agroforestry system and land-use in central Alberta, Canada (Banerjee et al., 2016; Baah-Acheamfour et al., 2020)..... 183

Appendix 3-2. Percentage contribution of select variables to the C stability profile..... 184

Appendix 3-3. Pearson correlation coefficients of basic soil properties, soil organic carbon biological and thermal indices (n=12)..... 185

Appendix 4-1. Basic soil properties of the four studied hedgerow system sites [mean ±standard error]. 187

Appendix 4-2. Average daily soil CO_2 and N_2O emissions in the five-day long heat wave period under control and heat wave treatments in both forest and cropland soils. 188

Appendix 4-3. Spearman correlation coefficients of basic soil properties, soil labile C and soil CO_2 and N_2O emissions (n=4). 189

List of Tables

Table Page

Table 2-1. The relative proportion (%) of carbon functional groups (mean ± standard error) derived from CP MAS NMR spectra of SOC in different land-use in the hedgerow system (n=12). 32

Table 2-2. Carbon structural indices (mean ± standard error, n=12) in forest and cropland land-use and soil depth (0-10 cm and 10-30 cm) in the hedgerow system. 33

Table 2-3. Selected thermal indices (mean ± standard error, n=12) for SOC in forest and cropland land-use and soil depth (0-10 cm and 10-30 cm) of the hedgerow system. 34

Table 3-1. Soil organic carbon (SOC) biological stability indices (mean ± standard error, n=12) as affected by agroforestry system, land-use, and the interaction effects of agroforestry system and land-use in central Alberta, Canada. 67

Table 3-2. Soil organic carbon (SOC) thermal stability indices (mean ± standard error, n=12) as affected by agroforestry system, land-use, and the interaction effects of agroforestry system and land-use in central Alberta, Canada. 69

Table 4-1. Results of the analysis of variance (F and P values) on the effect of land-use type, heat wave treatment and their interaction on basal soil and cumulative CO_2 and N_2O emissions (n=4). 101

Table 4-2. Results from the analysis of variance (F and P values) on the effect of land-uses, heat wave treatment, and their interaction on the temporal changes of soil labile C [(permanganate oxidable C (POXC), microbial biomass C (MBC) and hot-water extractable organic C (HWEOC)] over the incubation. 102

Table 5-1. Estimated C stocks, the relative contribution of C stocks, land areas occupying different land-uses, and the incremental C values comprising different land-uses, found in various agricultural land-uses across 50 study plots and the greater study region of central Alberta, Canada. 131

List of Figures

Figure Page

Fig. 2-1. Carbon-13 CPMAS NMR spectra (mean) of the soil samples from (a) different land-use within a hedgerow system and (b) different soil depths (n = 12). 35

Fig. 2-2. The interaction effects of land-use by soil depth on alkyl index (A/OA) based on ^{13}C CPMAS NMR data. Data points are mean (± standard error, n=6, the hollow point and the middle line in each boxplot represent mean and median, respectively). Different lowercase letters indicate a significant difference at $p < 0.05$. 36

Fig. 2-3. Differential scanning calorimetry (DSC) thermograms (mean ± standard error, n=6) for the cropland and forest land-uses and two soil depths within the hedgerow system. 37

Fig. 2-4. The relationships between basic soil properties, carbon functional groups and thermal indices of soils collected at two depths from forest and cropland, using a PCA ordination with 95% confidence ellipses to describe the interaction effects of land-use by depth. 38

Fig 3-1. Maps of (a) Canada, (b) the province of Alberta showing the soil group information and locations of the study sites, and (c) the central Alberta region showing the soil group information and locations of the study sites. The triangles and circles represent hedgerow and shelterbelt sites, respectively. 70

Fig 3-2. Soil respiration rate (mean ± standard error) as affected by (a) agroforestry systems and (b) land-uses. 71

Fig 3-3. The interaction effects of agroforestry system by land-use on basal soil respiration and cumulative respiration. Data points are mean (± standard error, n=12, the hollow point

and the middle line in each boxplot represent mean and median, respectively). Different lowercase letters indicate a significant difference at $p < 0.1$.. 72

Fig 3-4. Differential scanning calorimetry (DSC) thermograms (mean ± SE) of SOC in different (a) agroforestry systems and (b) land-uses (SE denotes standard error)..... 73

Fig 3-5. The interaction effects of agroforestry system by land-use on thermal stability indices. Data points are mean (± standard error, n=12, the hollow point and the middle line in each boxplot represent mean and median, respectively). Different lowercase letters indicating a significant difference at $p < 0.1$..... 74

Fig. 3-6. Relationships between basic soil properties, SOC biological and thermal stabilities of soils collected from forest and cropland from shelterbelt and hedgerow systems, using a PCA ordination with 95% confidence ellipses to describe the interaction between agroforestry system and land-use. 75

Fig. 4-1. A diagram illustrating the experimental design and the timing of the soil and greenhouse gas samplings. The codes HW2 and HW3 represent the heat wave treatment with two and three heatwave events, respectively, in the experiment. The HW2 and HW3 treatments had the same soil and gas sampling frequency as the control. 103

Fig. 4-2. Daily soil CO_2 emissions (a), N_2O emissions (b), and cumulative N_2O emissions as affected by the land-use type and heat wave treatment in the hedgerow system. Vertical bars are standard errors of the means (n=4), and the same letter(s) indicate no significant differences at $P < 0.05$. 104

Fig. 4-3. Soil cumulative N_2O emissions as affected by the interaction effect of land-use type by heat wave treatment. Vertical bars are standard errors of the means (n=4), and the same letter(s) indicate no significant differences at $P < 0.05$. 105

Fig. 4-4. Soil cumulative N_2O emissions as affected by land-use type and heat wave treatment. Vertical bars are standard errors of the means (n=4), and the same letter(s) indicate no significant differences at $P < 0.05$..... 106

Fig. 4-5. Soil labile C [(permanganate oxidable C (POXC), microbial biomass C (MBC) and hot-water extractable organic C (HWEOC)] as affected by the land-use type and soil sampling time. Vertical bars are standard errors of the means (n=4), and different letters indicate significant differences at $p < 0.05$. 107

Fig. 4-6. The relationships among basic soil properties, soil labile C and soil CO_2 and N_2O emissions using a PCA ordination with 95% confidence ellipses to describe the effects of land-use and heat wave treatment. 108

Fig. 5-1. Location of the study area in Alberta, Canada, and selected plots for object-based supervised classification of land-use activity. 132

Fig. 5-2. Example of a study plot used to assess changes in land-use activity, including agroforestry systems. The cultivation extent means the grassland and cultivated cropland.. 133

Fig. 5-3. The areal extent of cultivation used within the Google Earth Engine to derive information on annual forest loss. The cultivation extent means the grassland and cultivated cropland. 134

Fig. 5-4. Estimated annual forest loss and associated C loss derived from the cropland (representing hedgerow forests) and grassland (representing silvopasture forests) areas within central Alberta, Canada, based on Global Forest Changes (2000–2020) from Hansen et al. (2013) using Google Earth Engine. 135

List of Abbreviations

ABMI: Alberta Biodiversity Monitoring Institute

ANOVA: analysis of variance

A/OA: alkyl index

ARM: aromaticity index

C: carbon

CO_2: carbon dioxide

CO_2-T_{50} : the temperature that 50% of the CO_2 is produced

CPMAS: cross-polarization magic-angle spinning

DOC: dissolved organic carbon

DON: dissolved organic nitrogen

DSC: differential scanning calorimetry

DSC-T_{50}: the temperature that 50% of the exothermic energy is released

Ea: activation energy

Ed: energy density

EGA: evolved gas analysis

GEE: google earth engine

GHG: greenhouse gas

HB/HI: hydrophobicity index

HF: hydrofluoric acid

HW: heat wave

HWEOC: hot water extractable organic carbon

LigR: lignin ratio

Mt: million ton

MBC: microbial biomass carbon

MBN: microbial biomass nitrogen

N: nitrogen

NMR: nuclear magnetic resonance

N_2O: nitrous oxide

PCA: principal component analysis

POXC: Permanganate oxidizable C

ROI: return on energy investment

RS: remote sensing

SOC: soil organic carbon

TG: thermogravimetry

TG-T_{50}: the temperature that 50% of the exothermic mass is lost

Chapter 1. Introduction

1 Background of the research

Agricultural land is not only one of the primary sources of anthropogenic greenhouse gas (GHG) emissions (Smith et al., 2008) but also one of the most susceptible sectors to climate change (Watson et al., 1998; Calzadilla et al., 2013). With increasing temperatures, the rate of soil organic carbon (SOC) decomposition will be increased (Yang et al., 2007) and result in further loss of SOC and increased GHG emissions, accelerating the positive feedback to climate change. The climate in Canada has become warmer and will continue to become warmer in the future, and the magnitude of warming in Canada, both past and future, will be around two times that of overall changes in global warming (Bush and Lemmen, 2019). Moreover, the warmer future will cause more extreme weather conditions, e.g., heat waves (Bush and Lemmen, 2019), which will increase the difficulty of mitigating climate change. Thus, Canada urgently needs to develop effective strategies to offset the influence of climate change.

Planting more trees across the landscape, including croplands, has been suggested as a cost-effective climate change mitigation method (Griscom et al., 2017). Hence, there are opportunities for Canada to reintroduce C to the terrestrial ecosystem and offset the influence of anthropogenic GHG emissions on the climate by incorporating perennial vegetation into annually cropped landscapes, including the development of agroforestry systems. Agroforestry is a sustainable and climate-smart land-use management system that consists of trees, crops and/or animals in the farming systems in a piece of land to generate ecological, economic, environmental and social benefits (Nair, 1993; Muschler, 2016; Paustian et al., 2016). By

reintroducing trees and/or shrubs into agricultural land, agroforestry systems can increase C input to the soil. Thus, agroforestry systems are also regarded as an effective strategy in reducing GHG emissions, sequestering biological C (Nair et al., 2009), and mitigating climate change (Schoeneberger et al., 2012). Agroforestry systems may even play a more significant role in helping humans offset global warming by increase SOC storage and other related environmental hazards under different climate change scenarios (Nair et al., 2009; Baah-Acheamfour et al., 2014; Lim et al., 2018). Hence the stability of SOC and practices that influence SOC storage in agroforestry systems should be studied in detail, and it is equally important to understand factors affecting the stability of the C sequestered in the soil to increase/maintain the SOC pool in the long term (Xu et al., 2020), which has been poorly researched in past studies.

The stability of SOC is one of the critical factors affecting the size of the SOC stock. Any practice that can increase the stabilized proportion of SOC will increase the mean residence time of SOC (Ohno et al., 2017), in turn increasing SOC stock. The stability of SOC can be measured by how easily SOC can be mineralized (Plante et al., 2011). Generally, there are three types of mechanisms involved in regulating C stability in soils (Christensen, 1996), the first of which is the biological/biochemical mechanism, which refers to the complex molecule structure (as indicated by indices such as aromaticity and hydrophobicity) of the SOC (Monda et al., 2018). The more complex the structure of the SOC, the higher the SOC stability. The refractory nature of SOC is a representation of the complex structure (Singh et al., 2018). Second, physical mechanisms are important, which include the formation of physical barriers between SOC and microbes; physical barriers increase the inaccessibility of SOC by microbes and protect SOC from decomposition (Coleman and Elliot, 1988). The third is the chemical mechanism, which reflects the chemical interaction between SOC and soil mineral surfaces (Singh et al., 2018).

Different aspects of SOC stability should be evaluated to understand the SOC being sequestered in agroecosystems.

The stability of SOC can be quantitatively analyzed by a variety of methods, of which the ^{13}C cross-polarization magic-angle spinning nuclear magnetic resonance (CPMAS NMR) spectroscopy (Li et al., 2014), thermal analysis method (Plante et al., 2011) and soil incubation to determine soil respiration rate (Plante et al., 2011) are commonly used to study SOC stability quantitatively. The ^{13}C CPMAS NMR spectroscopy technique can be used to infer the molecular structure of SOC (Näthe et al., 2017), by detecting the nuclei spin and relaxation of ^{13}C in the added magnetic field, ^{13}C solid-state NMR produce SOC chemical shifts that correspond to the chemical position and the relative proportion of protons. Chemical shifts can be attributed to corresponding C functional groups (e.g., carbonyl C, alkyl C, and aromatic C) (Monda et al., 2017). With such information, we can better understand SOC quality and associated structural stability. In comparison, the thermal analysis method interprets SOC stability differently, as this method measures the energy required to oxidize SOC and break any existing bonds within soil mineral functional groups (Plante et al., 2011). Through thermal gravimetric analysis (TGA), evolved gas analysis (EGA) and differential scanning calorimetry (DSC), the energy- and temperature-related indices can be obtained to quantitatively represent SOC thermal stability (Plante et al., 2011; Stone and Plante, 2015). Soil respiration is an indicator of soil microbes and roots metabolism (Karhu et al., 2014) and SOC biological stability (Plante et al., 2011). Soils with a high respiration rate indicate that SOC with low biological stability may have a sizeable labile C pool.

Climate extremes resulting from climate change are regarded as key factors influencing the terrestrial biosphere (Anjileli et al., 2021). The spatial coverage and frequency of climate

extremes will intensify in the 21st century (Meyer and Pachauri, 2014). For those climate extremes, heat wave event, a period with no less than three consecutive hotter days than normal (Perkins and Alexander, 2013; Jeong et al., 2016), is thought to have a more severe impact on terrestrial ecosystems than gradual climate warming, due to a greater response strength, albeit over short response durations (Teuling et al., 2010; Frank et al., 2015; Zhang and Cao, 2017). In turn, this will also influence terrestrial C cycles as well as global climate change (Reichstein et al., 2013). Heat wave events may weaken C sinks in terrestrial ecosystems (i.e., cropland and forest) and turn them into C sources. For example, the heat wave event in Europe in 2003 substantially increased CO_2 emissions, which approximates the amount of C sequestered for the previous four years (Ciais et al., 2005). Because soils are the largest C reservoir contained in terrestrial ecosystems, understanding the response of soil C to heat wave events is key to climate change mitigation and C sequestration, especially when heat wave events are predicted to become more frequent (Smoyer-Tomic et al., 2003; Jeong et al., 2016). However, such knowledge about the response of soil C to heat wave events is limited due to the rarity, randomness and unpredictability of heat wave events (Smith, 2011; Hoover et al., 2014; Teskey et al., 2015). Little is also known regarding how heat wave events affect agroforestry systems. Therefore, knowledge of the influence of heat wave events on agroforestry systems is needed for the mitigation of GHG emissions and C sequestration in agricultural soils.

The quantification of C stocks in agroforestry systems is essential to determine the full potential of agroforestry systems to provide a practical approach for C sequestration. A previous publication has studied C stocks in three typical agroforestry systems in central Alberta (Lim et al., 2018); however, few studies report on past C changes related to the presence or absence of agroforestry systems. Information on the current C sequestration status and future potentials of C

storage by expanding agroforestry systems across the larger landscape is limited, with studies of C sequestration potential instead of being limited to a few C pools of specific agroforestry systems (most commonly in shelterbelts – i.e., planted trees along the margins of fields) and then limited to specific regions (Amichev et al., 2016; Abbas et al., 2017; Amichev et al., 2020). In general, limited studies have investigated the regional scale C stocks and the potential of increasing C stocks through the expansion of agroforestry systems, much less the potential economic value of the C stocks in agroforestry systems at the regional scale, thereby limiting our understanding of where and how agroforestry systems may be an effective C sequestration strategy.

2. Objectives of the research

This research aims to enhance our understanding of SOC stability (structural, thermal and biological) in agroforestry systems, the influence of extreme heat waves on GHG emissions and soil labile C dynamics, and the estimation of regional C stock and associated economic value in central Alberta, which can help support sustainable agriculture for farmers practicing agroforestry management in Alberta. The work will provide data that can support the recommendation of the type of agroforestry systems to use for ecological, environmental and economic benefits to the farmers in Alberta (or elsewhere) who have not considered this management practice on their agricultural land.

The main objectives of this thesis research are:

1) To investigate the effects of land-use type and soil depth (0-10 vs. 10-30 cm) on SOC quality, and structural and thermal stabilities within a natural hedgerow system, one of the most common agroforestry systems in central Alberta, Canada
2) To explore the influence of two typical agroforestry systems (planted shelterbelts and natural hedgerows) and their component land-use types (forest and cropland) on the biological and thermal stabilities of SOC (0-10 cm) in central Alberta, Canada
3) To study the effect of heat wave events and their frequency on GHG emissions and soil labile C (0-10 cm) in a hedgerow system in central Alberta, Canada.
4) To quantify previous and existing forests and associated C stocks (include SOC to 75 cm depth) and economic values of three typical agroforestry systems (planted shelterbelt, natural hedgerow and silvopasture systems), and the potential for future expansion of shelterbelt forests in C sequestration, within central Alberta, Canada.

3. Structure of the thesis

The thesis has six chapters. The first chapter (this chapter) introduces the background and general objectives of the thesis research. The second chapter studies the influence of component land-use types (cropland and forest) of a hedgerow system and soil depth on SOC structural and thermal stabilities. The third chapter extends the study of SOC stability (biological and thermal stabilities) to both hedgerow and shelterbelt systems. The fourth chapter explores the influence of the heat wave frequency (0, 2 and 3 times heat wave events) on GHG emissions and soil labile C dynamics in cropland and forest of the hedgerow system. The fifth chapter estimates regional C stock and associated economic value of three typical agroforestry systems (hedgerow,

shelterbelt and silvopasture systems) commonly found in central Alberta. The sixth chapter summarizes the primary findings of the thesis research and draws general conclusions, and suggestions for future research are also given in this chapter. Chapters 2 to 5 each make up a manuscript that has either been published (Chapter 2), under review (Chapter3), or will be submitted for publication (Chapters 4 and 5).

References

Abbas, F., Hammad, H.M., Fahad, S., Cerdà, A., Rizwan, M., Farhad, W., Ehsan, S., Bakhat, H.F., 2017. Agroforestry: a sustainable environmental practice for carbon sequestration under the climate change scenarios - a review. Environ. Sci. Pollut. Res. 24, 11177-11191. https://doi.org/10.1007/s11356-017-8687-0.

Amichev, B.Y., Bentham, M.J., Kulshreshtha, S.N., Laroque, C.P., Piwowar, J.M., Van Rees, K.C., 2016. Carbon sequestration and growth of six common tree and shrub shelterbelts in Saskatchewan, Canada. Can. J. Soil Sci. 97, 368-381. https://doi.org/10.1139/cjss-2016-0107.

Amichev, B.Y., Laroque, C.P., Van Rees, K.C., 2020. Shelterbelt removals in Saskatchewan, Canada: implications for long-term carbon sequestration. Agrofor. Syst. 1-16. https://doi.org/10.1007/s10457-020-00484-8.

Anjileli, H., Huning, L.S., Moftakhari, H., Ashraf, S., Asanjan, A.A., Norouzi, H., AghaKouchak, A., 2021. Extreme heat events heighten soil respiration. Sci. Rep. 11, 1-9. https://doi.org/10.1038/s41598-021-85764-8.

Baah-Acheamfour, M., Carlyle, C.N., Bork, E.W., Chang, S.X., 2014. Trees increase soil carbon and its stability in three agroforestry systems in central Alberta, Canada. For. Ecol. Manag. 328, 131-139. https://doi.org/10.1016/j.foreco.2014.05.031.

Bush, E. and Lemmen, D.S., 2019. Canada's Changing Climate Report; Government of Canada, Ottawa, ON. 444 pp.

Calzadilla, A., Rehdanz, K., Betts, R., Falloon, P., Wiltshire, A., Tol, R.S., 2013. Climate change impacts on global agriculture. Clim. Change 120, 357-374. https://doi.org/10.1007/s10584-013-0822-4.

Christensen, B.T., 1996. Carbon in primary and secondary organomineral complexes. In: Carter, M.R., Stewart, B. A. (Eds), Structure and organic matter storage in agricultural soils. CRC Lewis Publishers, New York, 97-165 pp.

Ciais, P., Reichstein, M., Viovy, N., Granier, A., Ogée, J., Allard, V., Aubinet, M., Buchmann, N., Bernhofer, C., Carrara, A., 2005. Europe-wide reduction in primary productivity caused by the heat and drought in 2003. Nature 437, 529-533. https://doi.org/10.1038/nature03972.

Coleman, D., Elliot, E., 1988. Let the soil work for us. Ecol Bull 39, 23-32.

Frank, D., Reichstein, M., Bahn, M., Thonicke, K., Frank, D., Mahecha, M.D., Smith, P., Van der Velde, M., Vicca, S., Babst, F., 2015. Effects of climate extremes on the terrestrial carbon cycle: concepts, processes and potential future impacts. Glob. Chang. Biol. 21, 2861-2880. https://doi.org/10.1111/gcb.12916.

Griscom, B.W., Adams, J., Ellis, P.W., Houghton, R.A., Lomax, G., Miteva, D.A., Schlesinger, W.H., Shoch, D., Siikamäki, J.V., Smith, P., 2017. Natural climate solutions. PNAS 114, 11645-11650. https://doi.org/10.1073/pnas.1710465114.

Hoover, D.L., Knapp, A.K., Smith, M.D., 2014. Resistance and resilience of a grassland ecosystem to climate extremes. Ecology 95, 2646-2656. https://doi.org/10.1890/13-2186.1.

Jeong, D.I., Sushama, L., Diro, G.T., Khaliq, M.N., Beltrami, H., Caya, D., 2016. Projected changes to high temperature events for Canada based on a regional climate model ensemble. Clim. Dyn. 46, 3163-3180. https://doi.org/10.1007/s00382-015-2759-y.

Karhu, K., Auffret, M.D., Dungait, J.A., Hopkins, D.W., Prosser, J.I., Singh, B.K., Subke, J.A., Wookey, P.A., Ågren, G.I., Sebastia, M.T., 2014. Temperature sensitivity of soil respiration rates enhanced by microbial community response. Nature 513, 81-84. https://doi.org/10.1038/nature13604.

Li, Y., Zhang, J., Chang, S.X., Jiang, P., Zhou, G., Shen, Z., Wu, J., Lin, L., Wang, Z., Shen, M., 2014. Converting native shrub forests to Chinese chestnut plantations and subsequent intensive management affected soil C and N pools. For. Ecol. Manag. 312, 161-169. https://doi.org/10.1016/j.foreco.2013.10.008.

Lim, S.S., Baah-Acheamfour, M., Choi, W.J., Arshad, M.A., Fatemi, F., Banerjee, S., Carlyle, C.N., Bork, E.W., Park, H.-J., Chang, S.X., 2018. Soil organic carbon stocks in three Canadian agroforestry systems: From surface organic to deeper mineral soils. For. Ecol. Manag. 417, 103-109. https://doi.org/10.1016/j.foreco.2018.02.050.

Meyer, L. and Pachauri, R., 2014. The Fifth assessment report of the intergovernmental panel on climate change. Geneva: IPCC Secretariat.

Monda, H., Cozzolino, V., Vinci, G., Drosos, M., Savy, D., Piccolo, A., 2018. Molecular composition of the Humeome extracted from different green composts and their biostimulation on early growth of maize. Plant Soil 429, 407-424. https://doi.org/10.1007/s11104-018-3642-5.

Monda, H., Cozzolino, V., Vinci, G., Spaccini, R., Piccolo, A., 2017. Molecular characteristics of water-extractable organic matter from different composted biomasses and their effects

on seed germination and early growth of maize. Sci. Total Environ. 590, 40-49. https://doi.org/10.1016/j.scitotenv.2017.03.026.

Muschler, R.G., 2016. Agroforestry: essential for sustainable and climate-smart land use, in: Pancel, L., Köhl, M. (Eds.), Tropical forestry handbook. Springer, pp. 2013-2116.

Nair, P., Kumar, B., Nair, V.D., 2009. Agroforestry as a strategy for carbon sequestration. J. Plant. Nutr. Soil Sci. 172, 10-23. https://doi.org/10.1002/jpln.200800030.

Nair, P.R., 1993. An introduction to agroforestry. Springer Science & Business Media, Netherlands.

Näthe, K., Levia, D.F., Steffens, M., Michalzik, B., 2017. Solid-state ^{13}C NMR characterization of surface fire effects on the composition of organic matter in both soil and soil solution from a coniferous forest. Geoderma 305, 394-406. https://doi.org/10.1016/j.geoderma.2017.06.030.

Ohno, T., Heckman, K.A., Plante, A.F., Fernandez, I.J., Parr, T.B., 2017. ^{14}C mean residence time and its relationship with thermal stability and molecular composition of soil organic matter: A case study of deciduous and coniferous forest types. Geoderma 308, 1-8. https://doi.org/10.1016/j.geoderma.2017.08.023.

Paustian, K., Lehmann, J., Ogle, S., Reay, D., Robertson, G.P., Smith, P., 2016. Climate-smart soils. Nature 532, 49-57. https://doi.org/10.1038/nature17174.

Perkins, S.E. and Alexander, L.V., 2013. On the measurement of heat waves. J. Clim. 26, 4500-4517. https://doi.org/10.1175/JCLI-D-12-00383.1.

Plante, A.F., Fernández, J.M., Haddix, M.L., Steinweg, J.M., Conant, R.T., 2011. Biological, chemical and thermal indices of soil organic matter stability in four grassland soils. Soil Biol. Biochem. 43, 1051-1058. https://doi.org/10.1016/j.soilbio.2011.01.024.

Reichstein, M., Bahn, M., Ciais, P., Frank, D., Mahecha, M.D., Seneviratne, S.I., Zscheischler, J., Beer, C., Buchmann, N., Frank, D.C., 2013. Climate extremes and the carbon cycle. Nature 500, 287-295. https://doi.org/10.1038/nature12350.

Schoeneberger, M., Bentrup, G., De Gooijer, H., Soolanayakanahally, R., Sauer, T., Brandle, J., Zhou, X.H., Current, D., 2012. Branching out: Agroforestry as a climate change mitigation and adaptation tool for agriculture. J. Soil Water Conserv. 67, 128A-136A. https://doi.org/10.2489/jswc.67.5.128A.

Singh, M., Sarkar, B., Sarkar, S., Churchman, J., Bolan, N., Mandal, S., Menon, M., Purakayastha, T.J., Beerling, D.J., 2018. Stabilization of soil organic carbon as influenced by clay mineralogy. Adv. Agron. 148, 33-84. https://doi.org/10.1016/bs.agron.2017.11.001.

Smith, M.D., 2011. An ecological perspective on extreme climatic events: a synthetic definition and framework to guide future research. J. Ecol. 99, 656-663. https://doi.org/10.1111/j.1365-2745.2011.01798.x.

Smith, P., Martino, D., Cai, Z.C., Gwary, D., Janzen, H., Kumar, P., McCarl, B., Ogle, S., O'Mara, F., Rice, C., 2008. Greenhouse gas mitigation in agriculture. Philos. Trans. R. Soc. B, Biol. Sci. 363, 789-813. https://doi.org/10.1098/rstb.2007.2184.

Smoyer-Tomic, K.E., Kuhn, R., Hudson, A., 2003. Heat wave hazards: an overview of heat wave impacts in Canada. Nat. Hazards 28, 465-486. https://doi.org/10.1023/A:1022946528157.

Stone, M.M., Plante, A.F., 2015. Relating the biological stability of soil organic matter to energy availability in deep tropical soil profiles. Soil Biol. Biochem. 89, 162-171. https://doi.org/10.1016/j.soilbio.2015.07.008.

Teskey, R., Wertin, T., Bauweraerts, I., Ameye, M., McGuire, M.A., Steppe, K., 2015. Responses of tree species to heat waves and extreme heat events. Plant Cell Environ. 38, 1699-1712. https://doi.org/10.1111/pce.12417.

Teuling, A.J., Seneviratne, S.I., Stöckli, R., Reichstein, M., Moors, E., Ciais, P., Luyssaert, S., Van Den Hurk, B., Ammann, C., Bernhofer, C., 2010. Contrasting response of European forest and grassland energy exchange to heatwaves. Nat. Geosci. 3, 722-727. https://doi.org/10.1038/NGEO950.

Watson, R.T., Zinyowera, M.C., Moss, R.H., Dokken, D.J., 1998. The regional impacts of climate change. IPCC, Geneva.

Xu, H., Qu, Q., Wang, M., Li, P., Li, Y., Xue, S., Liu, G., 2020. Soil organic carbon sequestration and its stability after vegetation restoration in the Loess Hilly Region, China. Land Degrad. Dev. 31, 568-580. https://doi.org/10.1002/ldr.3472.

Yang, L., Pan, J., Shao, Y., Chen, J.M., Ju, W.M., Shi, X., Yuan, S., 2007. Soil organic carbon decomposition and carbon pools in temperate and sub-tropical forests in China. J. Environ. Manage. 85, 690-695. https://doi.org/10.1016/j.jenvman.2006.09.011.

Zhang, F.W. and Cao, G.M., 2017. Resilience of Energy and CO 2 Exchange to a Summer Heatwave in an Alpine Humid Grassland on the Qinghai-Tibetan Plateau. Pol. J. Environ. Stud. 26. https://doi.org/10.15244/pjoes/64912.

Chapter 2. Forest land-use increases soil organic carbon quality but not structural or thermal stability in a hedgerow system

1. Introduction

Agricultural lands can act as a carbon (C) sink if they are reforested with trees (IPCC, 2007; Nair et al., 2009; Baah-Acheamfour et al., 2014). Reintroducing trees into agricultural lands to form agroforestry systems has been promoted as an effective means to sequester atmospheric CO_2 (IPCC, 2007). By deliberately including trees and/or shrubs with annual crops or perennial pasture/animals on the same unit of land, agroforestry systems provide a variety of economic and environmental benefits (Nair, 2011). Those benefits make agroforestry systems a popular land management option not only for their multifunctionality (e.g., reducing soil erosion, increasing soil fertility and promoting biodiversity) over time and space (Nair et al., 2009; Jose, 2009), but also for their ability to mitigate climate change by increasing C sequestration in soil and vegetation (De Stefano and Jacobson., 2018; Lim et al., 2018).

Management practices can substantially influence not only the size of soil organic C (SOC) stock (Howlett et al., 2011) but also its stability (Xu et al., 2020). For example, reforestation of croplands has been shown to increase SOC stock (Zhang et al., 2010), while information about the change in C stability due to afforestation is scarce. The stability of sequestered SOC is an important consideration when studying C sequestration (Xu et al., 2020), because the stability of SOC is a crucial determinant of soil organic matter dynamics and reflects how easily SOC can be mineralized (Plante et al., 2011).

Higher SOC stability means SOC is less prone to decomposition than SOC with lower stability, typically due to a low SOC quality (Bosatta and Ågren, 1999), leading to a longer residence time (Fontaine et al., 2007). However, few studies have investigated SOC stability in agroforestry systems. The forested component of agroforestry systems has been reported to have greater SOC stocks and stability; however, the latter has only been assessed by quantifying SOC within different mineral fractions (Baah-Acheamfour et al., 2014). In contrast, Xu et al. (2020) found that reforestation in cropland enhanced SOC sequestration while reducing SOC stability. These contradictory results on the effect of land-use type on SOC stability need to be addressed by studying the various aspects of SOC stability to better understand SOC dynamics and the long-term storage potential of C in agroforestry systems.

The inherent structural characteristics of SOC (Fontaine et al., 2007) and the amount of energy produced when SOC decomposes can be important indicators of SOC stability (Plante et al., 2011; Nie et al., 2018). For example, the ^{13}C cross-polarization magic-angle spinning (CPMAS) nuclear magnetic resonance (NMR) method is frequently used to investigate the effect of land-use practices on the chemical composition of SOC (Šmejkalová et al., 2008; Simpson et al., 2011; He et al., 2009). The spectra of SOC could yield qualitative information on the relative (i.e., proportional) abundance of various organic C functional groups (also known as SOC chemical composition), such as alkyl C, aromatic C, and carbonyl C (Li et al., 2014). In their assessment of land-use practices on the chemical composition of SOC, Li et al. (2014) found that long-term intensive management, such as deep tillage, vegetation control and fertilization, altered the chemical composition of SOC in a native forest and led to

decreased aromatic C, O-alkyl C, and aromaticity. Similarly, various methods of thermal analysis [e.g., thermogravimetry, evolved gas analysis (EGA), and differential scanning calorimetry (DSC)] can yield quantitative information on the thermal energy needed to oxidize SOC to CO_2 or to break chemical bonds in molecules of SOC with adjacent soil mineral functional groups (Ohno et al., 2017; Peltre et al., 2013). Soil organic C with high thermal stability is generally low in quality but more resistant to breakdown, and therefore more likely to persist for a longer period of time due to the low energy content (Plante et al., 2011; Williams and Plante, 2018).

Despite significant progress in quantifying the size of SOC stocks in northern temperate agroforestry systems (Baah-Acheamfour et al., 2014; Oelbermann et al., 2014; Lim et al., 2018), there is limited knowledge on how land-use type and soil depth (0-10 vs. 10-30 cm) influence SOC quality and stability in agroforestry systems. This study aims to investigate the effects of land-use type and soil depth on SOC quality, and structural and thermal stabilities within a hedgerow system, one of the most common agroforestry systems in central Alberta, Canada (Baah-Acheamfour et al., 2015). We hypothesized that SOC quality, and structural and thermal stabilities, would be higher in forestland than in the cropland of the hedgerow system due to the SOC derived from perennial vegetation having a higher lignin content (Xia et al., 2021), and that SOC quality and associated structural and thermal stabilities would be higher in the surface than in the subsurface soil. This study will improve our understanding of SOC stability and its influential factors, with implications for the long-term storage of SOC in contemporary agroforestry systems.

2. Material and methods

2.1. Study area

This study was conducted using six hedgerow sites distributed across central Alberta, Canada (52°24′-53°53 N, 112°20′-113°39′ W) that had previously been studied for SOC storage (Baah-Acheamfour et al., 2014, 2015; Lim et al., 2018). Central Alberta is part of the northern Great Plains, which transitions into the boreal forest region. The six sites were 60-80 km apart and randomly selected from a larger group of 11 sites reported in Baah-Acheamfour et al. (2014). The mean annual precipitation of the six sites for the period 1981-2020 was 443 mm, and the average minimum and maximum temperatures were -3.2 °C and 9.0 °C, respectively (Alberta Agriculture and Forestry, 2020). All sites had very gentle slopes (< 5°) and Black Chernozemic soils (Appendix 2-1; Soil Classification Working Group, 1998) with high C and nitrogen (N) contents (Appendix 2-2). These hedgerow systems were comprised of linear forestlands 3-5 m wide (described as the "forest" land-use hereafter) found adjacent to cropped areas (hereafter the "cropland" land-use). The forest land-use was dominated by naturally regenerated broad-leaf deciduous trees, including *Populus balsamifera* L.*, Betula papyrifera* Marsh., and *Populus tremuloides* Michx., along with a variety of shrubs and herbaceous understory vegetation (Baah-Acheamfour et al., 2014). Tree age ranged from 40 to 100 years, and the mean tree density was 7776 ± 1425 stems ha^{-1} (Baah-Acheamfour et al., 2015). All neighbouring croplands were used to grow annual crops in rotation, often comprised of annual cereals such as barley (*Hordeum vulgare* L.), wheat (*Triticum*

aestivum L.), and canola (*Brassica napus* L.), with most farmers utilizing minimum tillage. Fertilizer application to croplands included N addition up to 120 kg ha^{-1} $year^{-1}$ (Baah-Acheamfour et al., 2014).

2.2. Sampling design

A split-plot experimental design was used in this study, with the land-use as the main plot factor and soil depth as the split-plot factor. During soil sampling in 2013, a 30-50 m transect was randomly laid out in each of the cropland and forest subplots at each site. Line transects were established in the center of the forest strip and within the cropland in parallel to the forest but > 30 m away from the edge of the forest to avoid edge effects. Considering the strong influence of geophysical properties on soil samples (e.g., landform, slope, elevation and drainage) (Pennock et al., 2008), we avoided strongly sloped valleys and river terraces to make sure that the two land-uses were on the same ecosite to minimize the confounding effects of growing conditions. Along each transect, ten soil cores (3.2 cm in diameter) were collected from two depths (0-10 and 10-30 cm) of the mineral soil, as soils in the 0-30 cm depth contained over half of organic C in the 0-100 cm profile (Batjes, 1996) and are sensitive to influences from land cover and management; samples were then combined to form a composite sample for each land-use at each depth.

2.3. Soil physical and chemical analysis

All visible roots and plant debris were manually removed from the soil samples, after which the samples were air-dried at room temperature (25 °C) and passed through a 2 mm sieve. Soil pH was measured with a digital pH meter (PHH-200, Omega Eng. Inc., Stamford, CT) with soil to $CaCl_2$ solution (0.01 M) ratio of 1:2 (*w:v*). A portion of each soil sample was ground to a fine powder with a ball mill (MM200, Retsch GmbH, Haan, Germany) and analyzed for C and N concentrations with an elemental analyzer (LECO Tru-Spec CN analyzer, Leco Corp., St. Joseph, MI). Soil bulk density was determined by dividing the oven-dry (at 105 °C) soil mass in a bulk density ring by the soil volume. Soil physical and chemical properties are provided in Appendix 2-2.

2.4. The ^{13}C CPMAS NMR analysis

The NMR spectra quality can be limited by certain factors, such as the existence of paramagnetic materials in the sample, spinning sidebands and baseline distortions (Šmejkalová et al., 2008); thus, proper pretreatment and careful processing of spectra are required to address some of those concerns. Air-dried samples (~ 5 g) were first treated with hydrofluoric acid (HF) to remove paramagnetic substances (Mn^{2+} and Fe^{3+}), which cause broad peaks and unpredictable chemical shifts, and can therefore negatively influence the signal-to-noise ratio (Mathers et al., 2002; Sun et al., 2013). Briefly, each sample was placed in a 50 mL centrifuge tube, then 25 mL of HF solution (10% v/v) was added, and the sample was shaken (120 rpm) in a reciprocating shaker for one hour. The samples were then centrifuged for 10 min at 1000 ×g. After that, the supernatants were decanted, and the residues remaining in the centrifuge tubes were treated again with HF.

The HF treatment process was repeated eight times with shaking times of 1 hr (4 times), 12 hr (3 times) and 24 hr (1 time) (Li et al., 2014; Zhuang et al., 2011). After the HF treatment, the remaining soil was washed by centrifuging with deionized water four times, then oven-dried at 40 ℃ for 48 hr, and ground by an agate mortar to pass a 0.25 mm mesh before NMR analysis (Li et al., 2014).

Carbon-13 NMR spectra were obtained with a Bruker Avance 300 MHz NMR Spectrometer (B_0 = 7.05 T, 300 MHz ^{1}H) equipped with a MAS NMR probe; the analysis was conducted in the Department of Chemistry at the University of Alberta. Samples were packed in 4 mm outside diameter zirconia rotors with Kel-F® caps and spun at 14 000 ± 2 Hz. The NMR spectra were obtained using the cross-polarization method, with a 4.0 μs 90° pulse, a 3.0 ms contact time, 10.0 ms acquisition time, and a 1.5 s recycle delay; the number of co-added transients ranged from 14 600 to 40 800.

Each sample spectrum was divided into seven chemical shift regions and assigned to the corresponding C functional groups (0–45 ppm, Alkyl + alpha-amino C; 45–60 ppm, N-alkyl C; 60–90 ppm, O-alkyl C; 90– 110 ppm, di-O-alkyl C; 110–140 ppm, H- and C-substituted aromatic C; 140–160 ppm, O-substituted aromatic C; and 160-200 ppm, Carbonyl C), using the methods developed in Sarker et al. (2018) and Águas et al. (2018). The area under the curve for each C functional group was calculated by integration using the MestreNova 12.0.3 software (Mestrelab Research SL, Santiago de Compostela, Spain) and expressed as a percentage of the total area under the spectrum. Structural properties of SOC were computed using four dimensionless indices based on CPMAS data [HB/HI (hydrophobicity index) = (0-45 + 110-160) / (45-60 + 60-110 + 160-200); A/OA (alkyl index) = (0-45) / (60-110); ARM (aromaticity index) = (110-160)

/ (0-45 + 60-110), and LigR (lignin ratio) = (45-60) / (140-160)] (Monda et al., 2018), of which A/OA and ARM were also used as indicators for the degree of SOC decomposition (Baldock et al., 1997; Hou et al., 2019). Although the data from CPMAS ^{13}C NMR spectra are not quantitative (Soucémarianadin et al., 2013), careful analysis of differences in the CPMAS NMR spectra among the treatments allows for qualitative assessment of the impact of land-use type or soil depth on SOC characteristics.

2.5. Thermal analysis

A Netzsch STA 409PC Luxx (Netzsch-Gerätebau GmbH, Selb, Germany) coupled to an LI-840 CO_2/H_2O infrared gas analyzer (IRGA) (LI-COR, Inc. Lincoln, NE) was used to perform the thermal analysis. A detailed description of the thermal analysis method can be found in Plante et al. (2011), Stone and Plante (2015) and Williams et al. (2018). Briefly, air-dried samples (< 50 mg of soil, containing ~ 1 mg C) were placed in a Pt/Rh crucible (with an identical empty crucible used as a control) and heated from room temperature (25 °C) to 125 °C at a rate of 10 °C min^{-1} under an oxidizing condition with a supply of 40 mL min^{-1} of synthetic air (20% oxygen and the balance as N_2 gas). Each sample was maintained at 125 °C for 15 min to remove soil moisture, then heated to 650 °C at a rate of 10 °C min^{-1}. Thermogravimetric (TG) mass loss, CO_2-EGA signals and DSC heat flux data were recorded at one-second intervals for each sample. Baselines of CO_2 and DSC data were corrected *a-posteriori* through the base R package and application of a smooth.spline() function. Furthermore, DSC integration was done by

applying the base R package and the sintergral() function following the method in Williams and Plante (2018).

To determine total exothermic energy (i.e., the energy released during the ramped combustion, in mJ), the DSC heat flux (mW) was integrated over the exothermic region of 125–650 °C, which corresponded to the range of temperature that SOC was oxidized under (Rovira et al., 2008). The TG mass loss was also calculated for the same temperature range, and this mass loss was considered mainly due to the combustion of SOC, with little contribution from dehydration of minerals (e.g., kaolinite) (Williams and Plante, 2018). The energy density (J mg^{-1} C) of SOC was calculated by dividing the energy content by the TG mass loss (Rovira et al., 2008; Plante et al., 2011). Another four indices were also used to evaluate the thermal stability of SOC (Plante et al., 2011; Peltre et al., 2013). These included TG-T_{50} (the temperature at which 50% of the exothermic mass was lost), DSC-T_{50} (the temperature at which 50% of the exothermic energy was released), CO_2-T_{50} (the temperature at which 50% of the CO_2 was produced) and energy content (the total energy yield normalized to sample mass).

2.6. Statistical analysis

Data acquired by the solid-state ^{13}C NMR and thermal analyses were analyzed using *agricolae* (De Mendiburu, 2019) and *lsmeans* packages (Lenth, 2016) in R software (R Core Team, 2018). Results were subject to normality tests to evaluate sample distribution, with a log transformation applied to O-substituted aromatic C, alkyl index and the aromaticity index to meet normality. As factors like clay content, drainage and slope may

influence SOC stability, we included those factors and accounted for them as covariates. Analysis of variance (ANOVA) was applied to test how soil C functional groups, structural indices and thermal stability indices were affected by the fixed effects of land-use (forest vs. cropland) and soil depth (0-10 vs. 10-30 cm). Mean separation was conducted on any significant interactions between land-use and soil depth using least-squares means in the *lsmeans* package (Lenth, 2016). All means in non-transformed data are presented as *lsmeans*, while for the log-transformed data above, *lsmeans* were back-transformed for straightforward interpretation. The Pearson correlation analysis was used to determine the relationships between variables, and principal component analysis (PCA) was used to study relationships among SOC structural stability, thermal stability and basic soil properties such as soil total C, pH and bulk density by reducing the dimensionality of the datasets and improving the interpretability of patterns among treatments (Jolliffe and Cadima, 2016). All statistical significance was set at $\alpha = 0.05$ unless otherwise stated.

3. Results

3.1 Characterization of SOC by ^{13}C NMR spectroscopy

The interaction effects of land-use by soil depth were not significant for all C functional groups (Table 2-1). Forest SOC had a higher proportion of O-alkyl C than cropland SOC ($p = 0.02$). In comparison, SOC in cropland had a higher proportion of H- and C-substituted aromatic C than in forest ($p = 0.03$) (Table 2-1). All ^{13}C CPMAS NMR spectra had pronounced peaks for alkyl + alpha-amino C, H- and C-substituted aromatic C, carbonyl C

and O-alkyl C, regardless of the land-use and soil depth (Fig. 2-1). Among the seven C functional groups, the H- and C-substituted aromatic C region comprised the highest proportion, while di-O-alkyl C accounted for the lowest proportion. The proportions of di-O-alkyl C, H- and C-substituted aromatic C, N-alkyl C and O-alkyl C, all changed with soil depth; the 0-10 cm soil had higher di-O-alkyl C ($p = 0.01$), N-alkyl C ($p < 0.01$) and O-alkyl C ($p < 0.01$) than the 10-30 cm soil, while H- and C-substituted aromatic C was higher in 10-30 cm soil than the 0-10 cm soils ($p < 0.01$) (Table 2-1).

Interaction effects of land-use by soil depth were found for A/OA ($p < 0.01$) (Table 2-2). Soil organic carbon in both the 0-10 and 10-30 cm layers of the forest and the 0-10 cm layer of cropland had similar A/OA, while the greatest A/OA was found in the 10-30 cm layer of cropland (Fig. 2-2). Both HB/HI and ARM were influenced by land-use. Cropland SOC had higher HB/HI ($p = 0.01$) and ARM ($p = 0.02$) than the forest SOC. HB/HI, ARM and LigR were all influenced by soil depth, with the SOC in the 10-30 cm layer having higher HB/HI ($p < 0.01$), ARM ($p < 0.01$) and LigR ($p = 0.01$) than SOC in the 0-10 cm depth.

3.2. SOC thermal stability

The exothermic DSC region was larger for the 0-10 cm layer than for the 10-30 cm soil depth in both the forest and cropland, and the observed exothermic peaks ranged from 335 to 338 ˚C but were similar between the two land-uses and depths (Fig. 2-3). No interaction effects of land-use by soil depth were found on SOC thermal indices. SOC energy density, energy content and TG-T_{50} were influenced by both land-use and soil depth. SOC in forest

soils had higher energy density (12.8 J mg^{-1} C) ($p = 0.04$) and energy content (1.6 J mg^{-1} soil) ($p < 0.01$) than those in adjacent cropland soils (11.6 J mg^{-1} C and 0.9 J mg^{-1} soil, respectively), and forest SOC had lower TG-T_{50} than the cropland SOC ($p < 0.03$) (Table 2-3). SOC in 0-10 cm layer was higher in both energy density ($p = 0.04$) and energy content ($p = 0.01$) than that in the 10-30 cm layer. TG-T_{50} showed contrasting results with energy density and energy content, as SOC in the 10-30 cm layer had higher TG-T_{50} than the 0-10 cm layer ($p < 0.01$). Both DSC-T_{50} and CO_2-T_{50} were not influenced by land-use or soil depth (Table 2-3).

3.3 Relations of basic soil properties with SOC structural and thermal stability

The PCA1 and PCA2 accounted for 44.6 and 18.4%, respectively, of the variation in C stability profiles (Fig. 2-4). The top five variables that contributed to PCA1 was select SOC functional groups (N-alkyl C and O-alkyl C) and several structural stability indices (A/OA, ARM and HB/HI), while PCA2 was mainly linked to variables related to SOC thermal indices (DSC-T_{50}, CO_2-T_{50}, energy density and energy content) and soil bulk density. Of the total variability in C composition within the SOC profile, cropland soils demonstrated clear divergence from forested soils, particularly along PCA1. Considerable overlap occurred in the forest and cropland soils of the 0-10 cm layer, while cropland SOC in the 10-30 cm layer had the most significant separation from all other treatments, particularly shallow forest soils (Fig. 2-4). Pearson correlation analysis showed that C and N were negatively correlated with bulk density and all SOC structural indices and positively correlated with energy content. Bulk density was positively correlated with HB/HI and

A/OA, while being negatively correlated with DSC-T_{50}, TG-T_{50}, energy density and energy content. Soil pH was negatively correlated with soil C and N content while being positively correlated with HB/HI, A/OA and TG-T_{50}. Both HB/HI and A/OA were positively correlated with TG-T_{50} while being negatively correlated with energy content. HB/HI also showed a positive correlation with CO_2-T_{50}. No correlations were evident of ARM or LigR to any of the thermal indices (Appendix 2-3).

4. Discussion

Croplands had less labile C, making the remaining C more stable than that in the forest land-use. The difference in A/OA between land-uses and soil depths suggests that SOC in the deeper soil layer of the cropland had a higher degree of prior decomposition (Baldlock et al., 1997; Hou et al., 2019). The similarity of SOC structural and thermal stability (Fig. 2-2 and Fig. 2-4) between the cropland surface soil and forest subsurface soil highlights the divergent impacts of land-use on soil functioning. This could suggest the forest surface soil was much less stable than the surface cropland soil, thereby putting the surface soil in the forest at greater risk of SOC loss. The significant positive relationship between soil pH and A/OA and TG-T_{50} indicates that pH affects soil microbial activities (Pietri and Brookes, 2008), and thus the degree of SOC decomposition and energy density (Stone and Plante, 2015). It is noted that the proportion of variance explained by axis 1 in the PCA was high (Fig. 2-4), which could reflect high collinearity among variables (especially thermal and structural indices) along this axis (Appendix 2-3). The vectors for TG-T_{50} and CO_2-T_{50} were orthogonal, and

therefore independent of each other, which may reflect their uniqueness as functional indicators of different SOC pools. The metric of TG-T_{50} is known to be highly linked to labile SOC pools (Soucémarianadin et al., 2018), while CO_2-T_{50} is related to stable SOC pools with a mean residence time of no less than 50 to 100 years (Cécillon et al., 2018).

4.1. Effects of soil depth on SOC structural and thermal stability

Both SOC structural and thermal indices were influenced by soil depth regardless of land-use. Overall, the structural complexity of SOC in the 0-10 cm layer was lower than that in the 10-30 cm soil, suggesting that SOC in the 0-10 cm soil layer was less stable and more prone to decomposition than SOC in the 10-30 cm soil layer. The abundance of Di-O-alkyl C and O-alkyl C, both of which belonged to easily decomposable C groups (Cepáková et al., 2016; Näthe et al., 2017; Sarker et al., 2018), were higher in the 0-10 cm layer than in the 10-30 cm soil, again suggesting the SOC in the topsoil is easily decomposable. Moreover, N-alkyl C, an index of lignin content, was higher in the 0-10 cm soil layer regardless of land-use, while LigR was higher in the 10-30 cm soil layer, suggesting that a higher abundance of N-alkyl C did not necessarily mean a higher lignin content (Incerti et al., 2018). It should be noted that the higher HB/HI in deeper soils suggested the SOC was more hydrophobic in deeper soil, favoring the long-term storage of C via hydrophobic protection (Piccolo et al., 1999).

The elevated ARM and A/OA within the 10-30 cm soil layer compared to the 0-10 cm soil layer suggested that SOC in the deeper soil layer had a higher degree of decomposition (Näthe et al., 2017). This finding, together with a higher LigR, HB/HI and

TG-T_{50}, suggested that SOC structural stability and thermal stability increased with soil depth in both land-uses. This is consistent with Hou et al. (2019), who found that thermal and molecular indices of SOC stability increased with depth, which may be due to energy-rich litter inputs at the surface soil that account for the heightened energy density and content near the soil surface (Williams et al., 2018). In comparison, less of this surface litter-based SOC is likely to make it into the deeper soil, with the latter containing more recalcitrant C that is low in energy content (Williams et al., 2018; Stone and Plante, 2015; Hou et al., 2019). Both the DSC-T_{50} and CO_2-T_{50} did not show any differences between the two soil depths, which is inconsistent with results reported in Plante et al. (2011), suggesting that DSC-T_{50} and CO_2-T_{50} may not be universally effective indicators of SOC thermal stability.

4.2. Effects of land-use on SOC structural and thermal stability

Forest SOC had a higher proportion of O-alkyl C and lower values for the structural indices (HB/HI, ARM and A/OA), suggesting that the SOC in forests was rich in easily decomposable C that was of high quality. The SOC energy density and content were higher in the forest than in cropland soils, indicating that SOC in the forest soil was more labile (Peltre et al., 2013). Previous investigations revealed that the forest land-use within agroforestry systems supported more abundant and species-rich bacterial communities than croplands due to the availability of nutrient-rich resources (Banerjee et al., 2016), and this may account for the increased lability of SOC within the forest land-use. The hedgerow forest in this study consisted of naturally regenerating deciduous trees

(*Populus balsamifera* L and *Populus tremuloides* Michx) and shrubs (*Prunus virginiana* and *Amelanchier alnifolia*) (Baah-Acheamfour et al., 2016), which may increase the quality of litter input into forest soils. Higher plant (forbs, shrubs and trees) diversity in the hedgerow forest likely led to more variable C chemical composition due to contrasting inputs of litterfall of different quality (Howlett et al., 2011; Duarte et al., 2013). Also, tree species are known to affect SOC stability; Angst et al. (2019) found that SOC stability under different tree species varied considerably. The chemistry of plant tissue ultimately controls the amount of C input to the soil and its transformation into stable C within mineral soils via various physical, biological and chemical processes (Six et al., 2004; Angst et al., 2019). Soil microorganisms preferentially decompose organic matter having high energy density or high quality (Barré et al., 2016), which may result in the SOC of forest soils having a greater rate of turnover.

In contrast, the higher proportion of H- and C-substituted aromatic C and higher HB/HI, ARM and A/OA of SOC in the cropland relative to the forest indicated that SOC in the cropland was more abundant in structurally complex C (i.e., stable C). This same SOC would be low in organic matter quality (less labile C), indicating that SOC in the cropland can be expected to decompose more slowly due to the requirement of greater energy input (higher T_{50}) by microorganisms in exchange for a smaller energy benefit during the consumption of substrates with low energy density (Rovira et al., 2008). Our data suggest that there was an energy barrier to ongoing decomposition in cropland (Plante et al., 2011), as SOC oxidized at higher temperatures is fundamentally more recalcitrant, i.e., having high thermal stability (Lopez-Capel et al., 2005; Plante et al., 2011). Moreover, regular cultivation of cropland soils may inherently change the timing,

amount, and quality of organic matter input to these soils (Sollins et al., 1996), as well as SOC decomposition rate, which in turn, influences not only SOC stability but also the rate of turnover and the size of the SOC pool being turned over (Barré et al., 2016). Unlike the cropland soils, the forest soils with their higher SOC content in these agroforestry systems (Baah-Acheamfour et al., 2014) may be expected to store a considerable amount of C, a substantial portion of which may be relatively labile and susceptible to loss in association with their low SOC stability metrics (Hou et al., 2020). Although cropland SOC had higher stability than SOC in the forest, this arises from a net decline in SOC concentration relative to adjacent forestlands, and thus was the 'effect' of the loss of more labile SOC. That is, croplands hold less SOC due to the loss of less protected carbon; this loss of labile or less protected C may strongly influence soil health. Land-uses may affect soil texture (especially clay content) and hydrophobicity, and thus influence SOC stability indirectly. Peltre et al. (2013) found that TG-T_{50} was greater in soils with a higher clay content but a low C content. However, the lack of a relationship between clay content and the structural and thermal stability indices examined in this study (Appendix 2-4) suggested that clay content may not be the primary factor influencing SOC stability. Clay may favor the formation of mineral-associated C (von Lützow et al., 2007), which is favorable for long-term storage of C. In this study, however, the clay content was similar between the cropland and forest soils due to the paired study design [supplementary data in Baah-Acheamfour et al. (2014)]. Thus, clay content alone may not be able to explain differences in SOC properties between the two land-use systems. Soil hydrophobicity is mainly caused by organic matter that either coats soil particle surfaces or accumulates as particulate organic matter, thereby

inhibiting the rate and extent of soil wetting and affecting soil organic matter resistance to microbial decomposition (Capriel, 1997: Blum et al., 2011). A high soil hydrophobicity would reduce water infiltration into the soil, decrease water availability and limit SOC decomposition, thus increasing the long-term SOC storage potential (Piccolo and Mbagwu, 1999). Olorunfemi and Fasinmirin (2017) found that forest soils had higher hydrophobicity than cropland soil, which contradicted our results; the greater hydrophobicity in the cropland soils of this study may result from the periodic addition of materials with high organic matter content (e.g., manure or biochar following historical burning of crop residue) (Elbl et al., 2014).

5. Conclusions

Forested land-uses, represented here by natural hedgerows, contain high-quality SOC that is characterized by higher O-alkyl C abundance and lower structural and thermal stability as compared with the adjacent cropland. As a result, the SOC in croplands may be more likely to persist within these agroforestry systems. Both SOC structural stability and thermal stability also increased with soil depth regardless of land-use type. The high-quality but less thermally stable SOC in the surface (0-10 cm) mineral soil layer, especially in the forest land-use, may pose a risk of large C loss from future anthropogenic disturbances such as cultivation and climate change. Incorporating trees to form agroforestry systems will not only increase soil C stock but alter the quality, structural and thermal stabilities of SOC, which needs to be considered when evaluating the long-term ability of agroforestry systems to sequester C.

Table 2-1. The relative proportion (%) of carbon functional groups (mean ± standard error) derived from CP MAS NMR spectra of SOC in different land-use in the hedgerow system (n=12).

Land-use / Depth	The relative proportion of carbon functional groups (%)						
	Alkyl+alpha-amino C (0-45 ppm)	N-alkyl C (45-60 ppm)	O-alkyl C (60-90 ppm)	Di-O-alkyl C (90-110 ppm)	H- and C-substituted aromatic C (110-140 ppm)	O-substituted aromatic C (140-160 ppm)	Carbonyl C (160-200 ppm)
Land-use (LU)							
Forest	18.1±0.3	7.2±0.3	19.2±0.7	5.8±0.3	22±0.9	8.0±1.0	17.1±0.5
Cropland	18.5±0.3	6.6±0.3	16.4±0.7	5±0.3	25±0.9	8.5±1.0	17.7±0.5
Depth (D)							
0-10 cm	18.1±0.3	7.5±0.3	19.9±0.7	5.9±0.3	21.2±0.9	7.8±1.0	16.9±0.5
10-30 cm	18.5±0.3	6.3±0.3	15.7±0.7	4.9±0.3	25.8±0.9	8.7±1.0	17.8±0.5
ANOVA							
Source of variation							
LU	0.36	0.11	**0.02**	0.09	**0.03**	0.37	0.36
D	0.34	**<0.01**	**<0.01**	**0.01**	**<0.01**	0.06	0.14
LU × D	0.34	0.78	0.77	0.29	0.86	0.51	0.34

Note: $P < 0.05$ is highlighted in bold

Table 2-2. Carbon structural indices (mean ± standard error, n=12) in forest and cropland land-use and soil depth (0-10 cm and 10-30 cm) in the hedgerow system.

Land-use/Depth	Carbon structural index			
	HB/HI	A/OA	ARM	LigR
Land-use (LU)				
Forest	1.03±0.03	1.13±0.04	0.69±0.07	0.80±0.06
Cropland	1.20±0.03	1.36±0.04	0.81±0.07	0.91±0.06
Depth (D)				
0-10	1.00±0.01	1.11±0.03	0.64±0.07	0.73±0.06
10-30	1.23±0.03	1.40±0.03	0.87±0.07	1.00±0.06
ANOVA				
Source of variation				
LU	**0.01**	**0.02**	**0.02**	0.13
D	**<0.01**	**<0.01**	**<0.01**	**0.01**
LU × D	0.31	**0.01**	0.46	0.74

Note: $P < 0.05$ is highlighted in bold. A/OA, alkyl index; ARM, aromaticity index; HB/HI, hydrophobicity index; LigR, lignin ratio.

Table 2-3. Selected thermal indices (mean ± standard error, n=12) for SOC in forest and cropland land-use and soil depth (0-10 cm and 10-30 cm) of the hedgerow system.

Land-use/Depth	TG-T_{50} (˚C)	DSC-T_{50} (˚C)	CO_2-T_{50} (˚C)	Energy density (J mg^{-1} C)	Energy content (J mg^{-1} soil)
Land-use (LU)					
Forest	364±2.1	360±2.0	383±1.9	12.8±0.5	1.6±0.2
Cropland	373±2.1	358±2.0	383±1.9	11.6±0.5	0.9±0.2
Depth (D)					
0-10 cm	361±2.7	359±1.9	382±1.6	13.0±0.5	1.6±0.2
10-30 cm	376±2.7	359±1.9	384±1.6	11.4±0.5	0.9±0.2
ANOVA					
Source of variation					
LU	**0.03**	0.38	0.88	**0.04**	**<0.01**
D	**<0.01**	0.88	0.41	**0.04**	**0.01**
LU × D	0.33	0.68	0.27	0.33	0.5

Note: $P < 0.05$ is highlighted in bold, and TG-T_{50}, the temperature that 50% of the exothermic mass is lost; DSC-T_{50}, the temperature that 50% of the exothermic energy is released; CO_2-T_{50}, the temperature that 50% of the CO_2 is produced.

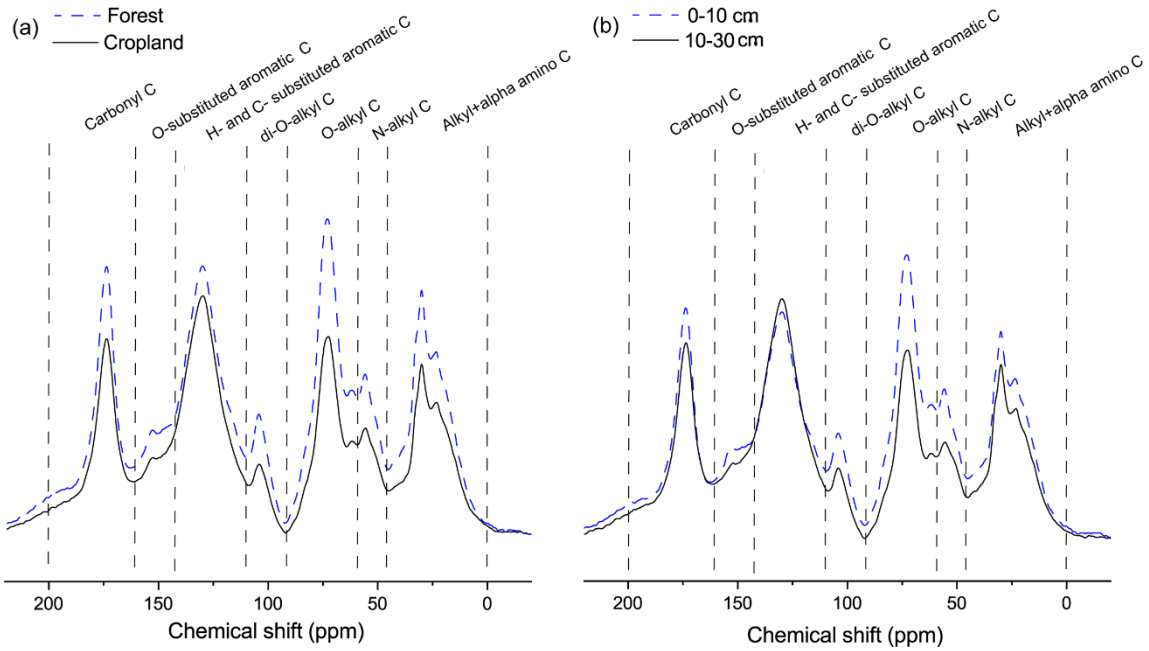

Fig. 2-1. Carbon-13 CPMAS NMR spectra (mean) of the soil samples from (a) different land-use within a hedgerow system and (b) different soil depths (n = 12).

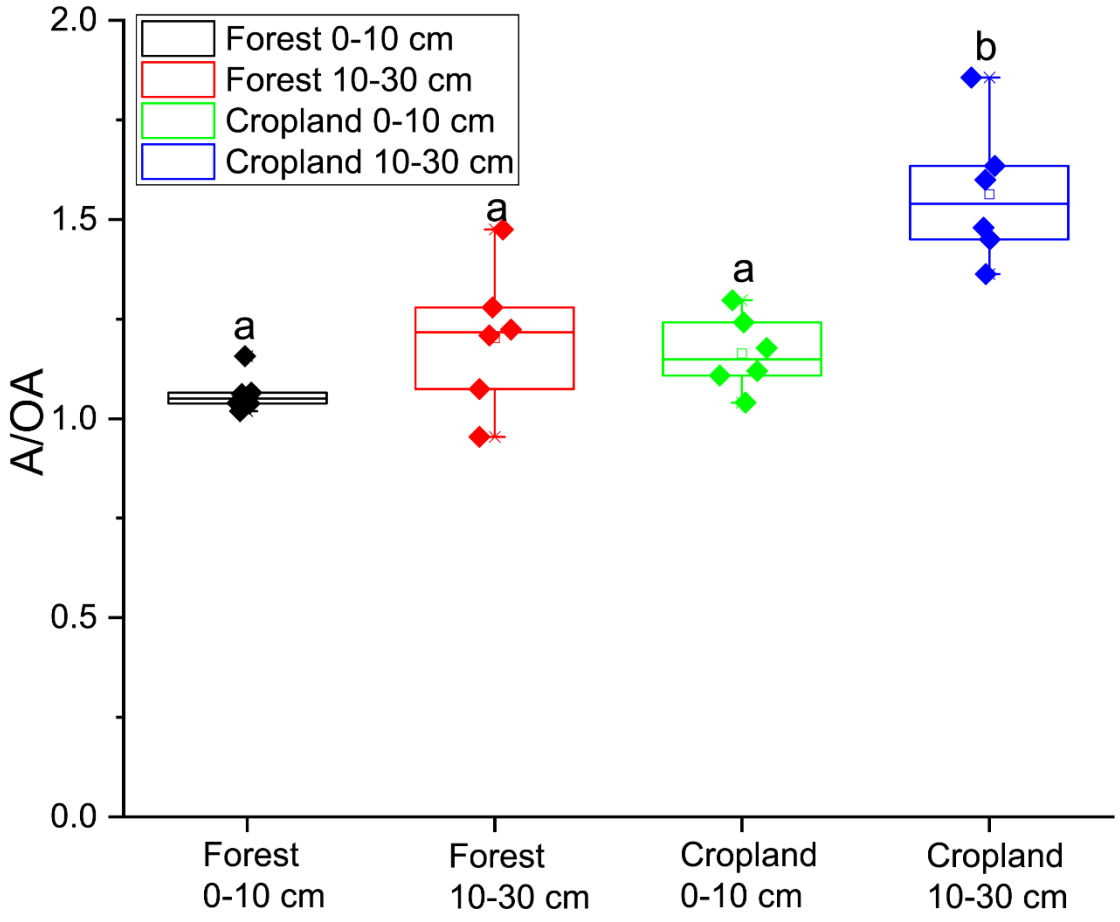

Fig. 2-2. The interaction effects of land-use by soil depth on alkyl index (A/OA) based on ^{13}C CPMAS NMR data. Data points are mean (± standard error, n=6, the hollow point and the middle line in each boxplot represent mean and median, respectively). Different lowercase letters indicate a significant difference at $p < 0.05$.

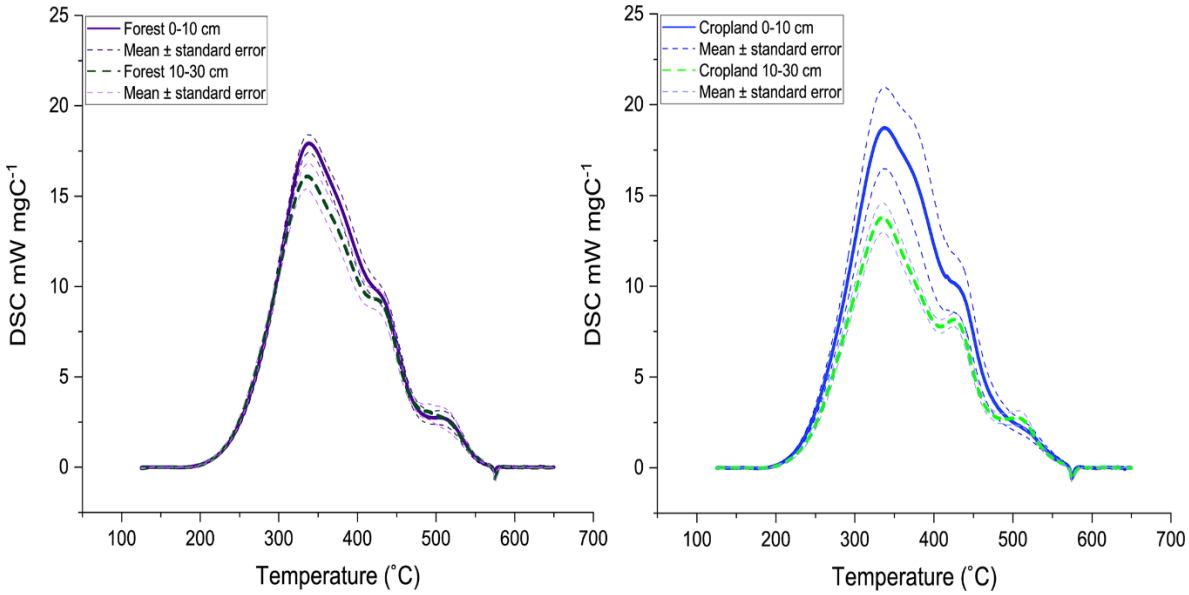

Fig. 2-3. Differential scanning calorimetry (DSC) thermograms (mean ± standard error, n=6) for the cropland and forest land-uses and two soil depths within the hedgerow system.

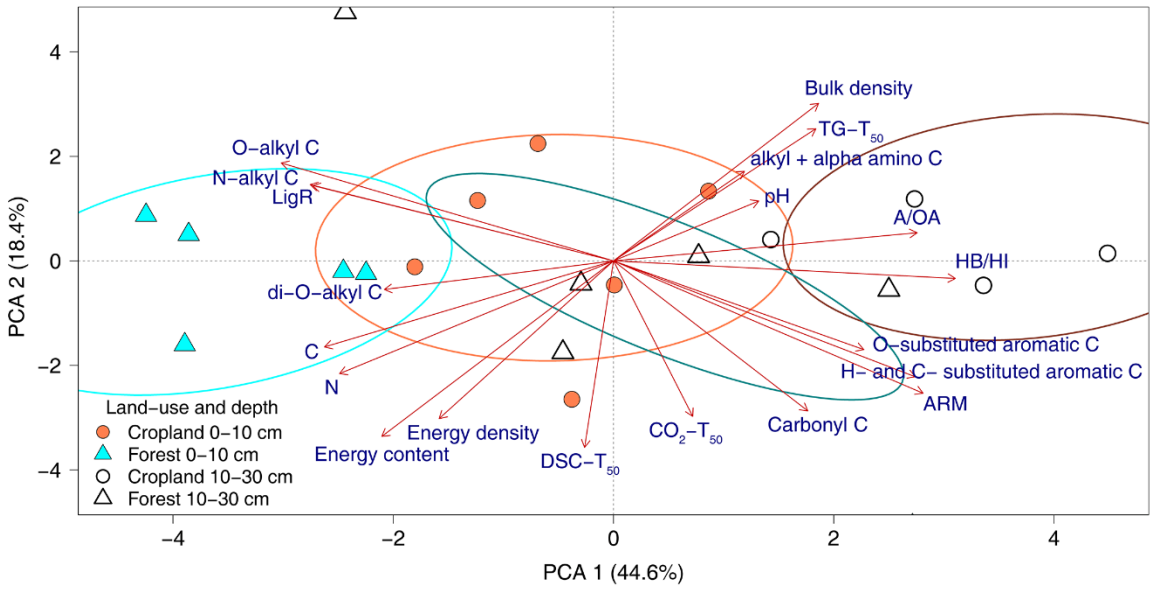

Fig. 2-4. The relationships between basic soil properties, carbon functional groups and thermal indices of soils collected at two depths from forest and cropland, using a PCA ordination with 95% confidence ellipses to describe the interaction effects of land-use by depth.

Note: HB/HI, hydrophobicity index; A/OA, alkyl index; ARM, aromaticity index; LigR, lignin ratio; TG-T_{50}, the temperature that 50% of the exothermic mass is lost; DSC-T_{50}, the temperature that 50% of the exothermic energy is released; CO_2-T_{50}, the temperature that 50% of the CO_2 is produced.

References

Águas, A., Incerti, G., Saracino, A., Lanzotti, V., Silva, J.S., Rego, F.C., Mazzoleni, S., Bonanomi, G., 2018. Fire effects on litter chemistry and early development of Eucalyptus globulus. Plant Soil 422, 495-514. https://doi.org/10.1007/s11104-017-3419-2.

Alberta Agriculture and Forestry, 2020. Interpolated Weather Data Since 1961 for Alberta Townships. Government of Alberta. https://acis.alberta.ca/township-data-viewer.jsp (accessed June 07, 2021).

Angst, G., Mueller, K.E., Eissenstat, D.M., Trumbore, S., Freeman, K.H., Hobbie, S.E., Chorover, J., Oleksyn, J., Reich, P.B., Mueller, C.W., 2019. Soil organic carbon stability in forests: distinct effects of tree species identity and traits. Glob. Change Biol. 25, 1529-1546. https://doi.org/10.1111/gcb.14548.

Baah-Acheamfour, M., Carlyle, C.N., Bork, E.W., Chang, S.X., 2014. Trees increase soil carbon and its stability in three agroforestry systems in central Alberta, Canada. For. Ecol. Manage. 328, 131-139. https://doi.org/10.1016/j.foreco.2014.05.031.

Baah-Acheamfour, M., Chang, S.X., Carlyle, C.N., Bork, E.W., 2015. Carbon pool size and stability are affected by trees and grassland use types within agroforestry systems of western Canada. Agric. Ecosyst. Environ. 213, 105-113. https://doi.org/10.1016/j.agee.2015.07.016.

Baah-Acheamfour, M., Carlyle, C.N., Lim, S.S., Bork, E.W., Chang, S.X. 2016. Forest and grassland cover types reduce net greenhouse gas emissions from agricultural soils. Sci. Total Environ. 571, 1115-1127.

https://doi.org/10.1016/j.scitotenv.2016.07.106.Batjes, N.H., 1996. Total carbon and nitrogen in the soils of the world. Eur. J. Soil Sci. 47, 151-163. https://doi.org/10.1111/j.1365-2389.1996.tb01386.x

Baldock, J.A., Oades, J.M., Nelson, P.N., Skene, T.M., Golchin, A., Clarke, P., 1997. Assessing the extent of decomposition of natural organic materials using solid-state ^{13}C NMR spectroscopy. Soil Res. 35, 1061-1084. https://doi.org/10.1071/S97004.

Banerjee, S., Baah-Acheamfour, M., Carlyle, C.N., Bissett, A., Richardson, A.E., Siddique, T., Bork, E.W., Chang, S.X., 2016. Determinants of bacterial communities in Canadian agroforestry systems. Environ. Microbiol. 18, 1805-1816. https://doi.org/10.1111/1462-2920.12986.

Barré, P., Plante, A.F., Cécillon, L., Lutfalla, S., Baudin, F., Bernard, S., Christensen, B.T., Eglin, T., Fernandez, J.M., Houot, S., Kätterer, T., 2016. The energetic and chemical signatures of persistent soil organic matter. Biogeochemistry 130, 1-12. https://doi.org/10.1007/s10533-016-0246-0.

Blum, W.E., de Baerdemaeker, J., Finkl, C.W., Horn, R., Pachepsky, Y., Shein, E.V., Konstankiewicz, K., Grundas, S., 2011. Encyclopedia of Agrophysics. Berlin, Germany, Springer. 378-382 pp.

Bosatta, E. and Ågren, G.I. 1999. Soil organic matter quality interpreted thermodynamically. Soil Biol. Biochem. 31, 1889-1891. https://doi.org/10.1016/S0038-0717(99)00105-4.

Capriel, P., 1997. Hydrophobicity of organic matter in arable soils: influence of management. Eur. J. Soil Sci. 48, 457-462. https://doi.org/10.1111/j.1365-2389.1997.tb00211.x.

Cécillon, L., Baudin, F., Chenu, C., Houot, S., Jolivet, R., Kätterer, T., Lutfalla, S., Macdonald, A., Oort, F.v., Plante, A.F., 2018. A model based on Rock-Eval thermal analysis to quantify the size of the centennially persistent organic carbon pool in temperate soils. Biogeosciences 15, 2835-2849. https://doi.org/10.5194/bg-15-2835-2018.

Cepáková, Š., Tošner, Z., Frouz, J., 2016. The effect of tree species on seasonal fluctuations in water-soluble and hot water-extractable organic matter at post-mining sites. Geoderma 275, 19-27. https://doi.org/10.1016/j.geoderma.2016.04.006.

De Mendiburu F., 2019. Agricolae: Statistical procedures for agricultural research. R Package Version 1.2-4.

De Stefano, A., Jacobson, M.G. 2018. Soil carbon sequestration in agroforestry systems: a meta-analysis. Agrofor. Syst. 92, 285-299. https://doi.org/10.1007/s10457-017-0147-9.

Duarte, R.M., Fernández-Getino, A.P., Duarte, A.C., 2013. Humic acids as proxies for assessing different Mediterranean forest soils signatures using solid-state CPMAS ^{13}C NMR spectroscopy. Chemosphere 91, 1556-1565. https://doi.org/10.1016/j.chemosphere.2012.12.043.

Elbl, J., Vaverková, M., Adamcová, D., Plosek, L., Kintl, A., Losak, T., Hynst, J., Kotovicová, J., 2014. Influence of fertilization on microbial activities, soil

hydrophobicity and mineral nitrogen leaching. Ecol. Chem. Eng. 21, 661. https://doi.org/10.1515/eces-2014-0048.

Fontaine, S., Barot, S., Barré, P., Bdioui, N., Mary, B., Rumpel, C., 2007. Stability of organic carbon in deep soil layers controlled by fresh carbon supply. Nature 450, 277-280. https://doi.org/10.1038/nature06275.

He, Y., Chen, C.R., Xu, Z.H., William, D., Xu, J.M., 2009. Assessing management impacts on soil organic matter quality in subtropical Australian forests using physical and chemical fractionation as well as ^{13}C NMR spectroscopy. Soil Biol. Biochem. 41, 640-650. https://doi.org/10.1016/j.soilbio.2009.01.008.

Hou, Y.H., Chen, Y., Chen, X. He, K.Y., Zhu, B., 2019. Changes in soil organic matter stability with depth in two alpine ecosystems on the Tibetan Plateau. Geoderma 351, 153-162. https://doi.org/10.1016/j.geoderma.2019.05.034.

Howlett, D.S., Mosquera-Losada, M.R., Nair, P.R., Nair, V.D., Rigueiro-Rodríguez, A., 2011. Soil carbon storage in silvopastoral systems and a treeless pasture in northwestern Spain. J. Environ. Qual. 40, 825-832. https://doi.org/10.2134/jeq2010.0145.

Incerti, G., Cartenì, F., Cesarano, G., Sarker, T.C., El-Gawad, A., Ahmed, M., D'Ascoli, R., Bonanomi, G., Giannino, F., 2018. Faster N release, but not C loss, from leaf litter of invasives compared to native species in Mediterranean ecosystems. Front. Plant Sci. 9, 534. https://doi.org/10.3389/fpls.2018.00534.

IPCC, 2007. Climate change 2007: The Physical Science Basis. Contribution of Working Group I to the Fourth Assessment Report of the Intergovernmental Panel on Climate Change. Geneva: IPCC.

Jolliffe, I.T. and Cadima, J., 2016. Principal component analysis: a review and recent developments. Philos. Trans. A. Math. Phys. Eng. Sci. 374(2065), 20150202. https://doi.org/10.1098/rsta.2015.0202.

Jose, S., 2009. Agroforestry for ecosystem services and environmental benefits: an overview. Agrofor. Syst. 76, 1-10. https://doi.org/10.1007/s10457-009-9229-7.

Lenth, R.V. 2016. Least-squares means: the R package lsmeans. J. Stat. Softw. 69, 1-33.

Li, Y.F., Zhang, J.J., Chang, S.X., Jiang, P.K., Zhou, G.M., Shen, Z.M., Wu, J.S., Lin, L., Wang, Z.H., Shen, M.C., 2014. Converting native shrub forests to Chinese chestnut plantations and subsequent intensive management affected soil C and N pools. For. Ecol. Manag. 312, 161-169. https://doi.org/10.1016/j.foreco.2013.10.008.

Lim, S.S., Baah-Acheamfour, M., Choi, W.J., Arshad, M.A., Fatemi, F., Banerjee, S., Carlyle, C.N., Bork, E.W., Park, H.J., Chang, S.X., 2018. Soil organic carbon stocks in three Canadian agroforestry systems: From surface organic to deeper mineral soils. For. Ecol. Manag. 417, 103-109. https://doi.org/10.1016/j.foreco.2018.02.050.

Lopez-Capel, E., Sohi, S.P., Gaunt, J.L., Manning, D.A., 2005. Use of thermogravimetry–differential scanning calorimetry to characterize modelable soil organic matter fractions. Soil Sci. Soc. Am. J. 69, 136-140. https://doi.org/10.2136/sssaj2005.0136a.

Mathers, N.J., Xu, Z., Berners-Price, S.J., Perera, M.S., Saffigna, P.G., 2002. Hydrofluoric acid pretreatment for improving ^{13}C CPMAS NMR spectral quality

of forest soils in south-east Queensland, Australia. Soil Res. 40, 665-674. https://doi.org/10.1071/SR01073.

Monda, H., Cozzolino, V., Vinci, G., Drosos, M., Savy, D., Piccolo, A., 2018. Molecular composition of the Humeome extracted from different green composts and their biostimulation on early growth of maize. Plant Soil 429, 407-424. https://doi.org/10.1007/s11104-018-3642-5.

Nair, P.R., 2011. Agroforestry systems and environmental quality: introduction. J. Environ. Qual. 40, 784-790. https://doi.org/10.2134/jeq2011.0076.

Nair, P.R., Nair, V.D., Kumar, B.M., Haile, S.G., 2009. Soil carbon sequestration in tropical agroforestry systems: a feasibility appraisal. Environ. Sci. Policy. 12, 1099-1111. https://doi.org/10.1016/j.envsci.2009.01.010.

Näthe, K., Levia, D.F., Steffens, M., Michalzik, B., 2017. Solid-state ^{13}C NMR characterization of surface fire effects on the composition of organic matter in both soil and soil solution from a coniferous forest. Geoderma 305, 394-406. https://doi.org/10.1016/j.geoderma.2017.06.030.

Nie, X.D., Li, Z.W., Huang, J.Q. Liu, L., Xiao, H.B., Liu, C., Zeng, G.M., 2018. Thermal stability of organic carbon in soil aggregates as affected by soil erosion and deposition. Soil Tillage Res. 175, 82-90. https://doi.org/10.1016/j.still.2017.08.010.

Oelbermann, M., Voroney, R.P., Gordon, A.M. 2004. Carbon sequestration in tropical and temperate agroforestry systems: a review with examples from Costa Rica and southern Canada. Agric. Ecosyst. Environ. 104, 359-377. https://doi.org/10.1016/j.agee.2004.04.001.

Ohno, T., Heckman, K.A., Plante, A.F., Fernandez, I.J., Parr, T.B.,2017. ^{14}C mean residence time and its relationship with thermal stability and molecular composition of soil organic matter: A case study of deciduous and coniferous forest types. Geoderma 308, 1-8. https://doi.org/10.1016/j.geoderma.2017.08.023.

Peltre, C., Fernández, J.M., Craine, J.M., Plante, A.F., 2013. Relationships between biological and thermal indices of soil organic matter stability differ with soil organic carbon level. Soil Sci. Soc. Am. J. 77, 2020-2028. https://doi.org/10.2136/sssaj2013.02.0081.

Pennock, D., Yates, T., and Braidek, J. 2008. Soil sampling designs. In M.R. Carter, Ed. Soil Sampling and Methods of Analysis, Canadian Society of Soil Science, Lewis Publishers, CRC Press, Boca Raton, 25-37 pp.

Piccolo, A. and Mbagwu, J.S., 1999. Role of hydrophobic components of soil organic matter in soil aggregate stability. Soil Sci. Soc. Am. J. 63, 1801-1810. https://doi.org/10.2136/sssaj1999.6361801x.

Piccolo, A., Spaccini, R., Haberhauer, G., Gerzabek, M.H., 1999. Increased sequestration of organic carbon in soil by hydrophobic protection. Naturwissenschaften, 86(10), 496-499.

Pietri, J.A. and Brookes, P.C., 2008. Relationships between soil pH and microbial properties in a UK arable soil. Soil Biol. Biochem. 40, 1856-1861. https://doi.org/10.1016/j.soilbio.2008.03.020.

Plante, A.F., Fernández, J.M., Haddix, M.L., Steinweg, J.M., Conant, R.T., 2011. Biological, chemical and thermal indices of soil organic matter stability in four

grassland soils. Soil Biol. Biochem. 43, 1051-1058. https://doi.org/10.1016/j.soilbio.2011.01.024.

R Core Team, 2018. R: A language and environment for statistical computing. R Foundation for Statistical Computing. Austria: Vienna.

Rovira, P., Kurz-Besson, C., Coûteaux, M.M., Vallejo, V.R., 2008. Changes in litter properties during decomposition: a study by differential thermogravimetry and scanning calorimetry. Soil Biol. Biochem. 40, 172-185. https://doi.org/10.1016/j.soilbio.2007.07.021.

Sarker, T.C., Incerti, G., Spaccini, R., Piccolo, A., Mazzoleni, S., Bonanomi, G., 2018. Linking organic matter chemistry with soil aggregate stability: insight from ^{13}C NMR spectroscopy. Soil Biol. Biochem. 117, 175-184. https://doi.org/10.1016/j.soilbio.2017.11.011.

Simpson, A.J., McNally, D.J., Simpson, M.J., 2011. NMR spectroscopy in environmental research: from molecular interactions to global processes. Prog. Nucl. Magn. Reson. Spectrosc. 3, 97-175. https://doi.org/10.1016/j.pnmrs.2010.09.001.

Six, J., Bossuyt, H., Degryze, S., Denef, K., 2004. A history of research on the link between (micro) aggregates, soil biota, and soil organic matter dynamics. Soil Tillage Res. 79, 7-31. https://doi.org/10.1016/j.still.2004.03.008.

Šmejkalová, D., Spaccini, R., Piccolo, A., 2008. Multivariate analysis of CPMAS ^{13}C-NMR spectra of soils and humic matter as a tool to evaluate organic carbon quality in natural systems. Eur. J. Soil Sci. 59, 496-504. https://doi.org/10.1111/j.1365-2389.2007.01005.x.

Soil Classification Working Group, 1998. The Canadian System of Soil Classification. NRC Research Press, Ottawa, Canada, 187 pp.

Sollins, P., Homann, P., Caldwell, B.A., 1996. Stabilization and destabilization of soil organic matter: mechanisms and controls. Geoderma, 74, 65-105. https://doi.org/10.1016/S0016-7061(96)00036-5.

Soucémarianadin, L.N., Cécillon, L., Guenet, B., Chenu, C., Baudin, F., Nicolas, M., Girardin, C., Barré, P., 2018. Environmental factors controlling soil organic carbon stability in French forest soils. Plant Soil 426, 267-286. https://doi.org/10.1007/s11104-018-3613-x.

Soucémarianadin, L.N., Quideau, S.A., MacKenzie, M.D., Bernard, G.M., Wasylishen, R.E., 2013. Laboratory charring conditions affect black carbon properties: a case study from Quebec black spruce forests. Org. Geochem. 62, 46-55. https://doi.org/10.1016/j.orggeochem.2013.07.005.

Stone, M.M., Plante, A.F., 2015. Relating the biological stability of soil organic matter to energy availability in deep tropical soil profiles. Soil Biol. Biochem. 89, 162-171. https://doi.org/10.1016/j.soilbio.2015.07.008.

Sun, S.H., Liu, J.J., Li, Y.F., Jiang, P.K., Chang, S.X., 2013. Similar quality and quantity of dissolved organic carbon under different land use systems in two Canadian and Chinese soils. J. Soils Sediments. 13, 34-42. https://doi.org/10.1007/s11368-012-0604-z.

von Lützow, M., Kögel-Knabner, I., Ekschmitt, K., Flessa, H., Guggenberger, G., Matzner, E., Marschner, B., 2007. SOM fractionation methods: relevance to

functional pools and to stabilization mechanisms. Soil Biol. Biochem. 39, 2183-2207. https://doi.org/10.1016/j.soilbio.2007.03.007.

Williams, E.K., Fogel, M.L., Berhe, A.A., Plante, A.F., 2018. Distinct bioenergetic signatures in particulate versus mineral-associated soil organic matter. Geoderma 330, 107-116. https://doi.org/10.1016/j.geoderma.2018.05.024.

Williams, E.K. and Plante, A.F. 2018. A bioenergetic framework for assessing soil organic matter persistence. Front. Earth Sci. 6: 143. https://doi.org/10.3389/feart.2018.00143.

Xia, S.P., Song, Z.L., Wang, Y.D., Wang, W.Q., Fu, X.L., Singh, B.P., Kuzyakov, Y., Wang, H.L., 2021. Soil organic matter turnover depending on land use change: Coupling C/N ratios, $\delta^{13}C$, and lignin biomarkers. Land Degrad. Dev. 32, 1591-1605. https://doi.org/10.1002/ldr.3720.

Xu, H.W, Qu, Q., Wang, M.G. Li, P., Li, Y.Z., Xue, S., Liu, G.B., 2020. Soil organic carbon sequestration and its stability after vegetation restoration in the Loess Hilly Region, China. Land Degrad. Dev. 31, 568-580. https://doi.org/10.1002/ldr.3472.

Zhang, K., Dang, H., Tan, S., Cheng, X., Zhang, Q., 2010. Change in soil organic carbon following the 'Grain-for-Green' programme in China. Land Degrad. Dev. 21, 13–23. https://doi.org/10.1002/ldr.954.

Zhuang, S.Y., Sun, X., Liu, G.Q., Wong, M.H., Cao, Z.H., 2011. Carbon sequestration in bamboo plantation soil with heavy winter organic mulching management. Bot. Rev. 77(3), 252. https://doi.org/10.1007/s12229-011-9081-0.

Chapter 3. Biological but not thermal stability of soil organic carbon differs between two agroforestry systems and their component land-uses in western Canada

1. Introduction

The soil has the largest organic carbon (C) pool in terrestrial ecosystems, with approximately 1550 Gigaton of soil organic C (SOC) stored in the top meter of soil, which is twice the amount stored in the atmosphere (Lal, 2004). Therefore, a small change in the SOC pool can significantly influence the carbon dioxide (CO_2) concentration in the atmosphere and the associated global climate (Lal, 2003; Jia et al., 2017). Soil C stocks are mainly controlled by C inputs from plant production and outputs through C mineralization (Jobbágy and Jackson, 2000). Agricultural practices such as cultivation, land-use change, and other forms of disturbance can cause a significant loss in SOC (Lal, 2004; 2007); for example, cultivation can reduce SOC content by 30 to 50% (Ogle et al., 2005). Because SOC is vital for soil system functioning, increasing it should help to improve soil productivity and mitigate climate change. Therefore, best management practices are urgently needed to increase SOC and its stability to reduce decomposition in agricultural land and improve sustainable land management.

Agroforestry systems are recognized as a climate-smart land management practice that can enhance SOC sequestration (Paustian et al., 2016). The introduction of perennial plants (trees and shrubs) into crop and animal farming practices show significant potential for C sequestration, climate change mitigation, and biodiversity enhancement relative to monocultural cropping systems (Nair et al., 2009; Jose and Bardhan, 2012;

Abbas et al., 2017). In Canada, about 5% of agricultural land is managed in some form of agroforestry systems (Thevathasan and Gordon, 2004), which store a substantial amount of C. However, C sequestration in agroforestry systems is a long process, especially in temperate ecosystems (Ma et al., 2020), so the stability of the sequestrated C should also be evaluated (Xu et al., 2020).

Extensive studies have been conducted to understand C sequestration in agroforestry systems (Lim et al., 2018), but limited studies have used different approaches to address SOC stability under different agroforestry systems, and more studies are needed to explore SOC stability using multiple approaches. For example, Baah-Acheamfour et al. (2014) studied SOC stability of three agroforestry systems using a physical fractionation approach that quantifies the C content in soil particle size fractions (silt, clay, and sand); An et al. (2021) explored SOC structural and thermal stability in a hedgerow system and found that the forest land-use had lower SOC structural and thermal stability than the cropland despite having greater SOC stock. Understanding the stability of C stored in different agroforestry systems and component land-uses is crucial because such studies will enhance our knowledge of the role of agroforestry systems in climate change mitigation. However, such knowledge is scarce, which is hindering our understanding of SOC stability in agroforestry systems.

The stability of SOC, viewed as the measure of the resistance and accessibility of organic molecules to microbial decomposition (Schädel et al., 2020), is an essential ecosystem property in maintaining SOC stock (Xu et al., 2020). The stability of SOC affects the extent to which SOC can persist for the long term in soils, and this stability can be characterized using various biological, chemical and physical methods (Baah-

Acheamfour et al., 2014; Plante et al., 2011; Stone and Plante, 2015; An et al., 2021). Soil respiration can act as an indicator of SOC biological stability; soil respiration reflects the breakdown of SOC by microbes. A higher soil respiration rate and the resulting C loss suggest lower biological stability (Stone and Plante, 2015). Because of such relationships between soil respiration and SOC quality and stability, measuring soil respiration through lab incubations could be the first approach in studying SOC stability. Thermal analysis is an integrated physicochemical method to study SOC stability. This method quantifies the energy required to break the bonds within and between SOC and soil minerals and provides information on the energy status of SOC as related to its persistence in the soil (Plante et al., 2011; Barré et al., 2016; Williams and Plante, 2018). Combing thermal and biological stability information will give us more insight into SOC stability.

Our previous study investigated SOC stability only for a hedgerow system in western Canada (An et al., 2021). Expanding the knowledge of SOC stability in other agroforestry systems will enhance our understanding of the role of different agroforestry systems on C sequestration. Therefore, it is crucial to understand SOC stability in other common agroforestry systems, such as planted shelterbelts, in western Canada. We used laboratory incubation and thermal analysis approaches to evaluate the influence of planted shelterbelts and natural hedgerows and their component land-use types (forest and cropland) on the biological and thermal stabilities of organic C in the surface soil (0-10 cm). We hypothesized that the shelterbelt system would have lower thermal and biological stabilities than the hedgerow system due to the less diverse tree species composition in the former than in the latter (Ma et al., 2020), and forest soils would have lower biological stabilities than the cropland due to the higher SOC quality in the forest

(An et al., 2021). This study will extend our understating of SOC stability in different agroforestry systems and their component land-uses.

2. Materials and methods

2.1 Study area and sampling design

The study area was located in the central parkland area of Alberta, Canada (Fig. 3-1). Based on climate data collected between 1981 and 2010 from 26 Environment Canada weather stations that were close to the study sites, the mean annual air temperatures in the north and south of the study area were 1.9 and 2.4 ºC, respectively, and the mean annual precipitation varied from 463 mm in the north to 448 mm in the south (Environment Canada, 2021). The study area encompasses three soil zones: Dark Gray Chernozemic and Gray Luvisolic soils were predominant in the north, while Black Chernozemic soils were dominant in the south (Fig. 1, Soil Classification Working Group, 1998). The physical and chemical properties of the soil in the 0-10 cm depth at the cropland and forested areas of the hedgerow and shelterbelt systems are presented in Appendix 3-1.

A detailed description of the study sites and the experimental design used in this study can be found in Baah-Acheamfour et al. (2014), Baah-Acheamfour et al. (2015) and Banerjee et al. (2016). In both systems, strips of vegetation (3-6 m wide) consisting of naturally regenerated or planted trees, shrubs, and grasses were managed around the edges of annual croplands. The hedgerow forests consisted of broadleaf deciduous tree-dominated stands. The dominant trees were balsam poplar (*Populus balsamifera*),

chokecherry (*Prunus virginiana*), saskatoon serviceberry (*Amelanchier alnifolia*), and trembling aspen (*Populus tremuloides*). The shelterbelt forests, which were planted, consisted of both deciduous and coniferous trees, were dominated by white spruce (*Picea glauca*), caragana (*Caragana arborescens*), box elder (*Acer negundo*) and willow (*Salix acutifolia*). Most of the shelterbelt forests had only one tree species, while a few had two tree species (Baah-Acheamfour et al., 2014). The average tree age and density of the trees were 28.1±1.4 yr and 7776±1425 ha^{-1} in the forested area in hedgerow; and 34.1±1.8 yr and 6323±1858 ha^{-1} in the forested area in shelterbelt (Lim et al., 2018). In both systems, the areas between rows of trees were used for annual crop production. Most landowners used minimum tillage and applied fertilizers (N ~120 kg ha^{-1} annually) in the cropland, with barley (*Hordeum vulgare*), canola (*Brassica napus*), corn (*Zea mays*), wheat (*Triticum aestivum*), soybean (*Glycine max*), and pea (*Pisum sativum*) grown in rotations.

The study was conducted using a split-plot design, where the agroforestry system (hedgerow and shelterbelt) was the whole-plot factor, and the paired land-use (forest and cropland) was the split-plot factor. Twenty-four agroforestry sites (12 hedgerow systems and 12 shelterbelt systems) were randomly selected in central Alberta, Canada (Fig. 3-1). A 30-50 m transect was then established in the center of each forested strip, while the transect in cropland was located no less than 30 m from the tree line to reduce the tree influence on the adjacent cropland. We revisited all the sites and recollected soil samples in 2018 for SOC biological and thermal stability assessment. In each sampling site, ten soil samples were collected from the 0-10 cm soil layer at regular intervals along each transect using an auger (3.2 cm diameter, 10 cm deep), then combined to make a composite sample. Each field moist sample was then sieved through a 2 mm mesh to

remove plant debris and visible roots. An aliquot of the sieved sample was air-dried and stored at room temperature (~ 25 °C), and the rest of the soil samples were stored at 4 °C for lab incubation.

2.2 Laboratory incubation to determine SOC biological stability

Soil water holding capacity was determined following the method using in Baah-Acheamfour et al. (2014). Twenty-gram oven-dried soil (48 h at 105 °C) was placed in a funnel and saturated in distilled water, then wrapped with polyvinyl chloride film to maintain moisture and placed vertically on top of a container to drip freely for 24 h, then reweighed. To determine the biological stability of SOC, six grams (dry weight equivalent, < 2 mm) of each soil sample was weighed into a 50-mL polyethylene centrifuge tube and incubated at 20 °C for 61-day in the dark in an incubator (Model 815, Precision, Winchester, VA) at 55% soil water holding capacity. All samples were pre-incubated for 24 h in the incubator under dark conditions. Emissions of CO_2 of the tubes were then measured every day for the first five days and every five days for the rest of the incubation with a 5 mL syringe; after each measurement, zero-air (CO_2-free) was used for flushing the tubes to reset the air within the tubes, and lids remained open before each measurement.

To measure CO_2 concentration on the designated day, the tubes were firstly flushed with zero-air for 3 minutes, capped, and the CO_2 concentration in the headspace was allowed to equilibrate for 1-2 minutes, then 2 mL baseline CO_2 (t = 0 h) was collected, and then 2 mL of gas sample was collected from each tube after 24 h. All gas samples

were analyzed using an LI-7000 CO_2/H_2O gas analyzer (LI-COR Biosciences, Lincoln, NE). The CO_2 concentration was determined as the difference of CO_2 concentration between the t = 0h and t = 24h and expressed as μg C g^{-1} soil. Basal soil respiration rate was determined following the method in Stone and Plante (2015) by averaging the gas flux of the last four times (last twenty days) in the incubation. Both basal respiration rate and cumulative CO_2 evolution were also normalized by soil C (μg mg^{-1} soil C day^{-1}) as indices of SOC decomposability, and by microbial biomass C (μg μg^{-1} MBC day^{-1}) as indices of specific metabolic activity. The proportion of C respired, which was determined by dividing the amount of C respired in the incubation by the total C, was used to assess the loss of C in the incubation (Trasar-Cepeda et al., 2008; Stone and Plante, 2015).

2.3 The thermal stability of SOC

To determine the SOC's thermal stability, thermal analysis was performed using a Netzsch STA 409PC Luxx (Netzsch-Gerätebau GmbH, Selb, Germany) coupled to an LI-840 CO_2/H_2O infrared gas analyzer (IRGA) (LI-COR, Inc., Lincoln, NE) as detailed in Plante et al. (2011), Stone and Plante (2015) and Williams and Plante (2018). Briefly, air-dried samples (approximate 1 mg C in each sample and sample mass should be less than 50 mg) were placed in a Pt/Rh crucible (with an identical and empty crucible used as the reference) and heated under an oxidizing condition (with a flow rate of 40 mL min^{-1} of synthetic CO_2-free air, which was made up of 20 mL min^{-1} oxygen and 20 mL min^{-1} nitrogen gas. The samples were heated up room temperature (25 °C) to 105 °C at a rate of

10 °C min^{-1} and maintained at 105 °C for 15 min to remove moisture. The samples were then heated up to 900 °C at a rate of 10 °C min^{-1}. Thermogravimetric (TG) mass loss, CO_2 evolved, and differential scanning calorimetry (DSC) heat-flux data were recorded every second for each sample, and the baselines of CO_2 and DSC thermograms were corrected a posteriori using a spline and linear baseline in the smooth.spline() function (Williams and Plante, 2018) in the R software (R Core Team, 2018).

The DSC heat flux (mW) was integrated over the exothermic region of 125 to 650 °C, corresponding to the temperature range that soil organic matter is oxidized (Rovira et al., 2008). The TG mass loss was calculated for the same temperature range. This mass loss is mainly due to the combustion of soil organic matter, with small contributions from the dehydration of minerals (e.g., kaolinite) (Stone and Plante, 2015; Williams and Plante, 2018). The energy density (J mg^{-1} C) of SOC was calculated by dividing the exothermic energy yield during the oxidation by TG mass loss, and the activation energy (kJ mol^{-1} CO_2) was calculated following the methods described in Williams et al. (2014) and Williams and Plante (2018). Four other thermal stability indices (TG-T_{50}, the temperature at which 50% of the exothermic mass was lost; DSC-T_{50}, the temperature at which 50% of the exothermic energy was released; CO_2-T_{50}, the temperature at which 50% of the CO_2 was produced; and ROI, return on energy investment, which is the ratio of energy density to activation energy) were also calculated to study SOC thermal stability (Plante et al., 2011; Stone and Plante, 2015; Harvey et al., 2016; Williams and Plante, 2018). Generally, SOC with greater thermal stability is associated with a greater TG-T_{50} and a lower energy density, DSC-T_{50}, CO_2-T_{50} and ROI (Plante et al., 2011; Peltre et al., 2013; Stone and Plante, 2015; Harvey et al., 2016;

Williams and Plante, 2018).

2.4 Statistical analyses

All statistical analyses were performed using R (R Core Team, 2018). All data were first checked for normality of distribution and homoscedasticity using the Shapiro-Wilk test and Levene's test, respectively. To meet the normality and homoscedasticity assumptions, basal respiration rate, cumulative respiration rate, soil energy density, activation energy, microbial biomass carbon (MBC) and nitrogen (MBN) were log-transformed prior to statistical analysis. Untransformed data are presented in figures and tables for ease of interpretation. We performed a two-way analysis of variance (ANOVA) using linear mixed-effect models in the *agricolae* package (De Mendiburu, 2019) to determine the effects of agroforestry systems, land-uses and their interactions on the biological and thermal stabilities of SOC. Agroforestry systems and land-uses were treated as fixed factors, and field replication was treated as a random factor within agroforestry systems and land-uses. Mean separation was conducted via Tukey's Honest Significant Difference. Parameters with significant interactions between agroforestry systems and land-uses were tested using least-squares means in the *lsmeans* package (Lenth, 2016). Standard error of the mean, which estimates the precision of the mean from the population mean, is determined as the result of standard deviation divided by the square root of the sample size (Nagele, 2003). Pearson correlation analysis was used to examine relationships between variables. Principal component analysis (PCA) was used to study the relationships among SOC biological stability, thermal stability, and basic soil

properties such as soil bulk density, pH, MBC and MBN.

Given that the study area covered a vast area (270 km from north to south and 150 km from east to west) and had a large variation in vegetation compositions and soil properties, a *p* value of 0.10 was used in this study to evaluate the significance to reduce the type II error (Baah-Acheamfour et al., 2014).

3. Results

3.1 Effects of agroforestry system and land-use on SOC biological stability

Daily soil respiration rate rapidly declined over the first five days of incubation, then the rate of decline slowed until the end of the incubation regardless of the agroforestry system and land-use (Fig. 3-2a-b). Basal soil respiration [both $\mu g\ g^{-1}$ soil day^{-1} and $\mu g\ \mu g$ MBC day^{-1}] was affected by an interaction between the agroforestry system and land-use. Cropland in the hedgerow system had the lowest basal soil respiration ($\mu g\ g^{-1}$ soil day^{-1}), and there was no difference among the basal soil respiration for cropland in the shelterbelt system and forest in both hedgerow and shelterbelt systems (Fig. 3-3a). Basal soil respiration normalized to MBC was the lowest in the forested land-use in the hedgerow system, but no difference between cropland in the hedgerow system, and between the two land-uses in the shelterbelt system (Fig. 3-3b).

Cumulative respiration ($\mu g\ C\ g^{-1}$ soil) was affected by agroforestry systems and land-uses, and the cumulative respiration normalized to soil MBC was interactively affected by agroforestry system and land-use (Table 3-1). Cumulative respiration (μg C

μg^{-1} MBC) was lowest for the forest in the hedgerow system and was similar to cropland in the hedgerow system and both land-uses in the shelterbelt system (Fig. 3-3c).

Basal soil respiration rate and cumulative respiration were neither affected by agroforestry systems nor by land-use when normalized to SOC. The proportion of C respired was affected by agroforestry system and land-use, with the shelterbelt system had 14.9% more C loss than the hedgerow system, and forest having 57.1% more C loss than the cropland (Table 3-1).

3.2 Effects of agroforestry system and land-use on SOC thermal stability

The thermograms were similar across all treatments, except for the difference in the height of the minor peak at 513 °C (Fig. 3-4). The soil organic matter was combusted between 225 and 600 °C, with a dominant peak at 325 °C, followed by a shoulder between 420 and 430 °C, and a minor peak between 510 and 520 °C. The TG-T_{50}, energy density, CO_2-T_{50}, DSC-T_{50} and ROI were interactively affected by the agroforestry system and land-use (Table 3-2). The cropland in the hedgerow system had the lowest CO_2-T_{50} and DSC-T_{50} (Fig. 3-5a-b), the highest TG-T_{50} was found in hedgerow cropland and hedgerow forest had the lowest TG-T_{50} (Fig. 3-5c). The energy density of SOC was the lowest for cropland in the shelterbelt system, and similar between cropland in the hedgerow system and forest in the shelterbelt system (Fig. 3-5d). The ROI was lowest for forest and highest for cropland in the shelterbelt system, but similar between the two land-uses in the hedgerow system (Fig. 3-5e). All agroforestry systems and land-uses had similar activation energy (Table 3-2).

3.3 Relationships among basic soil properties, SOC thermal and biological stabilities

The first five principal components (PC) accounted for 87.1% of the variance in the C stability profiles, of which PC1 and PC2 explained 31 and 21.1%, respectively, of the variance (Fig. 3-6). Variables MBC, total C, MBN and total nitrogen (N) contributed the most to PCA1, while SOC biological stability indices (proportion of C respired and basal soil respiration rate), soil sand content and pH contributed the most to PCA2 (Appendix 3-2). A considerable overlap occurred between the hedgerow and shelterbelt soils of the total variability in C composition within the SOC profile. Cropland SOC in the hedgerow differed the most from all other treatments, particularly the forest soils in hedgerow and cropland soils in shelterbelt (Fig. 3-6).

Pearson correlation analysis revealed that basal soil respiration was correlated with the proportion of C respired, SOC, DOC, MBC and clay content positively, while correlated with sand content, soil bulk density and TG-T_{50} negatively. The proportion of SOC respired was uncorrelated with the SOC, sand content, clay content, but negatively correlated with pH and ROI compared with basal soil respiration; the SOC content was positively correlated with pH, DOC, MBC, CO_2-T_{50}, DSC-T_{50} and ROI, while being negatively correlated with soil bulk density; pH was correlated with MBC and TG-T_{50} positively, while correlated with silt content negatively; the DOC was positively correlated with DON while both DOC and MBC were correlated with soil bulk density negatively. The sand content was positively while the silt content was negatively correlated with ROI; CO_2-T_{50} was strongly positively correlated with DSC-T_{50} (Appendix 3-3).

4. Discussion

This study examined the biological and thermal stability of SOC of forests and their adjacent croplands in hedgerow and shelterbelt systems and showed that the thermal stability of SOC in these systems depends on land-use types. The study also showed that SOC loss through respiration was more significant in the shelterbelt and forest as compared to the hedgerow and croplands, respectively, indicating that the hedgerow system is favorable in terms of C sequestration through enhancing SOC stability in the agroforestry system.

4.1 Biological stability of SOC in agroforestry systems and their component land-uses

The greater cumulative respiration and SOC loss in the shelterbelt system than the hedgerow system during the lab incubation (Table 3-1) indicate that the biological stability of SOC was lower in the shelterbelt than in the hedgerow system, suggesting that SOC in shelterbelt may contain more available C for decomposition. The C source used for soil respiration was dominated by the more bioavailable SOC and is mainly composed of microbially-derived C and fresh plant material, which was weakly protected by soil physical and chemical mechanisms (Angst et al., 2019). Thus, soil respiration and the proportion of C respired by microorganisms in the incubation provide a quantitative estimation of the labile C pool (Stone and Plante, 2015). Our supplementary data showed that MBC, MBN, DOC and DON were higher in the shelterbelt than in the hedgerow system (Appendix 3-1). The difference in biological stability may be due to the difference

in SOC input from plant sources, as tree species, tree species diversity and tree age may be important factors controlling SOC storage (Ma et al., 2020).

Tree species may affect the composition and thus the stability of SOC. The stability of SOC varied substantially among tree species, and this variability was independent of the amount of organic C in soils and tree species regulate SOC stability via the composition of their tissues, especially roots (Angst et al., 2019). A SOC composition with more recalcitrant C (higher hydrophobic C/hydrophilic C ratios, aromatic C/O-alkyl C and alkyl C/O-alkyl C) under birch than under pine and larch birch, suggesting that tree species selection should be considered as a potential approach for influencing the stability of SOC in addition to SOC concentration (Liang et al., 2021). Fissore et al. (2008) also found that SOC quality was higher in coniferous than in hardwood forests, suggesting that conifers may not be a better option for increasing stable C as compared with hardwood forests.

The shelterbelt system in this study consisted of planted trees that had only one or two tree species (either coniferous or broad-leafed trees, e.g., white spruce, trembling aspen, box elder and poplar) with a regular spacing, while the hedgerow system was dependent on tree regeneration and consisted of trees with mixed species (mostly broad-leafed trees), shrubs, and grasses in the lower strata of the vegetation, which in turn had higher species richness, evenness, and Shannon diversity than the forested land-use in the shelterbelt system [(supplementary data in Kwak et al. (2019)], and thus, the hedgerow system should have more diverse litter inputs and faster nutrient cycling than the shelterbelt system (Borden et al., 2020). Meanwhile, tree species diversity may increase the amount of root exudates and root biomass (Eisenhauer et al., 2017). Therefore, tree

species diversity may significantly affect soil CO_2 emission and SOC storage (Wang et al., 2016), for example, Wang et al. (2013) found that establishing a mixture of *Citrus hystrix* and *Pinus massoniana*, could be a better approach for SOC sequestration than planting monoculture *Citrus hystrix* plantation. Tree species diversity can also influence the bacterial community composition and soil C cycling. Monoculture plantations enhance the development of r-strategy bacteria, which would increase net C mineralization. In contrast, mixed tree species plantations can reduce SOC mineralization accompanied by decreased r- strategy bacteria (Zhang et al., 2018), which explains the higher cumulative respiration in the shelterbelt system than the hedgerow system in the current study, suggesting that higher tree species diversity may increase SOC storage, while the role of tree species identity effects on SOC stocks has not been studied and needs research in the future (Vesterdal et al., 2013). Moreover, monoculture cropland has lower abundances of soil bacteria and fungi compared with agroforestry systems due to the former having a rate of lower litter input (both above- and belowground) and a slower nutrient cycling (Beule et al., 2019), and thus a lower soil fertility. The SOC concentration and pools increased with tree age from 1- to 6-year agroforestry systems, and the increase was higher in soils with a loamy sand than those with a sandy clay texture, while soil type did not influence the SOC concentration and total SOC pool size (Gupta et al., 2009). The SOC stock accumulation rate in very old agroforestry systems may decrease due to the soil reaching a SOC stock equilibrium (Kim et al., 2016). However, the magnitude and direction of changes in SOC vary with soil property and the climate (Li et al., 2019). Future work should explore the influence of soil condition and tree characteristics on SOC stability in agroforestry systems.

The higher cumulative respiration and proportion of C respired in the forested land-use than in the cropland may have arisen from the fact that forest soils have higher labile C that is more easily decomposed than cropland soils (An et al., 2021), which is also consistent with Baah-Acheamfour et al. (2016), who reported that forest land-use had higher CO_2 emissions than the cropland. However, our biological stability result contradicts findings in Baah-Acheamfour et al. (2016) and Baah-Acheamfour et al. (2020), as they found that less CO_2 was emitted from the shelterbelt than from the hedgerow system and CO_2 emissions were more influenced by soil temperature than water content, and soil CO_2 emissions increased with soil temperature, based on field measurements conducted in the same study sites. The contradiction may be attributed to the different conditions between field and laboratory incubation studies. Laboratory incubation studies assess the physiological mechanisms of CO_2 yield and are better controlled than field studies (Zibilske, 1994) and offered more favourable conditions (e.g., moisture, temperature and aeration) to soil microbes in the current study, enhancing the SOC mineralization, meanwhile, aggregation abruption of soils during the incubation pretreatment may increase the availability of occluded C for decomposition, making a greater amount of C to be released in the lab incubation than in the field study (Salome et al., 2010).

4.2 Thermal stability of SOC in different agroforestry systems and land-uses

The thermal stability of SOC can be assessed by Ea, Ed and TG-T_{50} (Williams et al., 2018; An et al., 2021). The interaction effects of agroforestry system by land-use on the

thermal indices (except Ea) of SOC, with Ed and TG-T_{50} also influenced by land-use, suggest that biological and environmental conditions (such as vegetation, moisture and temperature) may have strong control on SOC stability (Williams and Plante, 2018). The shelterbelt and hedgerow systems differed from each other at soil properties, management practices and plant compositions (Baah-Acheamfour et al., 2014), which may influence SOC stability. For example, cultivation with different crop species may affect the SOC stability in croplands in agroforestry systems. Miao et al. (2012) found that continuous cultivation of soybean reduced SOC energy density, while cultivation of maize increased SOC stability, and soybean cultivation had higher SOC energy density than maize cultivation. In this study, different crop rotations were used at different agroforestry sites, which may cause the variation of SOC stability among sites. However, few have studied the effect of different crop rotations on SOC stability, and future work should address this knowledge gap. In addition, research on the impact of agroforestry practices on SOC stability should be expanded to other agroforestry systems to improve our knowledge of the role of agroforestry systems on C sequestration, especially for their importance in long-term C storage.

5. Conclusions

Our study expanded the understanding of the effect of agroforestry systems and their component land-uses on SOC biological and thermal stabilities. The hedgerow system had higher biological stability than the shelterbelt system, while interactions between agroforestry systems and land-uses affected the thermal stability of SOC. Incorporating

trees in agricultural land to form agroforestry systems changes SOC biological and thermal stabilities. Maintaining the hedgerow system and expanding agroforestry systems may enhance C stability, promote C sequestration, and mitigate climate change. Future work should investigate the effect of tree characteristics (i.e., tree age, species richness or identity) and other types of agroforestry systems on SOC stabilities.

Table 3-1. Soil organic carbon (SOC) biological stability indices (mean ± standard error, n=12) as affected by agroforestry system, land-use, and the interaction effects of agroforestry system and land-use in central Alberta, Canada.

Description	Basal respiration			Cumulative respiration			The proportion of SOC respired
	μg g^{-1} soil day^{-1}	μg mg^{-1} soil C_{org} day^{-1}	μg $μg^{-1}$ MBC day^{-1}	μg C g^{-1} soil	μg C mg^{-1} soil C_{org}	μg C $μg^{-1}$ MBC	%
Agroforestry system (AF)							
Hedgerow	9.33±1.00	0.20±0.02	0.02±0.01	692.36±68.78	15.09±1.39	1.47±0.16	0.67±0.07
Shelterbelt	11.35±0.89	0.24±0.02	0.03±0.01	806.05±67.00	17.20±1.57	2.05±0.22	0.77±0.07
Land-use (LU)							
Cropland	7.89±0.49	0.20±0.01	0.03±0.01	570.66±31.27	14.29±0.99	1.93±0.20	0.56±0.03
Forest	12.79±1.06	0.25±0.02	0.02±0.01	927.75±76.51	17.99±1.79	1.59±0.20	0.88±0.03

ANOVA

Source of variation							
AF	**0.03**	0.17	**0.05**	**0.08**	0.31	**0.09**	**0.09**
LU	**<0.01**	0.10	**0.09**	**<0.01**	0.12	0.11	**<0.01**
AF×LU	**0.06**	0.63	**0.07**	0.12	0.37	**0.06**	0.20

Note: P values < 0.1 are highlighted in bold.

Table 3-2. Soil organic carbon (SOC) thermal stability indices (mean ± standard error, n=12) as affected by agroforestry system, land-use, and the interaction effects of agroforestry system and land-use in central Alberta, Canada.

Description	CO_2-T_{50}	DSC-T_{50}	TG-T_{50}	Ea	Ed	ROI
	°C	°C	°C	kJ mol^{-1} CO_2	J mg^{-1} C	
Agroforestry system (AF)						
Hedgerow	378.0±1.3	359.1±1.5	363.0±1.2	69.86±0.80	14.43±0.60	0.22±0.01
Shelterbelt	381.4±1.7	360.2±1.7	362.0±0.9	70.59±1.00	13.58±0.66	0.21±0.01
Land-use (LU)						
Cropland	378.9±1.5	359.8±1.5	363.8±1.0	69.74±0.85	12.86±0.64	0.22±0.01
Forest	380.5±1.7	359.5±1.7	361.1±1.0	70.71±0.95	15.14±0.54	0.21±0.01
ANOVA						
Source of variation						
AF	0.24	0.7	0.54	0.61	0.3	0.55
LU	0.19	0.8	**0.01**	0.47	**0.01**	0.12
AF×LU	**0.07**	**<0.01**	**<0.01**	0.48	**0.02**	**<0.01**

Note: *P* values < 0.1 are highlighted in bold. Ea, activation energy; Ed, energy density; TG-T_{50}, the temperature that 50% of the exothermic mass is lost; DSC-T_{50}, the temperature that 50% of the exothermic energy is released; CO_2-T_{50}, the temperature that 50% of the CO_2 is produced; ROI, return on energy investment.

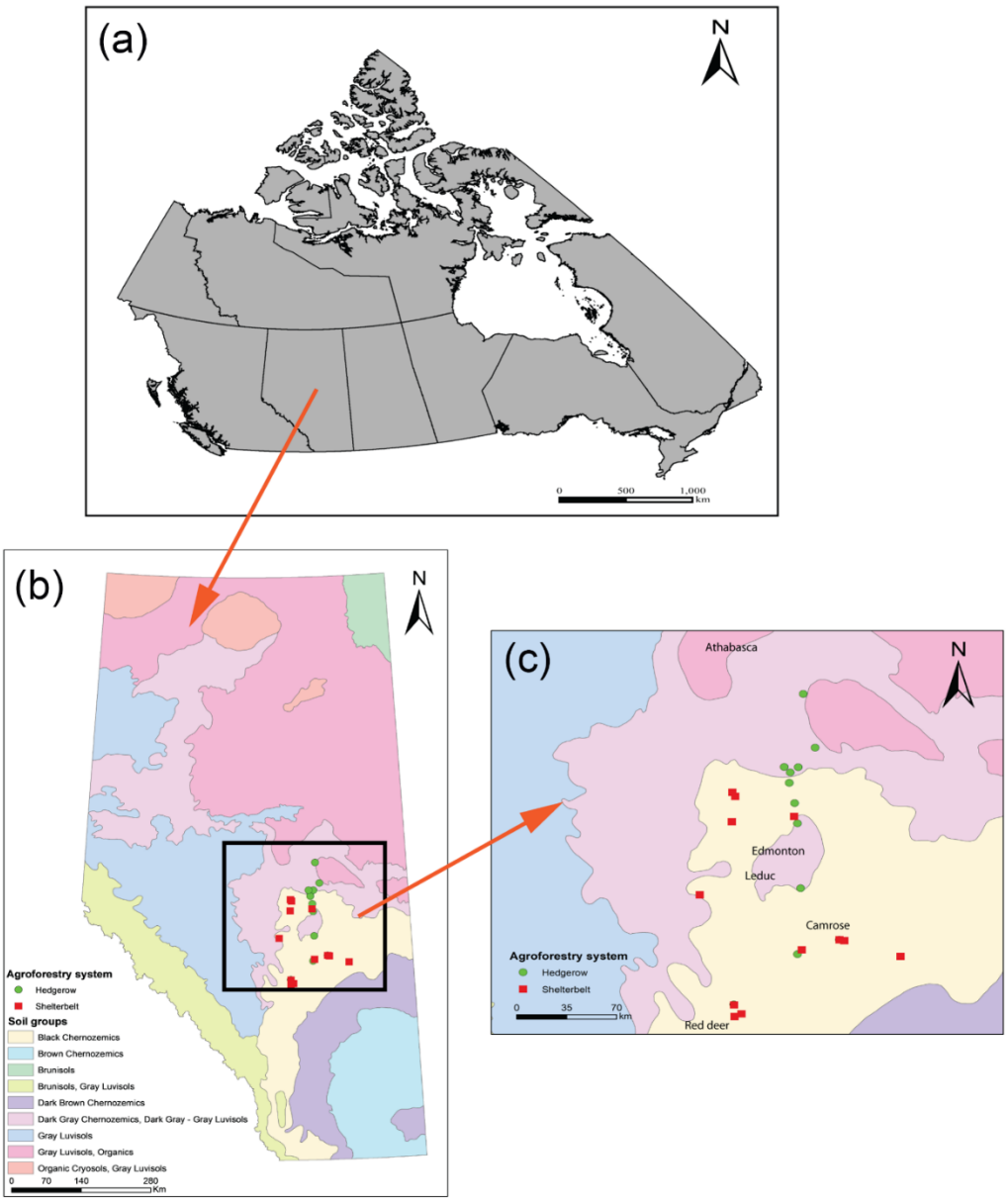

Fig 3-1. Maps of (a) Canada, (b) the province of Alberta showing the soil group information and locations of the study sites, and (c) the central Alberta region showing the soil group information and locations of the study sites. The triangles and circles represent hedgerow and shelterbelt sites, respectively.

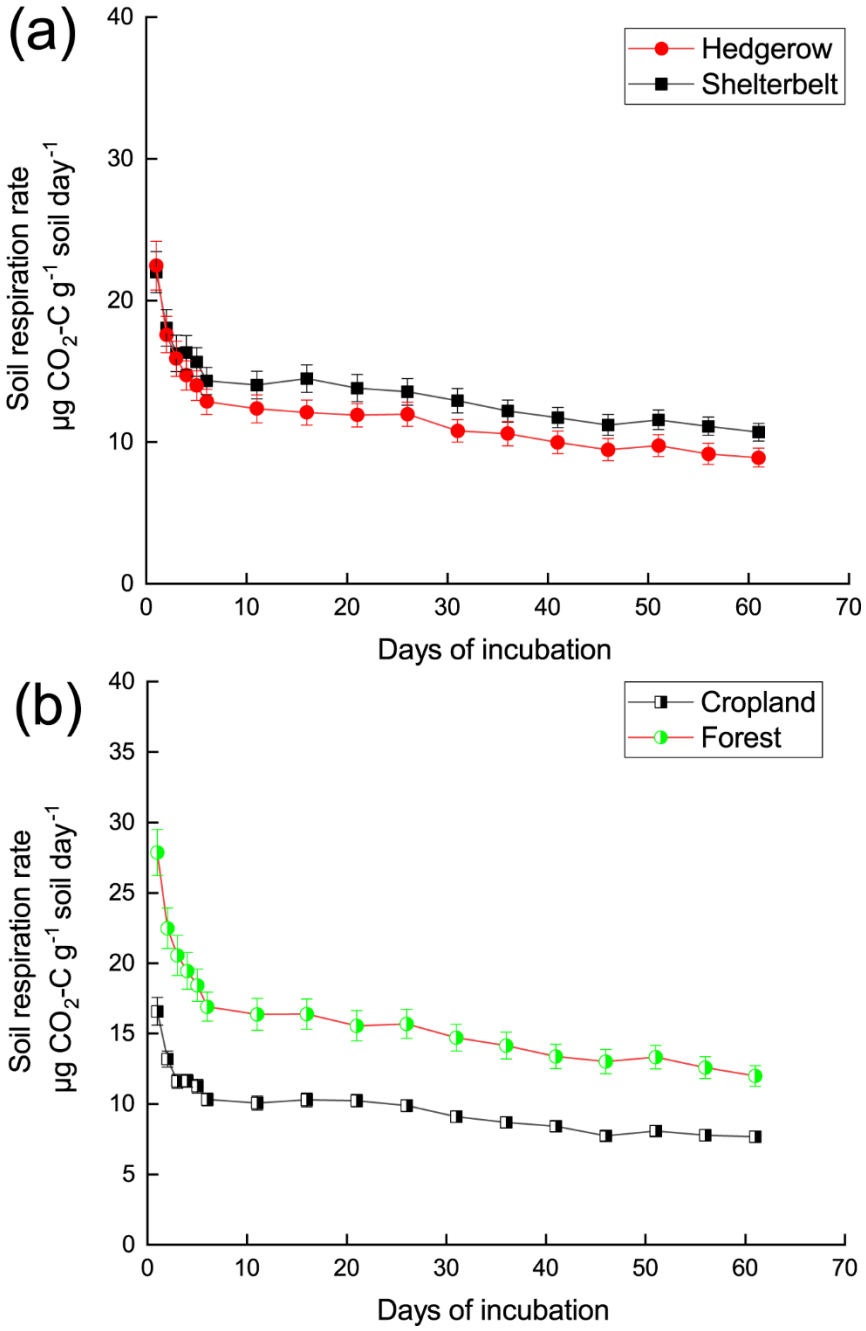

Fig 3-2. Soil respiration rate (mean ± standard error) as affected by (a) agroforestry systems and (b) land-uses.

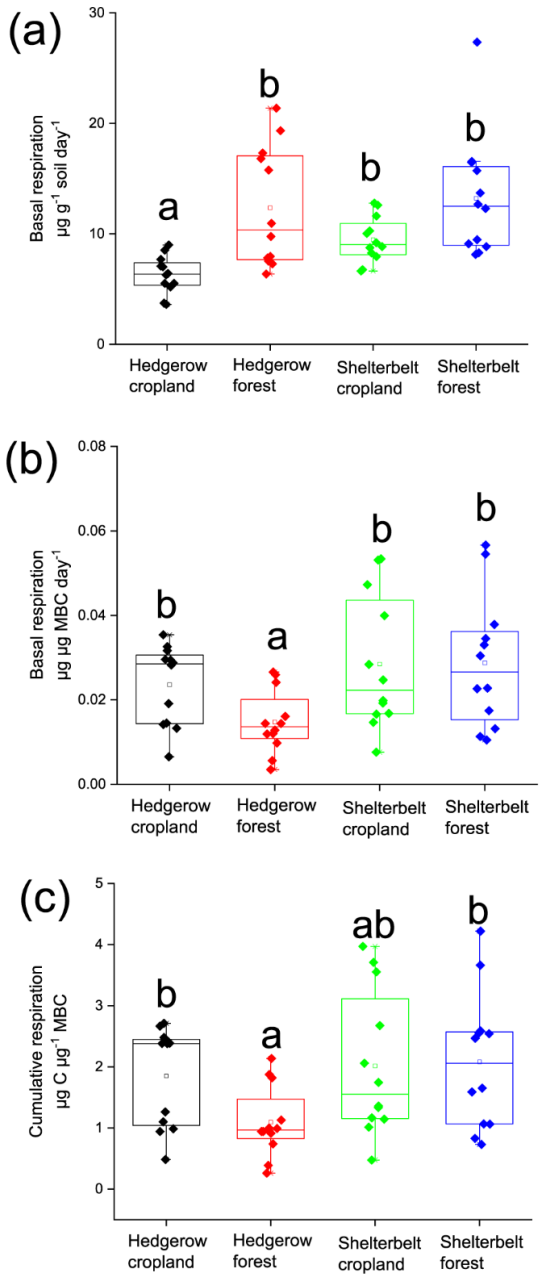

Fig 3-3. The interaction effects of agroforestry system by land-use on basal soil respiration and cumulative respiration. Data points are mean (± standard error, n=12, the hollow point and the middle line in each boxplot represent mean and median, respectively). Different lowercase letters indicate a significant difference at $p < 0.1$.

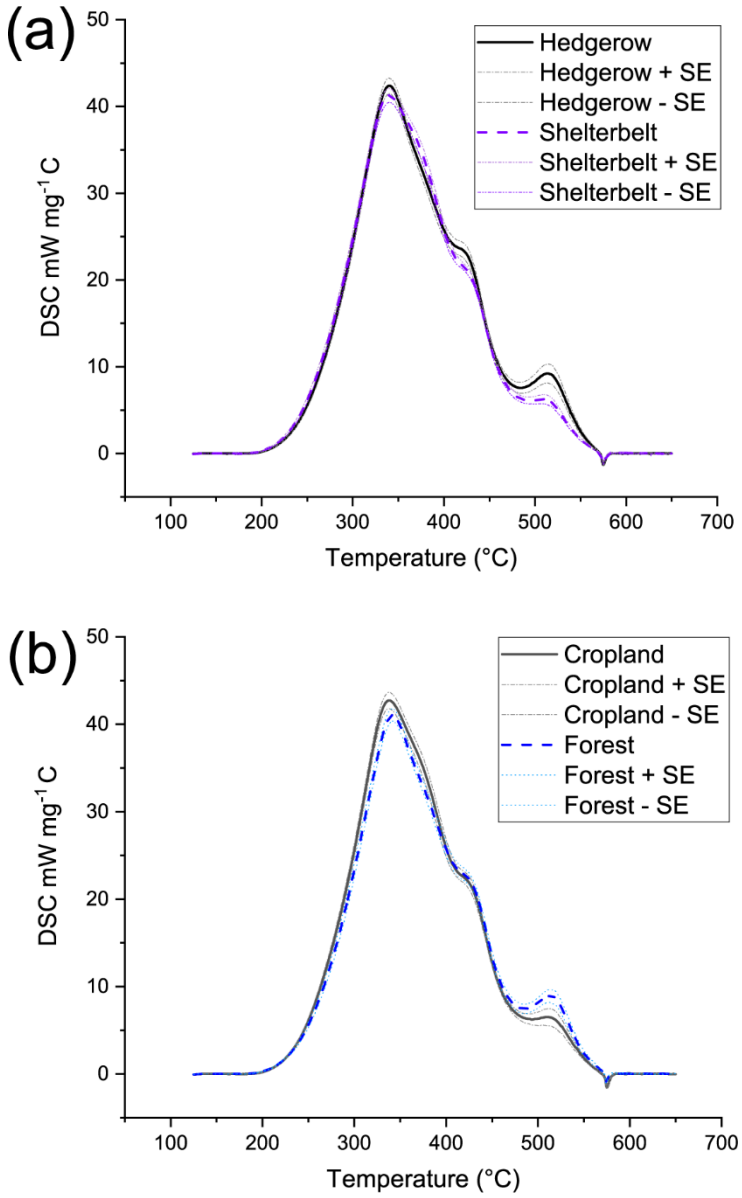

Fig 3-4. Differential scanning calorimetry (DSC) thermograms (mean ± SE) of SOC in different (a) agroforestry systems and (b) land-uses (SE denotes standard error)

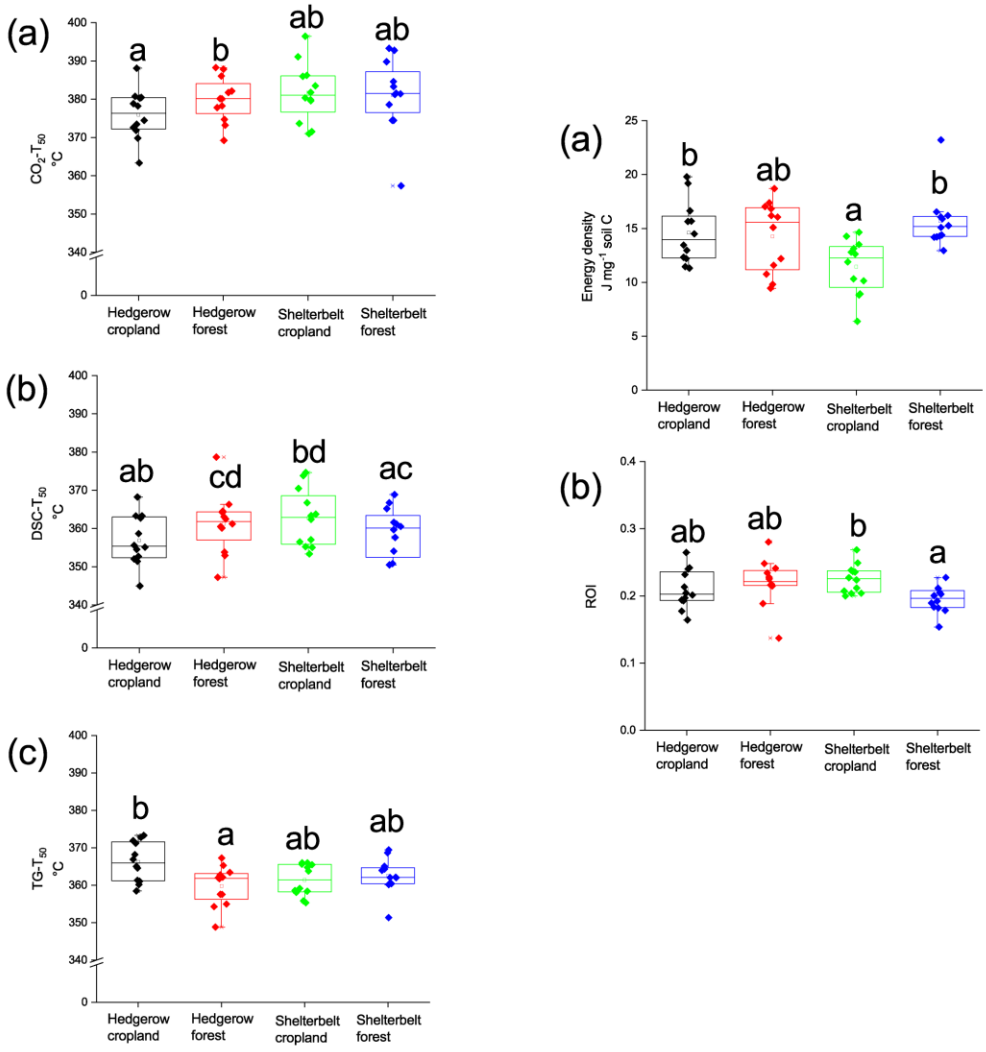

Fig 3-5. The interaction effects of agroforestry system by land-use on thermal stability indices. Data points are mean (± standard error, n=12, the hollow point and the middle line in each boxplot represent mean and median, respectively), with different lowercase letters indicating a significant difference at $p < 0.1$.

Note: TG-T_{50}, the temperature that 50% of the exothermic mass is lost; DSC-T_{50}, the temperature that 50% of the exothermic energy is released; CO_2-T_{50}, the temperature that 50% of the CO_2 is produced; ROI, energy density and return on energy investment.

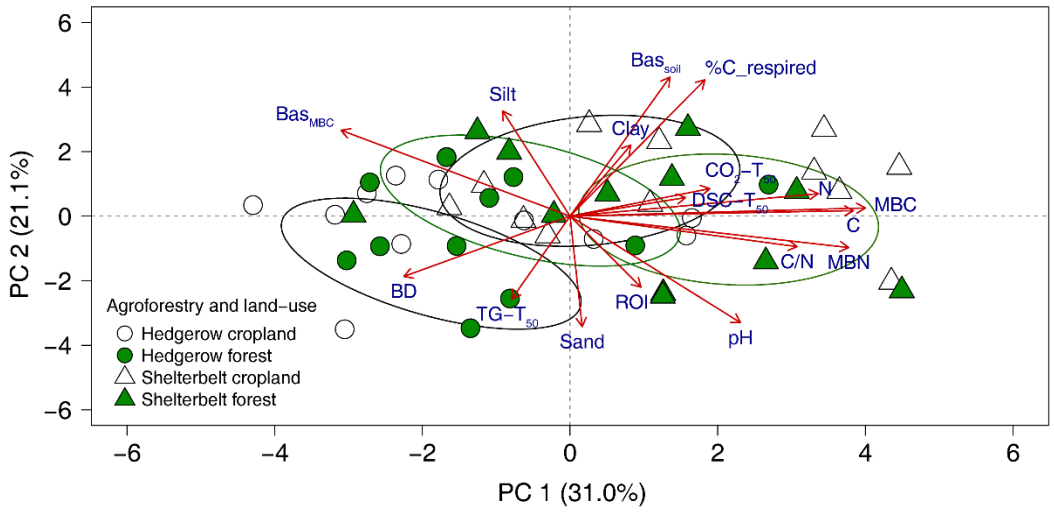

Fig. 3-6. Relationships between basic soil properties, SOC biological and thermal stabilities of soils collected from forest and cropland from shelterbelt and hedgerow systems, using a PCA ordination with 95% confidence ellipses to describe the interaction between agroforestry system and land-use.

Note: Ea, activation energy; BD, bulk density; Bas, basal respiration rate; Ed, energy density, Cum, cumulative respiration; %C_respired, the proportion of C respired; TG-T_{50}, the temperature that 50% of the exothermic mass is lost; DSC-T_{50}, the temperature that 50% of the exothermic energy is released; CO_2-T_{50}, the temperature that 50% of the CO_2 is produced; ROI, return on energy investment.

References

Abbas, F., Hammad, H.M., Fahad, S., Cerdà, A., Rizwan, M., Farhad, W., Ehsan, S., Bakhat, H.F. 2017. Agroforestry: a sustainable environmental practice for carbon sequestration under the climate change scenarios - a review. Environ. Sci. Pollut. Res. 24, 11177-11191. https://doi.org/10.1007/s11356-017-8687-0.

An, Z.F., Bernard, G.M., Ma, Z.L., Plante, A.F., Michaelis, V.K., Bork, E.W., Carlyle, C.N., Baah-Acheamfour, M., Chang, S.X. 2021. Forest land-use increases soil organic carbon quality but not structural or thermal stability in a hedgerow system. Agric. Ecosyst. Environ. 321, 107617. https://doi.org/10.1016/j.agee.2021.107617.

Angst, G., Mueller, K.E., Eissenstat, D.M., Trumbore, S., Freeman, K.H., Hobbie, S.E., Chorover, J., Oleksyn, J., Reich, P.B., Mueller, C.W. 2019. Soil organic carbon stability in forests: distinct effects of tree species identity and traits. Glob. Change Biol. 25, 1529-1546. https://doi.org/10.1111/gcb.14548.

Baah-Acheamfour, M., Carlyle, C.N., Bork, E.W., Chang, S.X. 2014. Trees increase soil carbon and its stability in three agroforestry systems in central Alberta, Canada. For. Ecol. Manag. 328, 131-139. https://doi.org/10.1016/j.foreco.2014.05.031.

Baah-Acheamfour, M., Carlyle, C.N., Bork, E.W., Chang, S.X. 2020. Forest and perennial herbland cover reduce microbial respiration but increase root respiration in agroforestry systems. Agric. For. Meteorol. 280, 107790. https://doi.org/10.1016/j.agrformet.2019.107790.

Baah-Acheamfour, M., Carlyle, C.N., Lim, S.S., Bork, E.W., Chang, S.X. 2016. Forest and grassland cover types reduce net greenhouse gas emissions from agricultural soils. Sci. Total Environ. 571, 1115-1127. https://doi.org/10.1016/j.scitotenv.2016.07.106.

Baah-Acheamfour, M., Chang, S.X., Carlyle, C.N., Bork, E.W. 2015. Carbon pool size and stability are affected by trees and grassland cover types within agroforestry systems of western Canada. Agric. Ecosyst. Environ. 213, 105-113. https://doi.org/10.1016/j.agee.2015.07.016.

Banerjee, S., Baah-Acheamfour, M., Carlyle, C.N., Bissett, A., Richardson, A.E., Siddique, T., Bork, E.W., Chang, S.X. 2016. Determinants of bacterial communities in Canadian agroforestry systems. Environ. Microbiol. 18, 1805-1816. https://doi.org/10.1111/1462-2920.12986.

Barré, P., Plante, A.F., Cécillon, L., Lutfalla, S., Baudin, F., Bernard, S., Christensen, B.T., Eglin, T., Fernandez, J.M., Houot, S. 2016. The energetic and chemical signatures of persistent soil organic matter. Biogeochemistry 130, 1-12. https://doi.org/10.1007/s10533-016-0246-0.

Beule, L., Corre, M.D., Schmidt, M., Göbel, L., Veldkamp, E., Karlovsky, P., 2019. Conversion of monoculture cropland and open grassland to agroforestry alters the abundance of soil bacteria, fungi and soil-N-cycling genes. PloS One 14, e0218779. https://doi.org/10.1371/journal.pone.0220713.

Borden, K.A., Thomas, S.C., Isaac, M.E., 2020. Variation in fine root traits reveals nutrient-specific acquisition strategies in agroforestry systems. Plant Soil, 453, 139-151. https://doi.org/10.1007/s11104-019-04003-2.

De Mendiburu F., 2019. Agricolae: Statistical procedures for agricultural research. R Package Version 1.2-4.

Eisenhauer, N., Lanoue, A., Strecker, T., Scheu, S., Steinauer, K., Thakur, M.P., Mommer, L., 2017. Root biomass and exudates link plant diversity with soil bacterial and fungal biomass. Sci. Rep. 7, 1-8. https://doi.org/10.1038/srep44641.

Environment Canada, 2021. Canadian Climate Normal 1981–2010. Government of Canada. https://climate.weather.gc.ca/climate_normals/(accessed June 08, 2021).

Fissore, C., Giardina, C.P., Kolka, R.K., Trettin, C.C., King, G.M., Jurgensen, M.F., Barton, C.D., McDowell, S.D. 2008. Temperature and vegetation effects on soil organic carbon quality along a forested mean annual temperature gradient in North America. Glob. Change Biol. 14, 193-205. https://doi.org/10.1111/j.1365-2486.2007.01478.x.

Gupta, N., Kukal, S., Bawa, S., Dhaliwal, G. 2009. Soil organic carbon and aggregation under poplar based agroforestry system in relation to tree age and soil type. Agrofor. Syst. 76, 27-35. https://doi.org/10.1007/s10457-009-9219-9.

Harvey, O.R., Myers-Pigg, A.N., Kuo, L.J., Singh, B.P., Kuehn, K.A., Louchouarn, P. 2016. Discrimination in degradability of soil pyrogenic organic matter follows a return-on-energy-investment principle. Environ. Sci. Technol. 50, 8578-8585. https://doi.org/10.1021/acs.est.6b01010.

Jia, Z.J., Yakov, K., Myrold, D., Tiedje, J. 2017. Soil organic carbon in a changing world. Pedosphere 27, 789-791. https://doi.org/10.1016/S1002-0160(17)60489-2.

Jobbágy, E.G. and Jackson, R.B. 2000. The vertical distribution of soil organic carbon and its relation to climate and vegetation. Ecol. Appl. 10, 423-436. https://doi.org/10.1890/1051-0761(2000)010[0423:TVDOSO]2.0.CO;2.

Jose, S., Bardhan, S. 2012. Agroforestry for biomass production and carbon sequestration: an overview. Agrofor. Syst. 86, 105-111. https://doi.org/10.1007/s10457-012-9573-x.

Kim, D.G., Kirschbaum, M.U., Beedy, T.L. 2016. Carbon sequestration and net emissions of CH_4 and N_2O under agroforestry: Synthesizing available data and suggestions for future studies. Agric. Ecosyst. Environ. 226, 65-78. https://doi.org/10.1016/j.agee.2016.04.011.

Kwak, J.H., Lim, S.S., Baah-Acheamfour, M., Choi, W.J., Fatemi, F., Carlyle, C.N., Bork, E.W., Chang, S.X. 2019. Introducing trees to agricultural lands increases greenhouse gas emission during spring thaw in Canadian agroforestry systems. Sci. Total Environ. 652, 800-809. https://doi.org/10.1016/j.scitotenv.2018.10.241.

Lal, R. 2003. Global potential of soil carbon sequestration to mitigate the greenhouse effect. Crit. Rev. Plant Sci. 22, 151-184. https://doi.org/10.1080/713610854.

Lal, R. 2004. Soil carbon sequestration impacts on global climate change and food security. Science 304, 1623-1627. https://doi.org/10.1126/science.1097396.

Lal, R. 2007. Carbon management in agricultural soils. Mitig. Adapt. Strateg. Glob. Chang. 12, 303-322. https://doi.org/10.1007/s11027-006-9036-7.

Lenth, R.V. 2016. Least-squares means: the R package lsmeans. J. Stat. Softw. 69, 1-33.

Li, Y., Bruelheide, H., Scholten, T., Schmid, B., Sun, Z.K., Zhang, N.L., Bu, W.S., Liu, X.J., Ma, K.P. 2019. Early positive effects of tree species richness on soil organic carbon accumulation in a large-scale forest biodiversity experiment. J. Plant Ecol. 12, 882-893. https://doi.org/10.1093/jpe/rtz026.

Liang, Q., Wang, C., Zhang, K.X., Shi, S.W., Guo, J.X., Gao, F., Liu, J., Wang, J.X., Liu, Y. 2021. The influence of tree species on soil organic carbon stability under three temperate

forests in the Baihua Mountain Reserve, China. Glob. Ecol. Conserv. 26, e01454. https://doi.org/10.1016/j.gecco.2021.e01454.

Lim, S.S., Baah-Acheamfour, M., Choi, W.J., Arshad, M.A., Fatemi, F., Banerjee, S., Carlyle, C.N., Bork, E.W., Park, H.J., Chang, S.X., 2018. Soil organic carbon stocks in three Canadian agroforestry systems: From surface organic to deeper mineral soils. For. Ecol. Manag. 417, 103-109. https://doi.org/10.1016/j.foreco.2018.02.050.

Ma, Z.L., Chen, H.Y., Bork, E.W., Carlyle, C.N., Chang, S.X., 2020. Carbon accumulation in agroforestry systems is affected by tree species diversity, age and regional climate: A global meta-analysis. Glob. Ecol. Biogeogr. 29, 1817-1828. https://doi.org/10.1111/geb.13145.

Miao, S.J., Qiao, Y.F., You, M.Y., Zhang, F.T. 2016. Thermal stability of soil organic matter was affected by 23-yr maize and soybean continuous cultivation in northeast of China. J. Therm. 123, 2045-2051. https://doi.org/10.1007/s10973-015-4709-7.

Nagele, P., 2003. Misuse of standard error of the mean (SEM) when reporting variability of a sample. A critical evaluation of four anaesthesia journals. Br. J. Anaesth. 90, 514-516. https://doi.org/10.1093/bja/aeg087.

Nair, P., Kumar, B., Nair, V.D., 2009. Agroforestry as a strategy for carbon sequestration. J. Plant. Nutr. Soil Sci. 172, 10-23. https://doi.org/10.1002/jpln.200800030.

Ogle, S.M., Breidt, F.J., Paustian, K. 2005. Agricultural management impacts on soil organic carbon storage under moist and dry climatic conditions of temperate and tropical regions. Biogeochemistry 72, 87-121. https://doi.org/10.1007/s10533-004-0360-2.

Paustian, K., Lehmann, J., Ogle, S., Reay, D., Robertson, G.P., Smith, P., 2016. Climate-smart soils. Nature 532, 49-57. https://doi.org/10.1038/nature17174.

Peltre, C., Fernández, J.M., Craine, J.M., Plante, A.F., 2013. Relationships between biological and thermal indices of soil organic matter stability differ with soil organic carbon level. Soil Sci. Soc. Am. J. 77, 2020-2028. https://doi.org/10.2136/sssaj2013.02.0081.

Plante, A.F., Fernández, J.M., Haddix, M.L., Steinweg, J.M., Conant, R.T., 2011. Biological, chemical and thermal indices of soil organic matter stability in four grassland soils. Soil Biol. Biochem. 43, 1051-1058. https://doi.org/10.1016/j.soilbio.2011.01.024.

R Core Team. 2018. R: A language and environment for statistical computing. R Foundation for Statistical Computing. Austria: Vienna.

Rovira, P., Kurz-Besson, C., Coûteaux, M.M., Vallejo, V.R., 2008. Changes in litter properties during decomposition: a study by differential thermogravimetry and scanning calorimetry. Soil Biol. Biochem. 40, 172-185. https://doi.org/10.1016/j.soilbio.2007.07.021.

Schädel, C., Beem-Miller, J., Aziz Rad, M., Crow, S.E., Hicks Pries, C.E., Ernakovich, J., Hoyt, A.M., Plante, A., Stoner, S., Treat, C.C., 2020. Decomposability of soil organic matter over time: the Soil Incubation Database (SIDb, version 1.0) and guidance for incubation procedures. Earth Syst. Sci. Data 12, 1511-1524. https://doi.org/10.5194/essd-12-1511-2020.

Soil Classification Working Group, 1998. The Canadian System of Soil Classification. NRC Research Press, Ottawa, Canada, 187 pp.

Stone, M.M. and Plante, A.F. 2015. Relating the biological stability of soil organic matter to energy availability in deep tropical soil profiles. Soil Biol. Biochem. 89, 162-171. https://doi.org/10.1016/j.soilbio.2015.07.008.

Thevathasan, N., Gordon, A. 2004. Ecology of tree intercropping systems in the North temperate region: Experiences from southern Ontario, Canada. New Vistas in Agroforestry. Springer, pp. 257-268.

Trasar-Cepeda, C., Leirós, M., Gil-Sotres, F. 2008. Hydrolytic enzyme activities in agricultural and forest soils. Some implications for their use as indicators of soil quality. Soil Biol. Biochem. 40, 2146-2155. https://doi.org/10.1016/j.soilbio.2008.03.015.

Vesterdal, L., Clarke, N., Sigurdsson, B.D., Gundersen, P. 2013. Do tree species influence soil carbon stocks in temperate and boreal forests? For. Ecol. Manag. 309, 4-18. https://doi.org/10.1016/j.foreco.2013.01.017.

Wang, H., Liu, S.R., Wang, J.X., Shi, Z.M., Lu, L.H., Zeng, J., Ming, A.G., Tang, J.X., Yu, H.L. 2013. Effects of tree species mixture on soil organic carbon stocks and greenhouse gas fluxes in subtropical plantations in China. Forest Ecol. Manag. 300, 4-13. https://doi.org/10.1016/j.foreco.2012.04.005.

Wang, S.J., Wang, H., Li, J.H. 2016. Does tree species composition affect soil CO_2 emission and soil organic carbon storage in plantations? Trees 30, 2071-2080. https://doi.org/10.1007/s00468-016-1434-1.

Williams, E.K., Fogel, M.L., Berhe, A.A., Plante, A.F., 2018. Distinct bioenergetic signatures in particulate versus mineral-associated soil organic matter. Geoderma 330, 107-116. https://doi.org/10.1016/j.geoderma.2018.05.024.

Williams, E.K. and Plante, A.F. 2018. A bioenergetic framework for assessing soil organic matter persistence. Front. Earth Sci. 6: 143. https://doi.org/10.3389/feart.2018.00143.

Williams, E.K., Rosenheim, B.E., McNichol, A.P., Masiello, C.A. 2014. Charring and non-additive chemical reactions during ramped pyrolysis: Applications to the characterization

of sedimentary and soil organic material. Org. Geochem. 77, 106-114. https://doi.org/10.1016/j.orggeochem.2014.10.006.

Xu, H.W, Qu, Q., Wang, M.G. Li, P., Li, Y.Z., Xue, S., Liu, G.B., 2020. Soil organic carbon sequestration and its stability after vegetation restoration in the Loess Hilly Region, China. Land Degrad. Dev. 31, 568-580. https://doi.org/10.1002/ldr.3472.

Zhang, X., Liu, S.R., Huang, Y.T., Fu, S.L., Wang, J.X., Ming, A.G., Li, X.Z., Yao, M.J., Li, H. 2018. Tree species mixture inhibits soil organic carbon mineralization accompanied by decreased r-selected bacteria. Plant Soil 431, 203-216. https://doi.org/10.1007/s11104-018-3755-x.

Zibilske, L. 1994. Carbon mineralization. Methods of Soil Analysis: Part 2 Microbiological and Biochemical Properties 5, 835-863. https://doi.org/10.2136/sssabookser5.2.c38.

Chapter 4. Heat waves increase soil CO_2 and N_2O emissions from both cropland and forestland of an agroforestry system

1. Introduction

Climate extremes resulting from climate change are regarded as crucial factors influencing the terrestrial biosphere (Anjileli et al., 2021). The spatial extent and frequency of climate extremes are predicted to intensify quickly in the 21st century and will be continually enhanced, regardless of the Earth system models used to make the prediction (Meyer and Pachauri, 2014). For those climate extremes, heat waves, defined as periods with no less than three consecutive days with a higher temperature than the average temperature (Perkins and Alexander, 2013; Jeong et al., 2016), are thought to have a more significant impact on terrestrial ecosystems than gradual climate warming. This is due to their significant response strengths (greater than usual) despite a shorter response duration (i.e., few days) (Teuling et al., 2010; Frank et al., 2015; Zhang and Cao, 2017), which will also influence terrestrial carbon (C) cycling as well as global climate change (Reichstein et al., 2013).

Heat wave events may weaken C stocks in terrestrial ecosystems (i.e., cropland and forestland) and turn them into C sources. For example, a series of heat wave events in Europe in 2003 from June to August substantially increased CO2 emissions, which released an amount of C equivalent to that sequestered in the previous four years (Ciais et al., 2005). Because soils are the largest C reservoir in terrestrial ecosystems, understanding the response of soil C to heat wave events is critical to C sequestration and climate change mitigation, especially when heat wave events are predicted to be more frequent (Smoyer-Tomic et al., 2003; Jeong et al., 2016).

However, such knowledge about the response of soil C to heat wave events remains limited due to the rarity, randomness and unpredictability of such natural extreme events (Smith, 2011; Hoover et al., 2014; Teskey et al., 2015). Little is also known regarding how heat wave events affect agroforestry systems, especially the role of agroforestry systems in regulating greenhouse gas (GHG) mitigation and C sequestration in soils.

Heat wave events will change soil C dynamics; for example, heat wave events can accelerate soil respiration and reduce C uptake by the soil (Anjileli et al., 2021), affecting the annual productivity of forests (Tatarinov et al., 2016; Yuan et al., 2016). Griebel et al. (2019) found that forest turned into a net C source with an increase of 137% in ecosystem respiration during a heat wave event, suggesting that forests may not always be a net sink of C and the role of forest as a net C sink may depend highly on climatic conditions (i.e., temperature and moisture content). Soil labile C is a critical component of soil organic C (SOC); labile C decomposes rapidly (ranging from days to years) and can have a strong influence on soil nutrient cycling (Gu et al., 2004; Xu et al., 2010). Soil labile C may be an early indicator of changes in soil C as affected by heat wave events, as soil labile C can act as a proxy for the changing conditions in soils and respond more quickly to the change than the total C (Benbi et al., 2015). For example, Ghani et al. (2003) found that hot water (at 80 °C) extractable organic C (HWEOC) is one of the most sensitive indicators in reflecting changes in the soil organic matter that resulted from soil management practices, with a positive relationship to soil microbial activities. Microbial biomass C (MBC) reflects crucial processes such as nutrient availability and cycling that are sensitive to management changes, including reduced tillage and use of cover crops (Xu et al., 2013). Permanganate oxidizable C (POXC) is a sensitive proxy for tracking soil C change, which accounted for 1~4% of SOC and actively reacted to nutrient management. The POXC is

also commonly used for measuring soil quality change and is regarded as a critical soil health indicator (Weil et al., 2003). However, how labile C responds to heat wave events is still largely unknown. Moreover, most studies on the influence of heat wave events have been limited to either post-event analysis of heat wave effects or the short-term effect of high-temperature stress on plants (Teskey et al., 2015), and the focus of most climate change research has been on natural ecosystems (i.e., grasslands or forests). In comparison, studies of extreme weather effects on the soil environment in agroecosystems are lacking (Acosta-Martinez et al., 2014), which hinders our understanding of heat wave effects in changing climate conditions.

No study has investigated the influence of heat wave events and their frequency on GHG emissions and C dynamics in agroforestry systems, while the Prairies in western Canada have had frequent heat wave events with high temperatures (Smoyer-Tomic et al., 2003). This study explores the effect of heat wave events and their frequency on C dynamics and GHG emissions in a typical hedgerow system in central Alberta, Canada. We hypothesized that heat wave events would increase GHG emissions and labile soil C loss in the forested and cropped components of a hedgerow system. In addition, forest soils may have more GHG emissions than the cropland under heat wave conditions due to the lower SOC stability (An et al., 2021), and the influence of heat wave events on GHG emission and soil labile C would intensify with higher heat wave frequency.

2. Material and methods

2.1 Soil properties

This study was conducted using surface soil samples (0-10 cm) collected from four hedgerow sites in central Alberta, Canada, as surface soils are directly influenced by heat wave events and will respond quickly to changes resulting from extreme heat. A detailed description of the hedgerow system, which is characterized as a boundary agroforestry system, can be found in An et al. (2021). The hedgerow systems were comprised of 3-5 m wide linear forestlands next to croplands. Naturally regenerated deciduous broad-leaf trees (e.g., *Populus tremuloides* Michx., *Populus balsamifera* L., *Betula papyrifera* Marsh.) dominated hedgerow forests and along with a variety of native shrubs and herbaceous understory vegetation (Baah-Acheamfour et al., 2014). Tree age ranged from 40 to 100-yr with a mean tree density of 7776 ± 1425 stems ha^{-1} (Baah-Acheamfour et al., 2015). The cropland grew annual crops (e.g., wheat, canola and barley) in rotation with minimum tillage and a fertilization rate of about 120 kg N ha^{-1} $year^{-1}$ (Baah-Acheamfour et al., 2014). The soil type in all the hedgerow sites was Black Chemozemic soils. The properties of soil samples (n=4) in each land-use type are listed in Appendix 4-1. For the period of 1981-2020, the mean annual precipitation of the four sites was 443 mm, and the mean minimum and maximum temperatures were -3.2 °C and 9.0 °C, respectively (Alberta Agriculture and Forestry, 2020).

2.2 Laboratory incubation

A split-plot design (the main plot: land-use type, the split-plot: heat wave treatment) was used to study the influence of heat wave events in different land-use components of the agroforestry system in central Alberta. The temperature in the heat wave event was set to 35 ºC, the duration of the heat wave event was 5 days, and the frequency of heat wave events was set to 0, 2 and 3 times over a 95-day study period. From 1916 to 2003, the central Alberta region suffered more

than ten times of three-day-long heat wave events, which was more than two times the frequency of 5-day long heat wave events (Smoyer-Tomic et al., 2003). With the influence of continuing high rates of anthropogenic GHG emissions and the resulting global warming, the average length of a heat wave event is projected to increase from 1~2 days in 1976-2005 to 5~6 days in 2051-2080, and that of extremely hot (> 34 ºC) days will increase from ~1 day to 6~7 days in a year (The Climate Atlas of Canada, 2019). The above climate change scenarios led us to decide the frequency and the temperature of the heat wave events. The experiment consisted of 3 heat wave treatments: 1) control, the incubation was done at 20 ºC, with the temperature maintained constant throughout the experiment, 2) two heat wave events (HW2), two 5-day long heat wave (35 ºC) events, and 3) three heat wave events (HW3), three 5-day long heat wave (35 ºC) events, over a period of 95 days of the experiment.

Field moist soil samples (< 2 mm), equivalent to 6 g dry weight, were used for the laboratory incubation experiment. The samples were placed into 50 mL polyethylene centrifuge tubes and then kept in the dark and maintained at 55% soil water holding capacity (Bradford et al., 2008) during the incubation. First, all treatments were incubated at 20 ºC for ten days, allowing microbial activities to be stabilized. Then the control treatment remained at 20 ºC while the HW2 and HW3 treatments were placed into a refrigerated incubator (3710, Forma Scientific, Inc., Marietta, Ohio, USA) that was set to 35 ºC for 5 days. Then the HW2 and HW3 treatments were immediately placed back to 20 ºC when the heat wave period was over. Emission rates of CO_2 and N_2O of the tubes in each treatment were measured by taking a gas sample at t = 0 and 24 h after closing the tube to create an air-tight condition on the day of sampling, and the same procedure was repeated every 5 days for the non-heat wave period and at the beginning and end of each heat wave period. The tubes in the incubation experiment were loosely capped to avoid

excessive water loss and anoxia between sampling events. A 5 mL gas sample was collected using a syringe and injected into a 3 mL pre-evacuated glass vial at each gas sampling point. The gas samples were then analyzed using a gas chromatograph (Varian CP-3800, Varian Canada, Mississauga, Canada). Another set of tubes was prepared for soil sampling with the same experimental setup as those used for gas sampling. Soil samples were destructively collected from the tubes at the beginning of the experiment, the end of the pre-incubation period, the beginning and end of each heat wave event, and the end of the incubation (Fig. 4-1). All tubes were checked for soil water loss every two days, and the water content was adjusted by adding deionized water into the tube to ensure that the sample remained at 55% soil water holding capacity. The basal emission of CO_2 (mg C kg^{-1} soil day^{-1}) and N_2O (mg N kg^{-1} soil day^{-1}), which indicate the steady rate of soil CO_2 and N_2O emissions, were determined as the average of the emission rates of CO_2 and N_2O, respectively, in the last 4 samplings in the incubation (Stone and Plante, 2015).

2.3 Analysis of soil POXC, HWEOC and MBC

Soil permanganate oxidizable C (POXC) was analyzed following the modified method of Weil et al. (2003) as described in Culman et al. (2012). Briefly, ~ 2.5 g air-dried soil samples (< 250 μm) were placed into 50 mL polypropylene centrifuge tubes, and 18 mL deionized water and a 2 mL of 0.2 M KMnO4 solution were added to each tube. Then the tubes were shaken for 2 min at 120 rpm on an oscillating shaker. After the tubes were let to settle for 10 min, 0.5 mL of the supernatant was transferred into a 50 mL centrifuge tube preloaded with 49.5 mL of deionized water and shaken to mix the content. Finally, an aliquot (1.5 mL) of each sample from the diluted

tube was transferred into a disposable cuvette to read the absorbance. In addition to a blank (using deionized water), a soil standard and a solution standard based on lab reference sample were used for quality control, and four $KMnO_4$ standard solutions were necessary to develop a standard curve (at 0.05, 0.1, 0.15, and 0.2 mmol L^{-1}, respectively) were included in the analysis. The absorbance of samples was analyzed at 550 nm wavelength using a UV-Vis spectrometer (Genesys 10-S, Thermo Scientific Inc., Rochester, NY, USA). The following equation was used to calculate POXC (mg kg^{-1} soil) following Weil et al. (2003):

$$POXC = [0.02 - (a+b \times A)] \times 9000 \times V \times M$$

Where 0.02 is the $KMnO_4$ concentration (mol L^{-1}); a and b are the intercept and slope of the standard curve, respectively; A is the absorbance of the sample, 9000 is the amount of C (mg) oxidized by 1 mol of MnO_4 (Mn^{7+} to Mn^{4+}); M is the soil mass (kg) used in the reaction and V is the volume (L) of $KMnO_4$ used (0.02 L).

Hot-water extractable organic C (HWEOC) was determined with a modified method of Ghani et al. (2003) and Plante et al. (2011). Briefly, approximately 2 g of air-dried soil and 20 mL deionized water were placed into each 50 mL polypropylene centrifuge tube. Then the tubes were shaken for half an hour at 120 rpm in a reciprocating shaker, then incubated in a water bath at 80 ºC for 18 hours without shaking. Next, the mixture was vortexed and centrifuged for 30 min at 6000 × g. The supernatant was filtered using a 0.45µm nitrocellulose membrane filter, and the filtrates were stored in 20 mL Nalgene bottles. Finally, the filtrate was analyzed using a TOC-V CSN analyzer (TNM-1, Shimadzu Corporation, Kyoto, Japan).

Soil MBC was analyzed by the chloroform fumigation-extraction method (Vance et al., 1987; Joergensen, 1996). Briefly, soil samples (with an equivalent of 10 g dry soil) were fumigated for 24 h with chloroform in an evacuated glass desiccator. Both non-fumigated and fumigated soil samples were extracted with 50 mL of a 0.1 mol L^{-1} K_2SO4 solution by shaking for one hour at 120 rpm in a reciprocating shaker and then filtered. Extractable C and N were analyzed using a TOC-V CSN analyzer (TNM-1, Shimadzu Corporation, Kyoto, Japan). Finally, MBC content was calculated as the difference in extractable C between fumigated and non-fumigated soil samples using an extraction coefficient of 0.45.

2.4 Statistical analysis

Two-way analysis of variance (ANOVA) was used to test the effects of land-use type and heat wave treatment on soil CO_2 and N_2O emissions (both cumulative and basal CO_2 and N_2O emissions), and a three-way ANOVA was undertaken to test the effects of land-use type, heat wave treatment and soil sampling time on soil POXC, HWEOC and MBC using the R software (R Core Team, 2018). Data were subjected to the Shapiro-Wilk test and Levene's test to evaluate the normality of data distribution and homogeneity of variance, respectively. The basal N_2O emissions, cumulative CO_2 and N_2O emissions, HWEOC and MBC were log-transformed to meet the normality requirement; however, non-transformed data were presented for the ease of interpretation of the results. The Spearman correlation analysis was used to explore the relationship among gas emissions, different C concentrations and soil properties. Principal component analysis (PCA) was used to explore the relationship between basic soil properties, soil labile C pools and soil CO_2 and N_2O emissions. We used LS-means in the "*lsmeans*"

package in R (Lenth and Lenth, 2018) and Fisher's protected test to identify differences between treatment means when ANOVA showed significant effects of treatments and interactions ($P < 0.05$).

3. Results

3.1 Soil CO_2 and N_2O emissions

Soil CO_2 and N_2O emissions decreased gradually in the control over time, while increasing dramatically when heat wave events occurred during HW2 and HW3 in both the forest and cropland soils (Fig. 4-2a and 2b). Soil basal CO_2 emissions were influenced by land-use type ($p < 0.001$) and heat wave treatment ($p = 0.043$) (Table 4-1), soil basal CO_2 emissions in forest soils were 1.3 times that in cropland soils (Fig 4-3a). Among heat wave treatments, HW3 had lower soil basal CO_2 emissions than HW2 and the control, while there was no difference between HW2 and control treatments with respect to soil basal CO_2 emissions (Fig 4-3b). No influence was found on neither land-use type nor heat wave frequency on soil basal N_2O emissions (Table 4-1). During the five-day heat wave period, daily soil CO_2 and N_2O emissions increased dramatically, the average daily soil CO_2 and N_2O during the heat wave period was 3.6 and 35.5 times that in the control of forest soils, and 3.7 and 10.0 times that of the control in the cropland soils (Appendix 4-2). We also observed a restoration of the daily soil CO_2 and N_2O emissions to pre-heat wave period a day after the end of the heat wave period (i.e., daily emissions of soil CO_2 and N_2O decreased to emissions in the non-heat wave period) (Fig. 4-2a and 2b).

Cumulative soil CO_2 emission was influenced by land-use type ($p < 0.01$) and heat wave frequency ($p < 0.01$) (Table 4-1). Cumulative soil CO_2 emissions were 1.4 times greater ($p < 0.01$) in the forest than in the cropland (Fig 4-3c). In the cropland, cumulative soil CO_2 emissions during the heat wave periods accounted for 19.7, 53.3 and 74.1% of the total CO_2 emissions in the control, HW2 and HW3 treatments, respectively. While in the forest, cumulative soil CO_2 emissions in the heat wave periods accounted for 19.9, 57.5 and 67.3% of the total CO_2 emissions in the control, HW2 and HW3 treatments, respectively. Among the heat wave treatments, CO_2 emissions in HW2 and HW3 were 1.3 ($p < 0.01$) and 1.4 times ($p < 0.01$), respectively, that in the control, while there was no significant difference between HW2 and HW3 (Fig 4-3d). The cumulative soil N_2O emission was significantly increased under heat wave treatments, and the cumulative soil N_2O emissions were influenced by land-use type, heat wave treatment and the interaction effects of land-use by heat wave treatment (Table 4-1). Cumulative soil N_2O emissions were higher under the two heat wave treatments (HW2 and HW3) than the control ($p < 0.01$) but were not different between HW2 and HW3 in either land-use type (Fig 4-4).

3.2 Changes in soil labile carbon

Land-use type significantly influenced soil POXC ($p < 0.01$, Table 4-2), with its concentration in forest soils 1.1 times that in cropland soils (Fig. 4-5a). Soil MBC was affected by land-uses, sampling time and their interactions (Table 4-2). Forest soil MBC declined significantly during the incubation due to heat wave treatment, even though forest soils had the highest MBC in the first sampling and decreased gradually over time. Similarly, MBC in cropland soils showed a

decreasing trend ($p > 0.05$) from the beginning of the incubation (Fig. 4-5b). Soil HWEOC was influenced by the land-use type and soil sampling time. Forest soils had higher HWEOC than cropland soils (Fig. 4-5c), while soil HWEOC decreased at the second sampling and increased afterward through the fourth sampling, then decreased until the end of the incubation (Fig. 4-5d).

3.3 Relations of basic soil properties with soil CO_2 and N_2O emissions

The PCA1 and PCA2 explained 43.7 and 19.2%, respectively, of the total variance in the dataset comprised of basic soil properties, soil labile C and soil CO_2 and N_2O emissions (Fig. 4-6a and 6b). The first five variables attributed to PCA1 were soil total C, MBC, HWEOC, POXC and C/N; basal CO_2 emissions, cumulative CO_2 emissions, soil pH, clay content, and basal N_2O emissions were the first five variables attributed to PCA2. There was a minor overlap of the 95% confidence ellipses between cropland and forest soils (Fig. 4-6a), while among heat wave treatments, the overlap was substantial, and the overlap decreased as the frequency of heat wave events increased (Fig. 4-6b).

Soil sand content was positively correlated with soil pH and MBC, while being negatively correlated with clay and silt content. Clay content was negatively correlated with soil pH; silt content was negatively correlated with HWEOC and MBC; Soil total C, N, C/N and pH were positively correlated with HWEOC, POXC and MBC, while soil pH was being negatively correlated with basal CO_2 emissions. The three types of soil labile C studied were positively correlated with one another (Appendix 4-3).

4. Discussion

4.1 Influence of land-use type and heat wave treatment on soil CO_2 and N_2O emissions

The current study showed that heat wave treatments affected both soil CO_2 and N_2O emissions from cropland and forest soils, suggesting that short-term elevated temperatures can stimulate soil CO_2 and N_2O emissions (Hagedorn et al., 2010; Butterbach-Bahl et al., 2013; Lu et al., 2013). In addition, forest soils were more susceptible to heat wave events than the cropland soils within the hedgerow system as there was a greater response of CO_2 and N_2O emissions to the heat wave treatment within the forest soil (Fig. 4-2), which may be due to a higher amount of high-quality and less stable C than cropland soils (Jílková et al., 2020; An et al., 2021). Moreover, the CO_2 and N_2O emissions increased with the increasing frequency of the heat wave events in both land-uses, suggesting that the hedgerow system may be a source of CO_2 and N_2O when more frequent and severe heat wave events occur. However, during the heat wave periods in HW2 and HW3, daily soil CO_2 and N_2O emissions increased dramatically relative to the control in both land-use types, especially in forest soils (Appendix 4-2). This indicates that forest soils might be a source of CO_2 and N_2O under future heat wave events (Hagedorn et al., 2010; Butterbach-Bahl and Dannenmann, 2011). Special attention should be paid to both forest and cropland soils in agroforestry systems, as those soils may be a significant source of GHG under increasing heat wave frequencies in the future.

The significantly increased CO_2 and N_2O emissions by the heat wave treatment (control vs. HW2 and/or HW3), and the gradual increase in the more frequent heat wave treatment, regardless of the land-use type, are similar to Ciais et al. (2005) and Li et al. (2020) on heat

waves leading to increased CO_2 emissions but is inconsistent with Li et al. (2020) on the lack of heat wave effects on soil N_2O emissions. This difference may be attributed to the difference in soil water regime, as the current study maintained constant moisture content, which may have favoured the nitrification and denitrification processes that enhanced N_2O emissions (Brown et al., 2012; Liu et al., 2017).

4.2 Influence of land-use type and heat wave treatment on soil labile carbon

The current study showed that the forested land-use had higher soil labile C (HWEOC, POXC and MBC) than cropland soils in the hedgerow system, which is in accordance to An et al. (2021), who found that SOC in forest soils is more labile and with a higher quality relative to that in cropland soils. However, the current study did not observe a significant decrease of either HWEOC, POXC or MBC among heat wave treatments, rejecting our hypothesis that heat wave treatment may increase soil labile C loss, which may be due to the short heat wave duration in the current study if it was not strong enough to induce significant changes. Meanwhile, Hagedorn et al. (2010) reported that there was no immediate change of soil labile C (dissolved organic C) to increased temperature, and they found a 10% increase (not significant) in dissolved organic C after 2 months of constant soil warming under field conditions. Moreover, the stable C may have a higher sensitivity of decomposition to temperature than the labile C in soils (Knorr et al., 2005; von Lützow and Kögel-Knabner, 2009); while such investigation was not done in the current study, future studies need to study those relationships.

The three types of soil labile C studied in the current study had different responses to heat wave treatments (Fig. 4-5), suggesting that different types of soil labile C may have various

sensitivity to heat wave treatments. The relatively lower soil MBC in the control than the HW2 and HW3, suggesting that more soil labile C may be lost with the increasing heat wave frequency. As SOC in forest soils had a larger amount of labile C than cropland soils, which may be lost during heat wave events, attention should be paid to conserving labile soil C in the forest. Albeit SOC in cropland soils are more stable than that in forest soils in heat wave events (less CO_2 and N_2O emissions), cropland soils hold less SOC due to the loss of less protected carbon, which will have a significant influence on soil health in the cropland.

4.3 Limitations and implications of the current study

Heat wave events with constant high soil moisture content are uncommon (Teskey et al., 2015). The current study aimed to study the influence of temperature and the frequency of heat wave events on GHG emissions and soil labile C; thus, we controlled the soil moisture regime. However, the typical situation is to have a heat wave and associated water-deficit conditions (i.e., drought) (Teskey et al., 2015), especially in field conditions, making it hard to isolate the effects (e.g., thermal effect, drying effect) on C cycling processes (Hoover et al., 2017). Meanwhile, to simplify the incubation experiment, we also set the diurnal and nocturnal temperatures the same, which may have caused soil CO_2 and N_2O emissions to be over-estimated, as the nocturnal temperature would usually be lower than the diurnal temperature in the field.

Soil moisture may be more important than temperature in controlling soil CO_2 emissions. Hoover et al. (2016) reported that soil moisture content is the primary controlling factor in soil respiration, and more frequent and intense drought, rather than heat waves, may have a more substantial impact on soil CO_2 emissions to the atmosphere (Hoover et al., 2016). Meanwhile,

heat wave events may also decrease soil moisture content indirectly by increasing soil evapotranspiration (Hoover et al., 2014), resulting in further negative impacts on soil respiration. Therefore, moisture availability changes can offset temperature-driven changes in soil respiration (Felton et al., 2019), and should be examined in future investigations. In the current study, all treatments had constant soil moisture content, which is unlikely to be the case for soils experiencing heat wave events in the field. The variation of CO_2 and N_2O emissions needs to be further studied in the field to improve our understanding of the influence of water, temperature, and their interactions.

Due to the unpredictable and random nature of heat wave events, studies have been restricted to either analysis after heat wave events or the short-term effects of high-temperature, and few studies have been conducted to investigate the influence of heat wave events in the field (Teskey et al., 2015). Lab incubation offers better control and greater simplicity compared to field measurements. For example, temperature and moisture effects can be investigated separately and/or with interactions under lab incubation (Salome et al., 2010). In addition, most heat wave events are short and intense by nature and are likely one of the few climatic effects that can be tested in a laboratory incubation experiment quite robustly. However, the incubation study did not have organic matter (litter) input, and the lack of organic matter input may influence the microbial community composition, making it different from soil microbial communities in situ (Salome et al., 2010). On the other hand, heat waves are short and intense by nature, and likely are one of the few climatic effects that can be tested under incubation fairly robustly (regardless of the water issue). Moreover, soils are subjected to various degrees of disturbance during field collection and pre-treatment (i.e., sieving and mixing, rewetting) in the laboratory incubation. Those shortcomings need to be considered in designing future heat wave

studies. Notably, in the current study, only 0-10 cm soils were studied. While heat wave events may affect the respiration of roots and biomass in deeper soil (Jarvi and Burton, 2020), future studies should explore the influence of heat wave events on deeper soil. Although the advantages of incubations are evident when using lab incubation for C-related studies, e.g., C sensitivity to influential factors such as temperature and moisture (Salome et al., 2010; Shrestha et al. 2020), future research should combine both field and laboratory incubation studies to obtain a better understanding the effect of heat wave events on the C dynamics in agricultural systems.

In future warming climate conditions, heat waves are expected to become more common and may cause substantial GHG emissions from soils. As forest soils have more labile C and are possibly more sensitive to heat wave events, forests may be a source of GHG emissions, and thus, agroforestry systems may not function as effective C sinks (e.g., Baah-Acheamfour et al., 2014) under more frequent and extreme heat wave events. Moreover, the record-breaking heat wave events in Alberta, Canada, that lasted for a week with a peak temperature around 38 °C in late June 2021, including the highest temperature recorded in the history of Alberta since 1937, was in actuality 3 °C higher in temperature and 2 days longer than what we tested in this study. The region that experienced heat wave events spanned over the whole of western Canada, with some areas experienced more than 45°C for several days (e.g., Lytton, 49.6 °C) (Environment Canada, 2021), suggesting that future studies should focus on even more extreme conditions (both the temperature magnitude and duration). This includes studying the regional effect of heat waves on agroforestry system C dynamics, soil C sequestration, GHG mitigation, and the socio-economic impacts that landowners and policymakers need to respond to during such extreme heat wave events.

5. Conclusion

Under heat wave events, both forest and cropland soils in the hedgerow system had significantly higher CO2 and N2O emissions. The CO_2 and N_2O emissions increased with the increase of heat wave frequency. Soil labile C (MBC) showed a decreasing trend with the increasing heat wave events. Forest soils may be a source of soil CO_2 and N_2O, and the C in both forest and cropland soils appear to be at risk of loss under the condition of more heat wave events. Agroforestry systems may not always be C sinks, particularly under climate extreme conditions. Future studies need to consider the influence of such climate extremes on C sequestration and pay attention to the effects of the duration, frequency and associated soil moisture deficiency of heat wave events on soil C dynamics, which will provide a better understanding of the impact of heat wave events on C sequestration and GHG mitigation within those agroecosystems.

Table 4-1. Results of the analysis of variance (F and P values) on the effect of land-use type, heat wave treatment and their interaction on basal soil and cumulative CO_2 and N_2O emissions (n=4).

Description	Basal CO_2 emissions mg C kg^{-1} soil			Basal N_2O emissions mg N kg^{-1} soil			Cumulative CO_2 emissions mg C kg^{-1} soil			Cumulative N_2O emissions mg N kg^{-1} soil		
	df	*F*	*P*	df	*F*	*P*	df	*F*	*P*	df	*F*	*P*
Land-use (L)	1	**13.64**	**0.002**	1	1.97	0.181	1	**43.47**	**<0.001**	1	**85.70**	**<0.001**
Heat wave (H)	2	**3.93**	**0.043**	2	2.40	0.125	2	**14.63**	**<0.001**	2	**55.72**	**<0.001**
L × H	2	0.05	0.951	2	0.17	0.846	2	0.36	0.700	2	**6.75**	**<0.008**

Note: *F*-stats with $P < 0.05$ indicate the significance and are shown in bold.

Table 4-2. Results from the analysis of variance (*F* and *P* values) on the effect of land-uses, heat wave treatment, and their interaction on the temporal changes of soil labile C [(permanganate oxidable C (POXC), microbial biomass C (MBC) and hot-water extractable organic C (HWEOC)] over the incubation.

	POXC			MBC			HWEOC		
	mg kg^{-1} soil			mg kg^{-1} soil			mg kg^{-1} soil		
Description	df	F	P	df	F	P	df	F	P
Land-use (L)	1	**43.88**	**<0.01**	1	**239.93**	**<0.01**	1	**84.94**	**<0.01**
Heat wave(H)	2	0.18	0.84	2	1.04	0.35	2	0.9	0.4
L×H	2	0.4	0.67	2	2.29	0.11	2	1.35	0.26
Sampling time (S)	6	1.1	0.36	6	**12.3**	**<0.01**	6	**4.71**	**<0.01**
L×S	6	0.31	0.93	6	**3.04**	**<0.01**	6	0.51	0.8
H×S	12	1.76	0.06	12	0.43	0.95	12	0.43	0.95
L×H×S	12	0.18	0.99	12	0.51	0.91	12	0.53	0.89

Note: *F*-stats with $p < 0.05$ indicate the significance and are shown in bold.

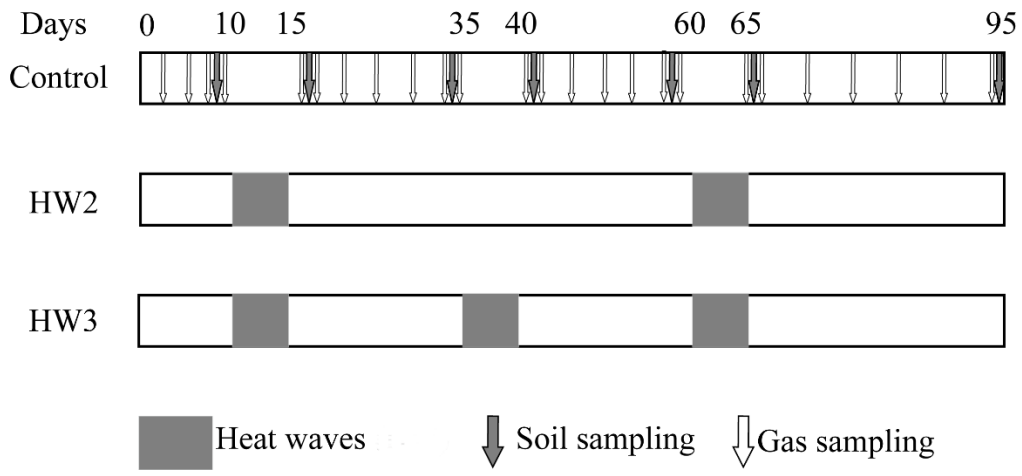

Fig. 4-1. A diagram illustrating the experimental design and the timing of the soil and greenhouse gas samplings. The codes HW2 and HW3 represent the heat wave treatment with two and three heatwave events, respectively, in the experiment. The HW2 and HW3 treatments had the same soil and gas sampling frequency as the control.

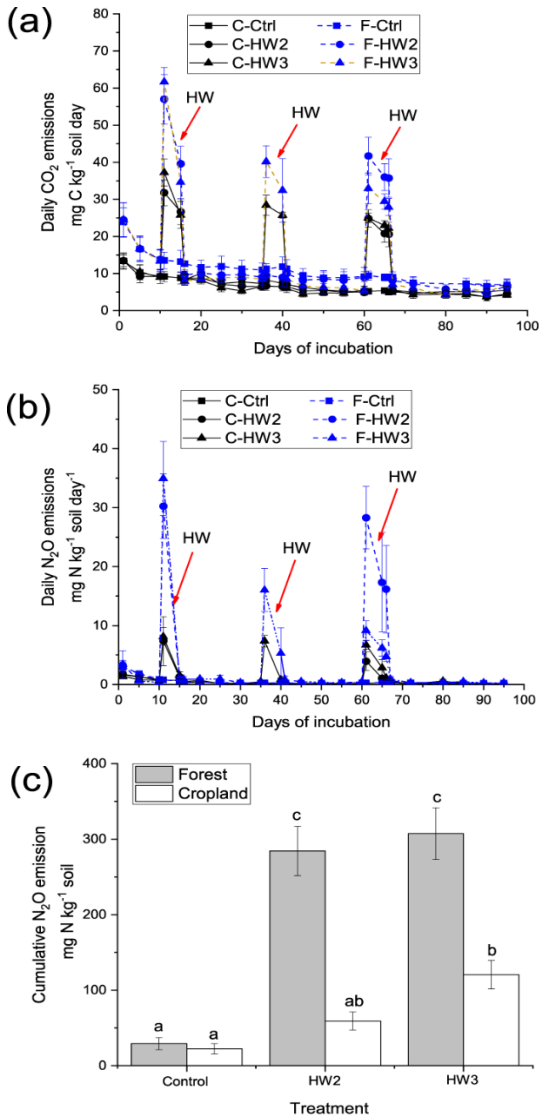

Fig. 4-2. Daily soil CO_2 emissions (a), N_2O emissions (b), and cumulative N_2O emissions as affected by the land-use type and heat wave treatment in the hedgerow system. Vertical bars are standard errors of the means (n=4), and the same letter(s) indicate no significant differences at $P < 0.05$.

Note: C-Ctrl and F-Ctrl indicate controls in the cropland and forest, respectively. C-HW2 and F-HW2 indicate two times heat wave treatment in the cropland and forest, respectively. C-HW3 and F-HW3 indicate three times heat wave treatment in the cropland and forest, respectively.

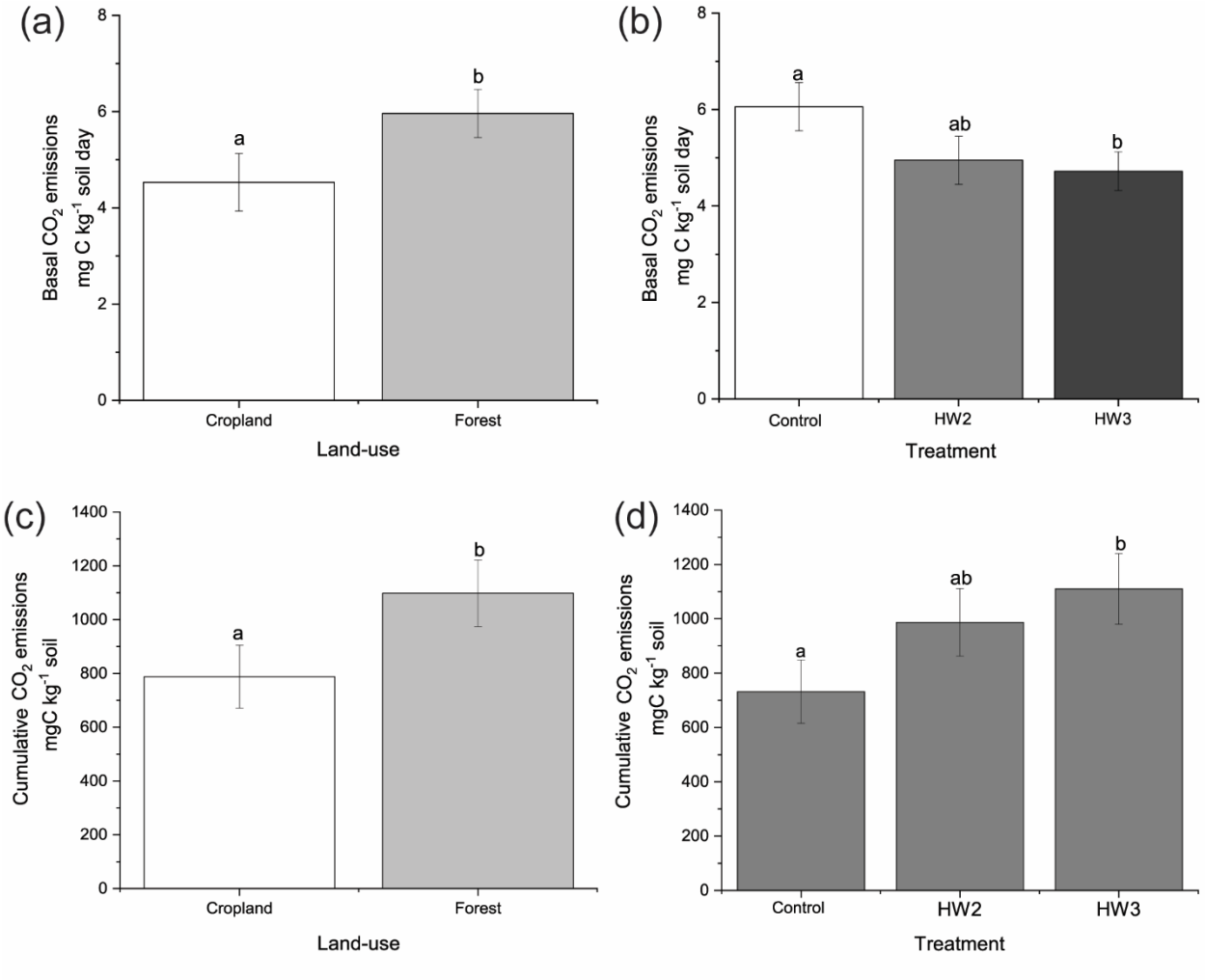

Fig. 4-3. Soil basal and cumulative CO_2 emissions as affected by land-use type and heat wave treatment. Vertical bars are standard errors of the means (n=4), and the same letter(s) indicate no significant differences at $P < 0.05$.

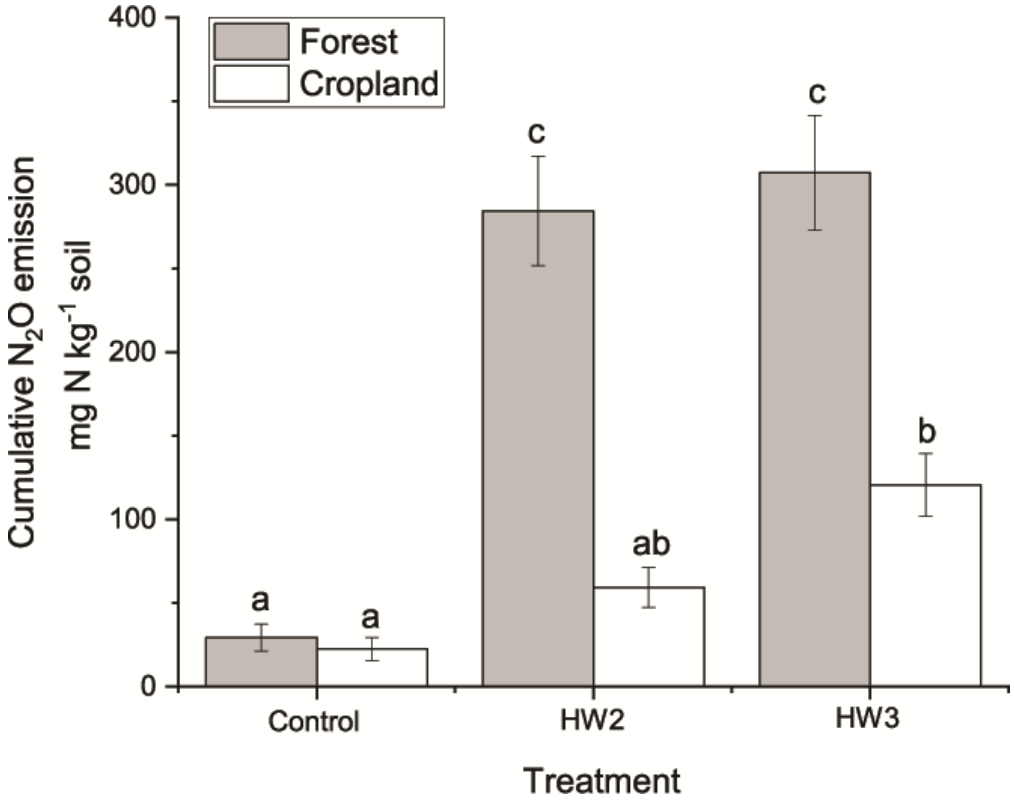

Fig. 4-4. Soil cumulative N_2O emissions as affected by the interaction effect of land-use type by heat wave treatment. Vertical bars are standard errors of the means (n=4), and the same letter(s) indicate no significant differences at $P < 0.05$

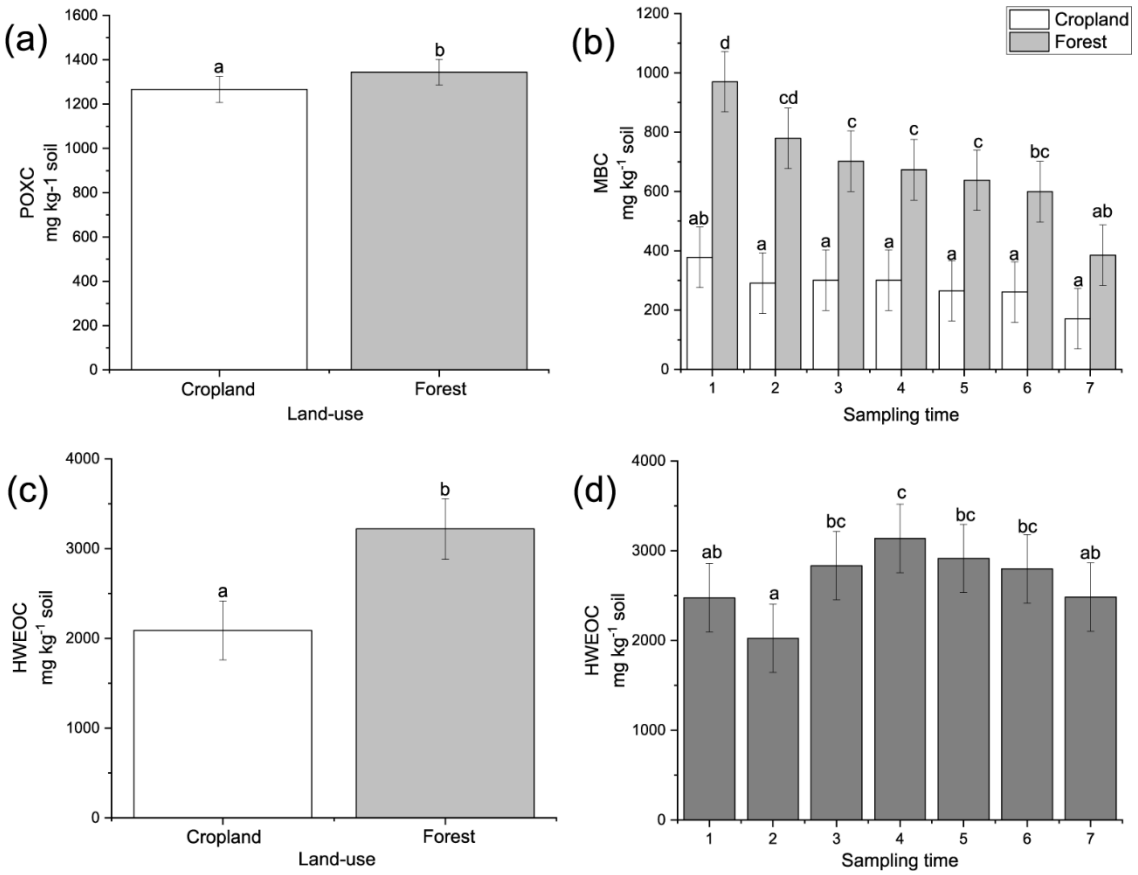

Fig. 4-5. Soil labile C [(permanganate oxidable C (POXC), microbial biomass C (MBC) and hot-water extractable organic C (HWEOC)] as affected by the land-use type and soil sampling time. Vertical bars are standard errors of the means (n=4), and different letters indicate significant differences at $p < 0.05$.

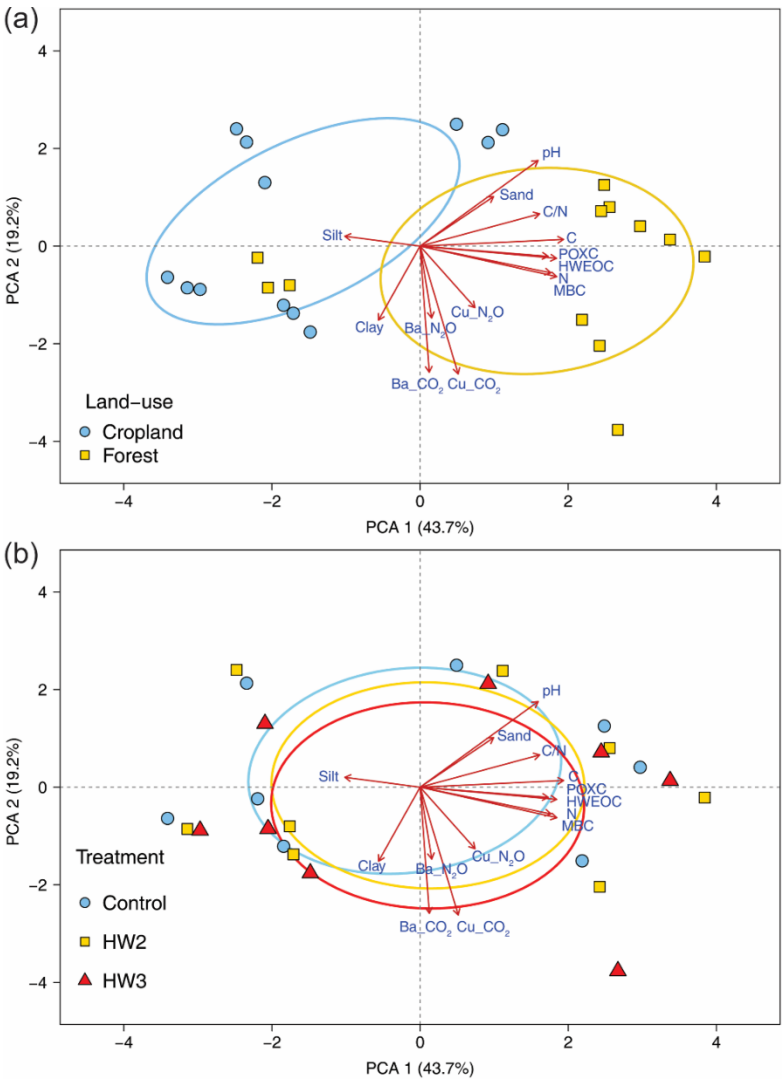

Fig. 4-6. The relationships among basic soil properties, soil labile C and soil CO_2 and N_2O emissions using a PCA ordination with 95% confidence ellipses to describe the effects of land-use and heat wave treatment.

Note: Ba_CO_2 and Ba_N_2O, Basal CO_2 and N_2O rate; Cu_CO_2 and Cu_N_2O, cumulative CO_2 and N_2O emissions; C, soil total C; N, soil total nitrogen; C/N. C to nitrogen ratio; POXC, permanganate oxidable C; MBC, microbial biomass C; HWEOC, hot-water extractable organic C.

References

Acosta-Martinez, V., Moore-Kucera, J., Cotton, J., Gardner, T. and Wester, D., 2014. Soil enzyme activities during the 2011 Texas record drought/heat wave and implications to biogeochemical cycling and organic matter dynamics. Appl. Soil Ecol. 75, 43-51. https://doi.org/10.1016/j.apsoil.2013.10.008.

Alberta Agriculture and Forestry, 2020. Interpolated Weather Data Since 1961 for Alberta Townships. Government of Alberta. https://acis.alberta.ca/township-data-viewer.jsp (accessed June 07, 2021).

An, Z.F., Bernard, G.M., Ma, Z.L., Plante, A.F., Michaelis, V.K., Bork, E.W., Carlyle, C.N., Baah-Acheamfour, M., Chang, S.X. 2021. Forest land-use increases soil organic carbon quality but not structural or thermal stability in a hedgerow system. Agric. Ecosyst. Environ. 321, 107617 https://doi.org/10.1016/j.agee.2021.107617.Anjileli, H., Huning, L.S., Moftakhari, H., Ashraf, S., Asanjan, A.A., Norouzi, H., AghaKouchak, A., 2021. Extreme heat events heighten soil respiration. Sci. Rep. 11, 1-9. https://doi.org/10.1038/s41598-021-85764-8

Baah-Acheamfour, M., Carlyle, C.N., Bork, E.W. and Chang, S.X., 2014. Trees increase soil carbon and its stability in three agroforestry systems in central Alberta, Canada. For. Ecol. Manag. 328, 131-139. https://doi.org/10.1016/j.foreco.2014.05.031.

Baah-Acheamfour, M., Chang, S.X., Carlyle, C.N. and Bork, E.W., 2015. Carbon pool size and stability are affected by trees and grassland cover types within agroforestry systems of western Canada. Agric. Ecosyst. Environ. 213, 105-113. https://doi.org/10.1016/j.agee.2015.07.016.

Benbi, D.K., Brar, K., Toor, A.S. and Singh, P., 2015. Total and labile pools of soil organic carbon in cultivated and undisturbed soils in northern India. Geoderma 237, 149-158. https://doi.org/10.1016/j.geoderma.2014.09.002.

Brown, J.R., Blankinship, J.C., Niboyet, A., van Groenigen, K.J., Dijkstra, P., Le Roux, X., Leadley, P.W. and Hungate, B.A., 2012. Effects of multiple global change treatments on soil N_2O fluxes. Biogeochemistry 109, 85-100. https://doi.org/10.1007/s10533-011-9655-2.

Butterbach-Bahl, K., Baggs, E.M., Dannenmann, M., Kiese, R. and Zechmeister-Boltenstern, S., 2013. Nitrous oxide emissions from soils: how well do we understand the processes and their controls? Philos. Trans. R. Soc. Lond. B Biol. Sci. 368, 20130122. https://doi.org/10.1098/rstb.2013.0122.

Ciais, P., Reichstein, M., Viovy, N., Granier, A., Ogée, J., Allard, V., Aubinet, M., Buchmann, N., Bernhofer, C. and Carrara, A., 2005. Europe-wide reduction in primary productivity caused by the heat and drought in 2003. Nature 437, 529-533. https://doi.org/10.1038/nature03972.

Culman, S.W., Snapp, S.S., Freeman, M.A., Schipanski, M.E., Beniston, J., Lal, R., Drinkwater, L.E., Franzluebbers, A.J., Glover, J.D., Grandy, A.S., 2012. Permanganate oxidizable carbon reflects a processed soil fraction that is sensitive to management. Soil Sci. Soc. Am. J. 76, 494-504. https://doi.org/10.2136/sssaj2011.0286.

Environment Canada, 2021. Weather Information. https://weather.gc.ca (accessed July 01, 2021).

Felton, A.J., Knapp, A.K., Smith, M.D., 2019. Carbon exchange responses of a mesic grassland to an extreme gradient of precipitation. Oecologia 189, 565-576. https://doi.org/10.1007/s00442-018-4284-2.

Frank, D., Reichstein, M., Bahn, M., Thonicke, K., Frank, D., Mahecha, M.D., Smith, P., Van der Velde, M., Vicca, S. and Babst, F., 2015. Effects of climate extremes on the terrestrial carbon cycle: concepts, processes and potential future impacts. Glob. Chang. Biol. 21, 2861-2880. https://doi.org/10.1111/gcb.12916.

Ghani, A., Dexter, M. and Perrott, K., 2003. Hot-water extractable carbon in soils: a sensitive measurement for determining impacts of fertilisation, grazing and cultivation. Soil Biol. Biochem. 35, 1231-1243. https://doi.org/10.1016/S0038-0717(03)00186-X.

Griebel, A., Bennett, L.T., Metzen, D., Pendall, E., Lane, P.N. and Arndt, S.K., 2019. Trading water for carbon: Sustained photosynthesis at the cost of increased water loss during high temperatures in a temperate forest. J. Geophys. Res. Biogeosci. 125. https://doi.org/10.1029/2019JG005239.

Gu, L., Post, W.M. and King, A.W., 2004. Fast labile carbon turnover obscures sensitivity of heterotrophic respiration from soil to temperature: a model analysis. Glob. Biogeochem. Cycles 18. https://doi.org/10.1029/2003GB002119.

Hagedorn, F., Martin, M., Rixen, C., Rusch, S., Bebi, P., Zürcher, A., Siegwolf, R.T., Wipf, S., Escape, C., Roy, J., 2010. Short-term responses of ecosystem carbon fluxes to experimental soil warming at the Swiss alpine treeline. Biogeochemistry 97, 7-19. https://doi.org/10.1007/s10533-009-9297-9.

Hoover, D.L., Knapp, A.K., Smith, M.D., 2014. Resistance and resilience of a grassland ecosystem to climate extremes. Ecology 95, 2646-2656. https://doi.org/10.1890/13-2186.1.

Hoover, D.L., Knapp, A.K. and Smith, M.D., 2016. The immediate and prolonged effects of climate extremes on soil respiration in a mesic grassland. J. Geophys. Res. Biogeosci. 121, 1034-1044. https://doi.org/10.1002/2015JG003256.

Hoover, D., Knapp, A. and Smith, M., 2017. Photosynthetic responses of a dominant C4 grass to an experimental heat wave are mediated by soil moisture. Oecologia 183, 303-313. https://doi.org/10.1007/s00442-016-3755-6.

Jarvi, M.P. and Burton, A.J., 2020. Root respiration and biomass responses to experimental soil warming vary with root diameter and soil depth. Plant Soil, 451, 435-446. https://doi.org/10.1007/s11104-020-04540-1.

Jeong, D.I., Sushama, L., Diro, G.T., Khaliq, M.N., Beltrami, H., Caya, D., 2016. Projected changes to high temperature events for Canada based on a regional climate model ensemble. Clim. Dyn. 46, 3163-3180. https://doi.org/10.1007/s00382-015-2759-y.

Jílková, V., Jandová, K., Cajthaml, T., Devetter, M., Kukla, J., Starý, J., Vacířová, A., 2020. Organic matter decomposition and carbon content in soil fractions as affected by a gradient of labile carbon input to a temperate forest soil. Biol. Fertil. Soils 56, 411-421. https://doi.org/10.1007/s00374-020-01433-4.

Joergensen, R.G., 1996. The fumigation-extraction method to estimate soil microbial biomass: calibration of the k_{EC} value. Soil Biol. Biochem. 28, 25-31. https://doi.org/10.1016/0038-0717(95)00102-6.

Knorr, W., Prentice, I.C., House, J., Holland, E., 2005. Long-term sensitivity of soil carbon turnover to warming. Nature 433, 298-301. https://doi.org/10.1038/s41467-020-17790-5.

Lenth, R. and Lenth, M.R., 2018. Package 'lsmeans'. Am. Stat. 34, 216-221.

Li, L.F., Qian, R.Y., Wang, W.J., Kang, X.M., Ran, Q.W., Zheng, Z.Z., Zhang, B., Xu, C., Che, R.X., Dong, J.F., 2020. The intra-and inter-annual responses of soil respiration to climate extremes in a semiarid grassland. Geoderma 378, 114629. https://doi.org/10.1016/j.geoderma.2020.114629.

Liu, R., Hayden, H.L., Suter, H., Hu, H.W., Lam, S.K., He, J.Z., Mele, P.M., Chen, D.L., 2017. The effect of temperature and moisture on the source of N_2O and contributions from ammonia oxidizers in an agricultural soil. Biol. Fertil. Soils 53, 141-152. https://doi.org/10.1007/s00374-016-1167-8.

Lu, M., Zhou, X.H., Yang, Q., Li, H., Luo, Y.Q., Fang, C.M., Chen, J.K., Yang, X., Li, B., 2013. Responses of ecosystem carbon cycle to experimental warming: a meta-analysis. Ecology 94, 726-738. https://doi.org/10.1890/12-0279.1.

Meyer, L. and Pachauri, R., 2014. The Fifth assessment report of the intergovernmental panel on climate change. Geneva: IPCC Secretariat.

Perkins, S.E. and Alexander, L.V., 2013. On the measurement of heat waves. J. Clim. 26, 4500-4517. https://doi.org/10.1175/JCLI-D-12-00383.1.

Plante, A.F., Fernández, J.M., Haddix, M.L., Steinweg, J.M. and Conant, R.T., 2011. Biological, chemical and thermal indices of soil organic matter stability in four grassland soils. Soil Biol. Biochem. 43, 1051-1058. https://doi.org/10.1016/j.soilbio.2011.01.024.

R Core Team, 2018. R: A language and environment for statistical computing. R Foundation for Statistical Computing. Austria: Vienna.

Reichstein, M., Bahn, M., Ciais, P., Frank, D., Mahecha, M.D., Seneviratne, S.I., Zscheischler, J., Beer, C., Buchmann, N. and Frank, D.C., 2013. Climate extremes and the carbon cycle. Nature 500, 287-295. https://doi.org/doi:10.1038/nature12350.

Salome, C., Nunan, N., Pouteau, V., Lerch, T.Z., Chenu, C., 2010. Carbon dynamics in topsoil and in subsoil may be controlled by different regulatory mechanisms. Glob. Change Biol. 16, 416-426. https://doi.org/10.1111/j.1365-2486.2009.01884.x.

Shrestha, B.M., Bork, E.W., Chang, S.X., Carlyle, C.N., Ma, Z., Döbert, T.F., Kaliaskar, D., Boyce, M.S., 2020. Adaptive Multi-Paddock Grazing Lowers Soil Greenhouse Gas Emission Potential by Altering Extracellular Enzyme Activity. Agronomy 10, p.1781. https://doi.org/10.3390/agronomy10111781.

Smith, M.D., 2011. An ecological perspective on extreme climatic events: a synthetic definition and framework to guide future research. J. Ecol. 99, 656-663. https://doi.org/10.1111/j.1365-2745.2011.01798.x.

Smoyer-Tomic, K.E., Kuhn, R., Hudson, A., 2003. Heat wave hazards: an overview of heat wave impacts in Canada. Nat. Hazards 28, 465-486. https://doi.org/10.1023/A:1022946528157.

Stone, M.M. and Plante, A.F. 2015. Relating the biological stability of soil organic matter to energy availability in deep tropical soil profiles. Soil Biol. Biochem. 89, 162-171. https://doi.org/10.1016/j.soilbio.2015.07.008.

Tatarinov, F., Rotenberg, E., Maseyk, K., Ogée, J., Klein, T., Yakir, D., 2016. Resilience to seasonal heat wave episodes in a Mediterranean pine forest. New Phytol. 210, 485-496. https://doi.org/10.1111/nph.13791.

Teskey, R., Wertin, T., Bauweraerts, I., Ameye, M., McGuire, M.A., Steppe, K., 2015. Responses of tree species to heat waves and extreme heat events. Plant Cell Environ. 38, 1699-1712. https://doi.org/10.1111/pce.12417.

Teuling, A.J., Seneviratne, S.I., Stöckli, R., Reichstein, M., Moors, E., Ciais, P., Luyssaert, S., Van Den Hurk, B., Ammann, C., Bernhofer, C., 2010. Contrasting response of European

forest and grassland energy exchange to heatwaves. Nat. Geosci. 3, 722-727. https://doi.org/10.1038/NGEO950.

The Climate Atlas of Canada, 2019. Climate Atlas of Canada, version 2, using BCCAQv2 climate model data. https://climateatlas.ca/climate-atlas-version-2.

Vance, E.D., Brookes, P.C., Jenkinson, D.S., 1987. An extraction method for measuring soil microbial biomass C. Soil Biol. Biochem. 19, 703-707. https://doi.org/10.1016/0038-0717(87)90052-6.

von Lützow, M. and Kögel-Knabner, I., 2009. Temperature sensitivity of soil organic matter decomposition—what do we know? Biol. Fertil. Soils 46, 1-15. https://doi.org//10.1007/s00374-009-0413-8.

Weil, R.R., Islam, K.R., Stine, M.A., Gruver, J.B. and Samson-Liebig, S.E., 2003. Estimating active carbon for soil quality assessment: A simplified method for laboratory and field use. Am. J. Alternative Agr., 3-17.

Xu, X., Cheng, X., Zhou, Y., Luo, Y., Ruan, H., Wang, J., 2010. Variation of soil labile organic carbon pools along an elevational gradient in the Wuyi Mountains, China. J. Res. Ecol. 1, 368-374. https://doi.org/10.3969/j.issn.1674-764x.2010.04.010.

Xu, X., Thornton, P.E., Post, W.M., 2013. A global analysis of soil microbial biomass carbon, nitrogen and phosphorus in terrestrial ecosystems. Glob. Ecol. Biogeogr. 22, 737-749. https://doi.org/10.1111/geb.12029.

Yuan, W.P., Cai, W.W., Chen, Y., Liu, S.G., Dong, W.J., Zhang, H.C., Yu, G.R., Chen, Z.Q., He, H.L. and Guo, W.D., 2016. Severe summer heatwave and drought strongly reduced carbon uptake in Southern China. Sci. Rep. 6, 1-12. https://doi.org/10.1038/srep18813.

Zhang, F.W. and Cao, G.M., 2017. Resilience of Energy and CO 2 Exchange to a Summer Heatwave in an Alpine Humid Grassland on the Qinghai-Tibetan Plateau. Pol. J. Environ. Stud. 26. https://doi.org/10.15244/pjoes/64912.

Chapter 5. Quantifying the past, current, and projected carbon stocks of forests associated with three agroforestry systems in central Alberta, Canada

1. Introduction

Agroforestry systems are known carbon (C) sinks, playing a critical role in C sequestration and, therefore, climate change mitigation in the Canadian Prairies (Kort and Turnock, 1998; Oelbermann et al., 2004; Baah-Acheamfour et al., 2014). Quantification of C stocks in agroforestry systems is essential to understand the full capability of agroforestry systems to provide a practical approach for C sequestration. However, few studies report on the past C declines, current C sequestration status, and future potentials of expanding agroforestry systems across the larger landscape. Studies of C sequestration capability in agroforestry systems are often limited to plot level, few C pools and specific agroforestry systems, such as shelterbelts (planted trees along field margins), within specific regions (Amichev et al., 2016; Abbas et al., 2017; Amichev et al., 2020). In general, few studies have investigated regional-scale C stocks and the potential to increase C stocks through agroforestry system expansion, thereby limiting our understanding of where and how agroforestry systems may be an effective C sequestration strategy.

The province of Alberta has the second largest agricultural land area, ~ 20.6 million ha, or 31.7% of the agricultural land in Canada (Statistics Canada, 2014) and has many different types of agroforestry systems (Baah-Acheamfour et al., 2017). Agroforestry systems (specifically hedgerow, shelterbelt and silvopasture) are critical for increasing C sequestration in agroecosystems in Canada (Acheamfour et al., 2014; Amichev et al., 2016; Lim et al., 2018). For

example, shelterbelt systems comprising 6 million trees in the agricultural landscape in the Canadian prairie could store 0.4 million tons (Mt) of additional C annually (Kort and Turnock, 1998) to offset increases in atmospheric CO_2 (Pankiw and Piwowar, 2010). However, regional C stock and associated C valuation in such agroforestry systems are not well documented. The availability of regional C stock data and understanding the potentials for C sequestration through agroforestry development will help the development of agroforestry systems.

Remote sensing (RS) is a readily available and effective tool to determine the area extent of agroforestry systems over vast areas (Wiseman et al., 2009). Imagery from Google, Bing and ESRI satellite image repository have high-resolution, georeferenced information suitable for land-use classification and the calculation of vegetation inventories, which can be used for quantifying C stocks. The Google Earth Engine is a cloud-based platform that is characterized by its strong parallel analysis capacity and large geophysical datasets(e.g., Landsat, MODIS, Sentinel, DEM, land-use) (Hansen et al., 2013; Gorelick et al., 2017), which brings immense computational power of Google to researchers studying large-scale environmental monitoring and analysis, such as climate monitoring (Ravanelli et al., 2018), land-use change and classification analysis with high efficiency (Jin et al., 2019; Liu et al., 2020). According to Hansen et al. (2013), it took 100-hr to process over half a million Landsat-7 images (~ 643 Tebibyte) within the Google Earth Engine. It produced global map forests; the method was thousands of times faster than traditional processing methods. However, no study has used the Google Earth Engine for regional C stock estimation for agroforestry systems.

This study aims to quantify the areal extent of existing forest land-use, loss of forest and the associated C stocks and economic values of forests within hedgerow, shelterbelt, and silvopasture systems, and the potential for expansion of shelterbelts and the associated C

sequestration in the agricultural landscape in central Alberta (hereafter central Alberta), Canada. We aimed to answer the following questions: 1) how much C is stored in existing forest land-use in agroforestry systems (hedgerow, shelterbelt and silvopasture systems) in central Alberta? 2) What is the amount of forest land-use and the associated C stocks lost from 2001 to 2020 in agricultural lands in central Alberta? And 3) to what extent could C storage be enhanced by the expansion of shelterbelt systems in central Alberta?

2. Materials and methods

2.1. Study area and dataset

This study focuses on the agricultural land of the central Alberta region (52° 20' ~ 55° 15' N, 110° 0' ~ 116° 39' W), which belongs to a humid continental climate and includes central parkland, central mixwood and dry mixwood ecoregions of Alberta (Environment and Parks, 2006). The annual precipitation and temperature of the region range from 474 ~ 432 mm and 1.6 ~ 2.5 °C from north to south, respectively (Environment Canada, 2020). The region is characterized by Gray Luvisolic and Dark Gray Chernozemic soils, based on the Canadian system of soil classification (Soil Classification Working Group, 1998; same below), in the north and Black Chernozemic and Dark Brown Chernozemic soils in the south. The extent of agricultural land was based on the shapefile "Organic Matter Content of Cultivated Soils" in the Alberta Open Government Program (Alberta Agriculture and Forestry, 2016), in which the total area under cultivation was provided. This dataset also allows for differentiation of hedgerows, shelterbelts and silvopasture systems across the study area. However, due to the considerable

time investment to map each agroforestry system for the whole study area, randomly selected plots were chosen (manually mapped each agroforestry system in those plots) to represent the region. The "3 × 7 km Sample-based Human Footprint Data" released by Alberta Biodiversity Monitoring Institute (ABMI) offered a selection of pre-defined plots (Alberta Biodiversity Monitoring Institute, 2017). However, ABMI plots were not uniformly distributed across the region and did not cover several areas (no ABMI plot available) in parts of central Alberta (Fig. 5-1). Thus, we randomly selected 35 plots from the ABMI plots and an additional 15 plots across the area where no ABMI plots were available (the 50 plots covered a total of 0.105 M ha, representing 1.9% of the central Alberta region). Within each plot, forests associated with the shelterbelt, hedgerow and silvopasture systems were recognized (Fig. 5-2) by object-based classification methods from the Bing Aerial Imagery, ESRI Satellite Imagery and Google Satellite Imagery.

Detailed descriptions of some of the characteristics of forests associated with hedgerows, shelterbelt and silvopasture systems that were used for obtaining the C density data for C stock estimation can be found in Baah-Acheamfour et al. (2014) and Lim et al. (2018). Briefly, hedgerow and shelterbelt forests have linear boundary features, and hedgerow forests are comprised of broadleaf deciduous trees (e.g., *Betula papyrifera* and *Populus tremuloides* with an average tree age of 28 years), along with various shrubs (e.g., *Prunus virginiana* and *Amelanchier alnifolia*) and herbaceous understory vegetation (e.g., *Bromus tectorum*) at field edges, while trees (e.g., *Picea glauca* and *Caragana arborescens*) with an average tree age of 34 years) in shelterbelt systems are planted. Silvopasture forests consist of mixtures of widely spaced trees (e.g., *Populus tremuloides* and *Betula papyrifera*) with an average tree age of 30 years) and grasslands and are grazed by livestock (Baah-Acheamfour et al., 2014; Lim et al.,

2018). As silvopasture forests were not linear and had unforested areas within each silvopasture forest, the forested area at each silvopasture site was manually determined after the delineation of each silvopasture site.

We estimated past forests loss focusing on hedgerow and silvopasture systems by assuming the loss of forest in cropland and grassland attributed to hedgerow and silvopasture systems, respectively. The road and field edges were marked as the potential areas for reforestation with shelterbelts and the potential for increasing C sequestration by planting shelterbelt systems over time (Fig. 5-2).

The extent of land area under grazed grassland and cultivated cropland within the plots (Fig. 5-3) was derived from the "Wall-to-Wall Human Footprint Inventory" (Alberta Biodiversity Monitoring Institute, 2018) and cross-validated with "Alberta Satellite Land Cover" (Alberta Agriculture and Forestry, 2018), "Central Parkland Vegetation Inventory (CPVI) Polygons" (Environment and Parks, 2012), Bing Aerial Imagery, ESRI Satellite Imagery, and Google Satellite Imagery. The annual forest loss from the agricultural area was obtained by extracting the yearly forest loss information from "Global Forest Change (2000–2020) v1.8" over the period 2001 to 2020 (Hansen et al., 2013), using the cultivated land area.

2.2. Carbon density in different agroforestry systems

The carbon density in the forest land-use component of hedgerow, shelterbelt and silvopasture systems were reported to be 369.0, 392.5 and 368.4 t ha^{-1} [these values included C stock in aboveground vegetation, roots, litter, partially decomposed litter and humus (referred to as LFH) as well as SOC stocks to 75 cm depth]; in contrast, the C stocks within the cropland and grazed

grassland land-use components of the agroforestry systems were 198.9 and 191.8 t ha^{-1}, respectively (Table 5-1; Lim et al., 2018). These C stocks were applied to each corresponding land-use area at the plot and regional scale for computation of C stocks and the estimation of C stock changes in combination with the spatial data in the current study under the assumption that those C densities are representative for the entire study area in central Alberta.

2.3 Calculation methods

The delineation of area under forest land-use within agroforestry systems and the potential area for shelterbelt forest expansion were done using QGIS 3.12.0 (QGIS Development Team, 2018) and ArcGIS Pro 2.7 (Esri Inc, 2020), with "NAD83 / Alberta 10-TM (Forest)" as the source coordinate reference systems. All map outputs were created in ArcGIS Pro 2.7 (Esri Inc, 2020). The information on areas and C stocks, both current and past, in each land-use within the 50 plots was used to represent the corresponding information (e.g., areas and distributions of agroforestry systems, carbon density) in the central Alberta region. Total C stocks within the forest land-use associated with the shelterbelt, hedgerow and silvopasture systems were obtained by multiplying the area under each forest type by the corresponding C stock density. Regional C stock size was calculated by summing the C stocks in cropland, grassland and forest land-use in the hedgerow, shelterbelt and silvopasture systems. Annual forest loss (total, hedgerow forests and silvopasture forests) was analyzed using the Google Earth Engine. The C loss in the hedgerow and silvopasture systems was calculated as the difference in C density between hedgerow forests and adjacent cropland, and between silvopasture forests and adjacent grazed grasslands. It should be noted that time lags of C loss with deforestation were not considered in

the current study, and riparian forests (forests that are adjacent to waterways and wetlands) were not included in the analysis. The C value of \$40 t^{-1} CO_2 equivalent for the year 2021 (Energy Rates, 2021) was used to estimate the potential value of C stocks in the region.

3. Results

3.1 Carbon stocks and their valuation of current agroforestry systems

The three agroforestry systems occupied 20936.1 ha in the 50 plots, accounting for 22.8% of the total agricultural land area in the 50 plots (Table 5-1). Shelterbelt and hedgerow forests accounted for 0.3 and 1.5% of the land area, respectively, while silvopasture forests occupied 21.0% of the land area. Grassland and cropland accounted for 23.0 and 54.1%, respectively, of the total agricultural land area in the 50 plots. The total linear length of hedgerow and shelterbelt forests was 1174.6 km in the 50 plots. The total C stock in the agricultural land area in the 50 plots was estimated to be 21.6 Mt, of which 0.5, 2.3, and 32.9% were stored in the shelterbelt, hedgerow, and silvopasture forests, respectively. In contrast, the grassland and cropland together comprised a total of 77.2% of the land area in the 50 plots, and stored 64.3% of the total C. The incremental economic value for C storage by planting forests to form shelterbelt and hedgerow in cropland and silvopasture in grassland were estimated to be \$28420.5, \$24970.7 and \$25924.9 ha^{-1}, respectively (Table 5-1).

The forest land-use associated with the three common agroforestry systems was estimated to occupy 24390 (shelterbelt), 122888 (hedgerow) and 1750791 ha (silvopasture) in central Alberta, Canada. The total C stock in the forest land-use in the three agroforestry systems in

central Alberta was estimated to be 699.9 Mt C (Table 5-1), worthing approximately $102.7 billion. Silvopasture forests stored the largest amount of C with 645 Mt C, followed by hedgerow and shelterbelt forests with 45.3 and 9.6 Mt C, respectively. Grassland and cropland stored 364.5 and 898.0 Mt C, respectively. The total length of shelterbelt forests (21263.5 km) and hedgerow forests (85228.4 km) were summed to be 106491.9 km. The incremental C value of shelterbelt, hedgerow and silvopasture forests compared with cropland and grassland was estimated to be $0.9, $2.9 and $45.1 billion (Table 5-1).

3.2 Loss of forest land-use in agroforestry systems between 2001 and 2020

The forest area within the agricultural region in central Alberta has declined, with a mean forest loss rate of 2425.2 ha yr^{-1} from 2001 to 2020. Annual forest loss rates peaked in 2016, slowing thereafter to a low of -770 ha in 2020 (Fig. 5-4a). The total forest area lost over the 20 years was 48503.4 ha, of which silvopasture forests represented over 80% of the total loss. The estimated C loss ranged from 0.1 to 1.0 Mt of C per year, with a mean loss rate of 0.4 Mt C yr^{-1} from 2001 to 2020. The C loss when the forest land-use in hedgerow and silvopasture was changed to cropland and grassland was 1.6 and 6.9 Mt C, respectively (Fig. 5-4b), which represented a net decline of 8.5 Mt C, representing a loss of $1247.8 M of sequestered C across the agricultural land in central Alberta from 2001 to 2020.

3.3 Future C stock increment with shelterbelt expansion

The total length of non-forested cropland field margins potentially available to plant shelterbelt forests was estimated to be 46285.3 km, a 230% increase in the current length of shelterbelt forests. The estimated potential increase in C stocks over time due to shelterbelt expansion was 21.8 M ton C, or 2.3 times the C stocks currently held in shelterbelt forests (9.6 M ton C).

4. Discussion

4.1. Past, current, and future carbon stocks in central Alberta

The current study showed that the loss of forest and associated C in the studied region due to converting forested areas to cropland and grassland (decrease in hedgerow and silvopasture systems) in the past 20 years was substantial, totalling 8.5 Mt C, highlighting the urgency to protect hedgerow and silvopasture systems for C sequestration and providing other ecological services. Annual C loss due to forest removal in cropland varied substantially from 2001 to 2020, while the C loss decreased dramatically since 2015, possibly due to the improving recognition of the importance of trees as well as change in policy. The loss of forest in agroforestry systems on the prairies is mainly due to the shortage of labour in maintenance, the need for more space for maneuvering large agricultural equipment, and tree ageing and death (Rempel et al., 2013; 2014). Meanwhile, trees in agroforestry systems may be harmful as they can be the host for pests, bacteria and invasive plants (Gordon et al., 2009), which may negatively influence crop yield and make landowners want to remove them. It should be noted that I did not consider time lags of C loss with deforestation and assumed that C stock changes in sync with land-use change

when evaluating past C loss. Moreover, most C from agroforestry removal is eventually burned (Rudd et al., 2021).

The current study unveiled that a significant amount of C (sum of cropland, grassland, and forests in the hedgerow, shelterbelt and silvopasture systems, both above- and belowground C and SOC to 75 cm) stored in agricultural lands in central Alberta (1962.4 Mt C), and agroforests stored a disproportionately large amount of C (699.9 Mt) relative to their land area (22.8%), which was around two times the C stored in grasslands (23.1% of the land area), suggesting that planting trees in agricultural land to form agroforestry systems is crucial for C sequestration and climate change mitigation in the region (Amichev et al., 2015; Amichev et al., 2016; Ha et al., 2019; Kort and Turnock, 1998; Piwowar et al., 2016).

There is also substantial potential for the region to increase C storage by implementing new shelterbelt systems on the road/field edges suitable for shelterbelt establishment. Over time, the C stored in the current shelterbelt forest can nearly be tripled by shelterbelt planting, with an approximate value of $3200.3 M of sequestered C. However, the increase of C stocks in shelterbelts is a long process, newly planted shelterbelts may take decades to reach the estimated valuation, and it should be noted that the shelterbelt planation can have an annual median SOC accrual rate of 0.7 t ha^{-1} yr^{-1} (Dhillon and Van Rees, 2017). Moreover, proper management practices in the cropped component are also key to C sequestration. For example, cover crops, no-till, manure and biochar amendments can increase C storage in agroforestry systems (Stavi and Lal., 2013; Gross et al., 2021).

4.2 Valuation of forests associated with agroforestry systems

Information on the value of C stored in the forest land-use in agroforestry systems is lacking but is key to promoting agroforestry practices for climate change mitigation. Using the current price of \$40 t^{-1} CO_2 that is charged to industrial emitters in Alberta, the total value of C in the agricultural lands was \$288.1 billion. The C value of agroforestry forests is about \$102.7 billion at the expense of 22.8% of the land area in central Alberta. In contrast, the area of forest associated with agroforestry systems was less than half of the cropland, highlighting the significant C storage brought about by current agroforestry systems and the potential for agroforestry expansion by converting cropland to agroforestry system. This valuation only accounts for C sequestration and does not include other ecosystem services (i.e., soil and water retention, wind protection, biodiversity conservation) provided by these forests (Jose, 2009). Additionally, agroforestry systems are the nexus of sustainable intensification (Van Noordwijk, 2020), and they may be essential means of balancing the environment and agricultural production. Agroforestry systems provide many benefits to societies and ecosystems. However, many of such benefits are not fully understood by the general public; thus, improved guidelines and economic incentives are advisable for promoting the development of agroforestry systems (Van Noordwijk, 2020). It should be noted that the C tax in Alberta keeps increasing each year (Energy Rates, 2021), the valuation of C in agroforestry systems will be even more substantial in the future.

4.3 Limitations and future recommendations

The datasets from the Open Government Program of the Alberta Government were validated and updated when released. All datasets need to be customized and combined with other data sources

for validation and analysis. Meanwhile, some image tiles used in this study may not be current due to delays in updating them by the source provider, which may introduce errors in the delineation of the agroforestry systems and in the subsequent calculation of C stocks in those agroforestry systems.

In the "Hansen Global Forest Change v1.8 (2000-2020)" (Hansen et al., 2013) used for estimating the annual forest loss and associated C loss in agroforestry systems, forest loss information was updated each year since the initial release of the database, while information on forest gains is not updated annually and only available for 2000-2012 (~ 970 ha forest gains in this period in central Alberta). No other dataset is available for the estimation of annual forest gain in the region. Future work should create forest gain information and combine it with forest loss information to understand net forest change in the region.

In estimating shelterbelt expansion, we only characterized road/field edges as the potential area for forest expansion. However, shelterbelt forests may be set up in the middle of the lands and surrounding farmyards, which were not easy to quantify; thus, our results likely underestimate the potential of shelterbelt expansion to enhance C stocks in central Alberta. Carbon stock estimation in this study utilized data from the average value of C stocks in 36 agroforestry systems (each has 12 sites of hedgerow, shelterbelt and silvopasture systems with average tree age > 20 years) (Lim et al., 2018), and all other values were extrapolated from those values. Those values may be expected to discount influential factors such as tree sizes, tree species, tree ages, diameters and ecosite qualities, all of which are known to be crucial factors in controlling C stocks (Ma et al., 2020); for example, large trees were reported to dominate C storage in forests (Mildrexler et al., 2020). Meanwhile, younger shelterbelts may show a loss of C stocks and thereafter require decades of growth to occur before shelterbelts show positive

effects on C sequestration potential (Dhillon and Van Rees, 2017). Management practices (e.g., tillage, irrigation, fertilizer, and herbicide) may influence the total C stock in agroforestry systems, Amichev et al. (2021) found that management practices increased carbon stocks for two thirds (4 out or 6) of the tree species studied regardless of tree spacing in the shelterbelt system, and the increase of C stocks due to management practices varied across planting design, land condition and tree species. The absence of management practices in C stocks estimation may cause doubtful information on the potential of C stocks sequestration (Amichev et al., 2021). Therefore, the C stocks in this study should be used with care.

In the future, more efforts should be given to collect detailed information about the factors that influence C stocks relative to different agroforestry systems, and further efforts put into calibrating and validating predictive models of C gain and loss (Kröbel et al., 2020). Meanwhile, increasing forests by afforestation (e.g., of shelterbelts) may be a key component enhancing C stocks in the region. Notably, attention should be paid to understory C (e.g., stock and stability) in agroforests, as the forest understory C may have a greater mean C age and take up a disproportional portion to the forest C sink (Hubau et al., 2019), which may also be a source of stable SOC, while such knowledge is limited in agroforestry systems. Future studies should also assess natural increases in the hedgerow forest, such as under ongoing fire suppression (Bailey and Wroe, 1974; Bork et al., 2021), to better understand the complete dynamics of agroforestry land-uses and associated C stocks.

5. Conclusions

This study quantified the past forest C loss, current C stocks, and potential future C stock increments of three agroforestry systems within a 9.3 M ha area of central Alberta, Canada. Hedgerows, shelterbelts, and silvopasture represent a substantial C storage, and there is potential for expanding shelterbelts in central Alberta, which could then sequester more C. Despite this, past land-use dynamics since 2001 show ongoing forest loss from hedgerow and silvopasture systems leading to a considerable loss in C storage (a net decline of 8.5 M t C from 2001-2020). Policymakers need to be aware of the ongoing risk of C losses due to the conversion of forested areas within agroforestry systems into cropland or grassland and opportunities to enhance C stocks with tree retention and planting. Meanwhile, policies should be implemented to promote the maintenance, renovation, and expansion of agroforestry systems. Future research should expand our understanding of the valuation of agroforestry systems, including the study of the complete suite of ecosystem services provided by forested areas and how ongoing forest gains or losses influence these services. In our assessment of C sequestration and valuation, it is clear that the benefits of maintaining and establishing or expanding agroforestry systems in central Alberta are substantial if this additional C stored by farmers using agroforestry systems were monetized

Table 5-1. Estimated C stocks, the relative contribution of C stocks, land areas occupying different land-uses, and the incremental C values comprising different land-uses, found in various agricultural land-uses across 50 study plots and the greater study region of central Alberta, Canada.

Land-use	Carbon density[a] (t ha^{-1})	Selected 50 plots				Central Alberta region			
		Estimated total C (Mt)	Percent of C stocks in various agricultural lands	Percent of the total agricultural land area[b]	Incremental C value[c]($\$ha^{-1}$)	Estimated total C (Mt)	Percent of C stocks in various agricultural lands	Percent of the total agricultural land area[b]	Incremental C value[c](Total $billion)
Shelterbelt forests	392.5	0.1	0.5	0.3	28420.5	9.6	0.5	0.3	0.9
Hedgerow forests	369	0.5	2.3	1.5	24970.7	45.3	2.3	1.5	2.9
Silvopasture forests	368.4	7.1	32.9	21	25924.9	645.0	32.9	21	45.1
Grassland	191.8	4	18.5	23.1	n.a	364.5	18.5	23.1	n.a
Cropland	198.9	9.9	45.8	54.1	n.a	898	45.8	54.1	n.a
Total	n.a	21.6	100%	100%	n.a	1962.4	100%	100%	n.a

Note: “a” indicates the C stocks included aboveground vegetation C stock, roots, LFH and soil C to 75 cm depth; “b” indicates that the percent of the total agricultural land area did not include urban-industrial, water, etc.; “c” indicates that the incremental C value is calculated based on \$40 ton^{-1} CO_2 equivalent and “n.a” indicates not available.

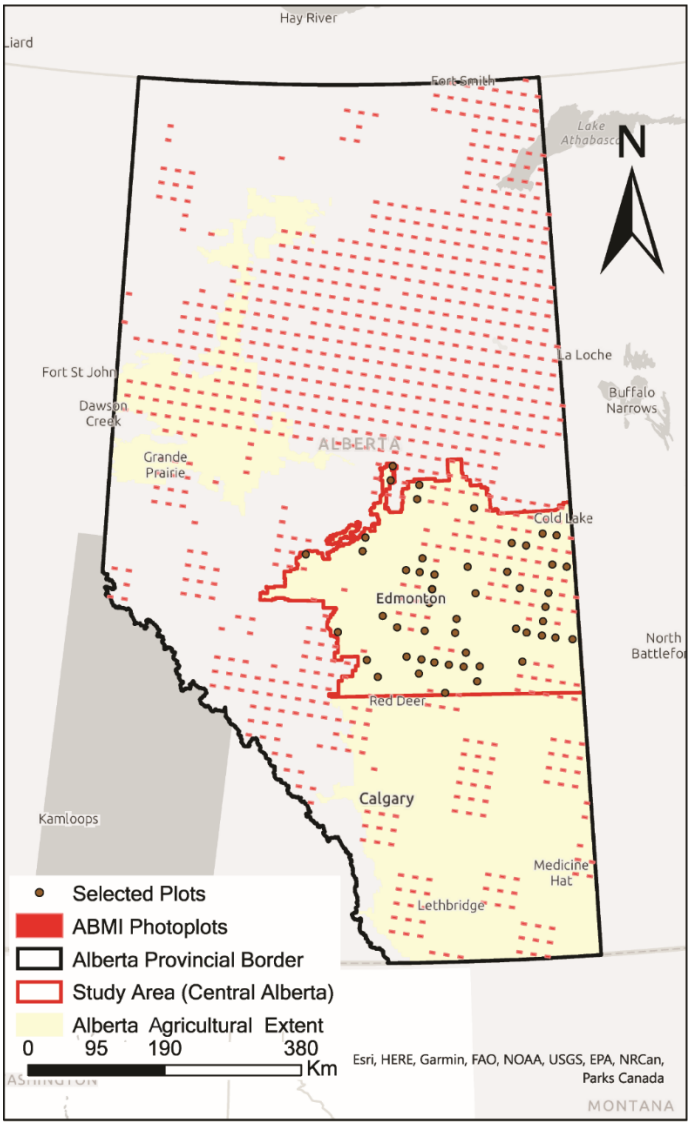

Fig. 5-1. Location of the study area in Alberta, Canada, and selected plots for object-based supervised classification of land-use activity.

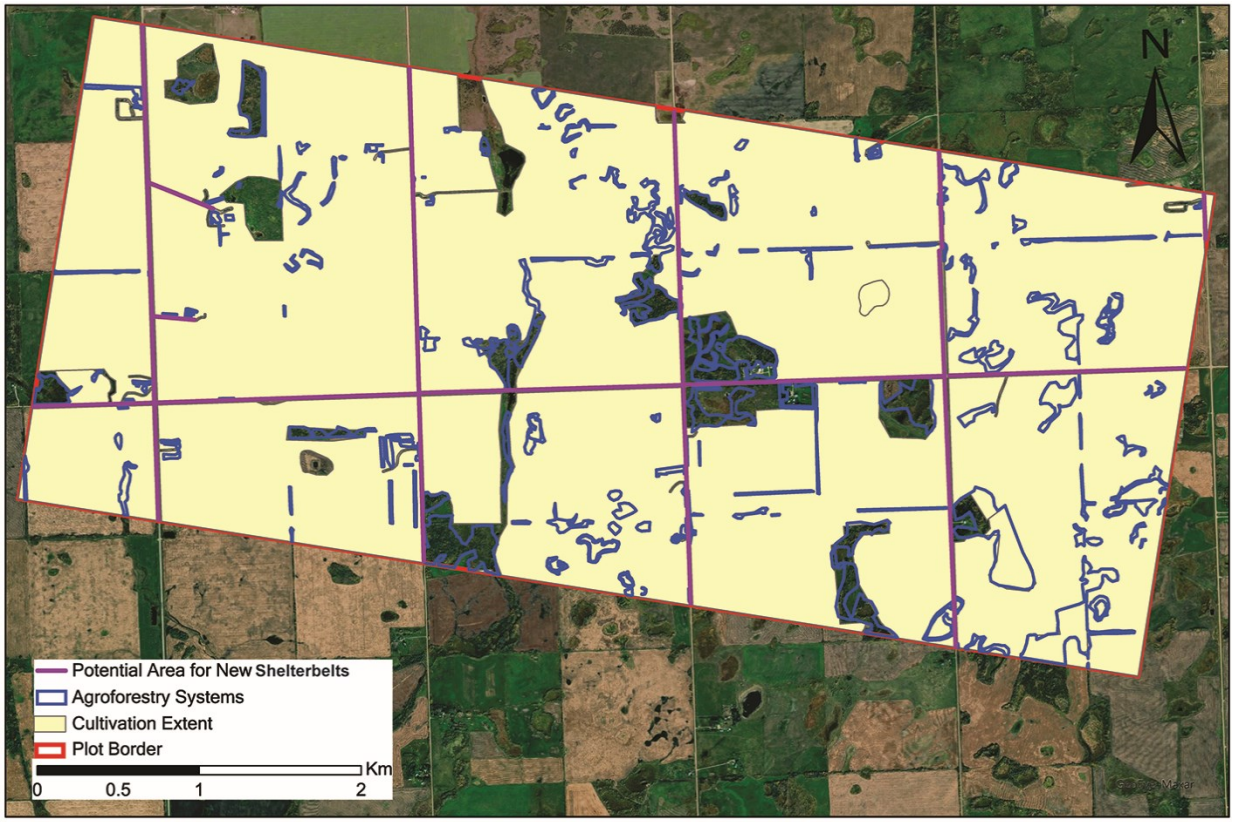

Fig. 5-2. Example of a study plot used to assess changes in land-use activity, including agroforestry systems. The cultivation extent means the grassland and cultivated cropland.

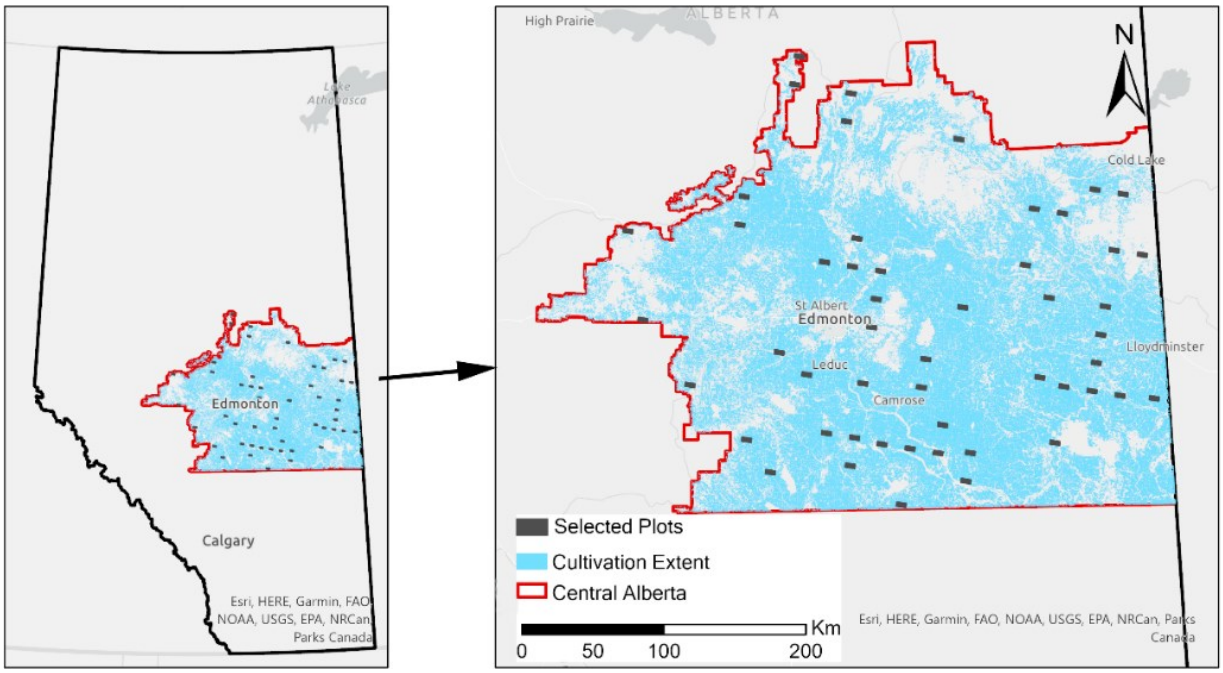

Fig. 5-3. The areal extent of cultivation used within the Google Earth Engine to derive information on annual forest loss. The cultivation extent means the grassland and cultivated cropland.

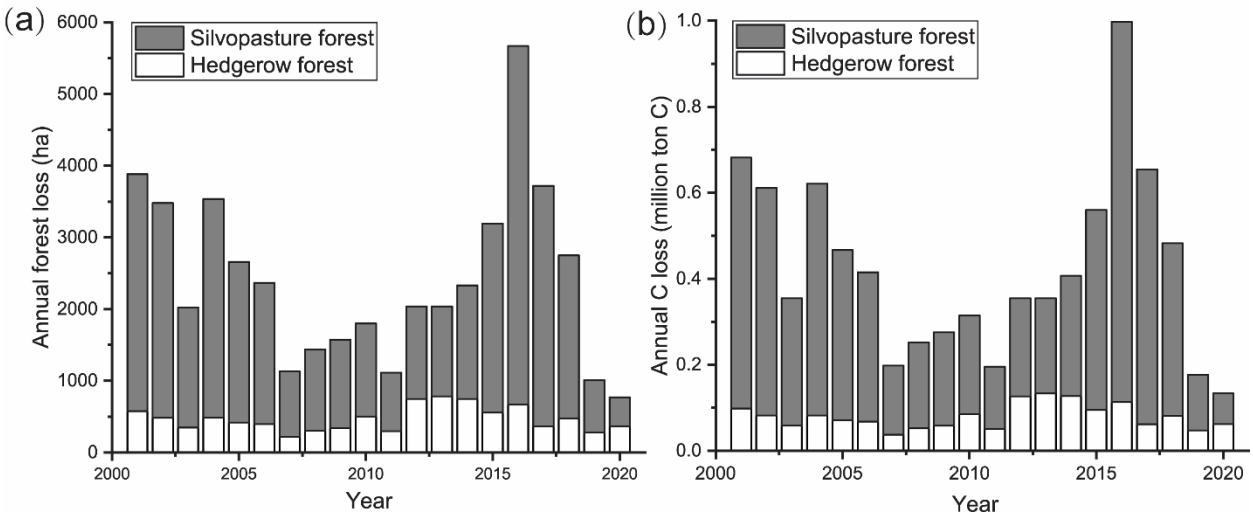

Fig. 5-4. Estimated annual forest loss and associated C loss derived from the cropland (representing hedgerow forests) and grassland (representing silvopasture forests) areas within central Alberta, Canada, based on Global Forest Changes (2000–2020) from Hansen et al. (2013) using Google Earth Engine.

References

Abbas, F., Hammad, H.M., Fahad, S., Cerdà, A., Rizwan, M., Farhad, W., Ehsan, S., Bakhat, H.F., 2017. Agroforestry: a sustainable environmental practice for carbon sequestration under the climate change scenarios—a review. Sci. Pollut. Res. 24, 11177-11191. https://doi.org/10.1007/s11356-017-8687-0.

Alberta Agriculture and Forestry, 2016. Organic Matter Content of Cultivated Soils. Government of Alberta https://open.alberta.ca/dataset/4921c409-eb2c-4953-8755-af6652323e2c#detailed. (accessed 12 December 2020).

Alberta Agriculture and Forestry, 2018. Alberta Satellite Land Cover. Government of Alberta https://open.alberta.ca/dataset/c0511ea4-bee5-40f6-ab4d-59de37bbbe66#detailed (accessed on 12 Dec 2020).

Alberta Biodiversity Monitoring Institute, 2017. 3 × 7 km Sample-Based Human Footprint Data. http://abmi.ca/home/data-analytics/da-top/da-product-overview/GIS-Human-Footprint-Land-Cover-Data/Human-Footprint-Sample-Based-Inventory.html (accessed on 12 Dec 2020).

Alberta Biodiversity Monitoring Institute, 2018. Wall-to-Wall Human Footprint Inventory. https://www.abmi.ca/home/data-analytics/da-top/da-product-overview/Human-Footprint-Products/HF-inventory.html (accessed on 12 Dec 2020).

Amichev, B.Y., Bentham, M.J., Cerkowniak, D., Kort, J., Kulshreshtha, S., Laroque, C.P., Piwowar, J.M., Van Rees, K.C., 2015. Mapping and quantification of planted tree and shrub shelterbelts in Saskatchewan, Canada. Agrofor. Syst. 89, 49-65. https://doi.org/10.1007/s10457-014-9741-2.

Amichev, B.Y., Bentham, M.J., Kulshreshtha, S.N., Laroque, C.P., Piwowar, J.M., Van Rees, K.C., 2016. Carbon sequestration and growth of six common tree and shrub shelterbelts in Saskatchewan, Canada. Can. J. Soil Sci. 97, 368-381. https://doi.org/10.1139/cjss-2016-0107.

Amichev, B.Y., Laroque, C.P., Van Rees, K.C., 2020. Shelterbelt removals in Saskatchewan, Canada: implications for long-term carbon sequestration. Agrofor. Syst. 1-16. https://doi.org/10.1007/s10457-020-00484-8.

Baah-Acheamfour, M., Carlyle, C.N., Bork, E.W., Chang, S.X., 2014. Trees increase soil carbon and its stability in three agroforestry systems in central Alberta, Canada. For. Ecol. Manag. 328, 131-139. https://doi.org/10.1016/j.foreco.2014.05.031.

Baah-Acheamfour, M., Chang, S.X., Bork, E.W., Carlyle, C.N., 2017. The potential of agroforestry to reduce atmospheric greenhouse gases in Canada: Insight from pairwise comparisons with traditional agriculture, data gaps and future research. For. Chron. 93, 180-189. https://doi.org/10.5558/tfc2017-024.

Bailey, A.W., Wroe, R.A., 1974. Aspen invasion in a portion of the Alberta parklands. Rangel Ecol. Manag. 27, 263-266. https://doi.org/10.2307/3896819.

Bork, E.W., Osko, T.J., Frerichs, L., Naeth, M.A., 2021. Low soil disturbance during boreal forest well site development enhances vegetation recovery after 10 years. For. Ecol. Manag. 482, 118849. https://doi.org/10.1016/j.foreco.2020.118849.

Gross, C.D., Bork, E.W., Carlyle, C.N., Chang, S.X., 2021 Biochar and its manure-based feedstock have divergent effects on soil organic carbon and greenhouse gas emissions in croplands. Sci. Total Environ. (Under review).

Dhillon, G.S. and Van Rees, K.C., 2017. Soil organic carbon sequestration by shelterbelt agroforestry systems in Saskatchewan. Can. J. Soil Sci. 97, 394-409. https://doi.org/10.1139/cjss-2016-0094.

Energy Rates, 2021. Alberta Carbon Tax and Rebates. Government of Alberta https://energyrates.ca/alberta/alberta-carbon-levy-rebates/ (accessed on 10 Aug 2021).

Environment and Parks, 2006. Natural regions and subregions of Alberta. Government of Alberta https://open.alberta.ca/publications/0778545725#detailed (accessed on 12 Dec 2020).

Environment and Parks, 2012. Central Parkland Vegetation Inventory (CPVI) Polygons. Government of Alberta https://open.alberta.ca/opendata/gda-351dd940-9110-4218-9cc9-cb159a9ac20a (accessed on 12 Dec 2020).

Environment Canada, 2020. Alberta weather condition. Government of Alberta https://weather.gc.ca/forecast/canada/index_e.html?id=AB (accessed in 12 December 2020).

Esri Inc, 2020. ArcGIS Pro (Version 2.7). Esri Inc. https://www.esri.com/en-us/arcgis/products/arcgis-pro/overview.

Gordon, A. M., Thevathasan, N., Nair, P. K. R., 2009. An agroecological foundation for temperate agroforestry. In "Temperate Agroforestry: Science and Practice" (H. E. Garrett and R. F. Fisher, Eds.), 25–44. American Society of Agronomy, Madison, WI.Gorelick, N., Hancher, M., Dixon, M., Ilyushchenko, S., Thau, D., Moore, R., 2017. Google Earth Engine: Planetary-scale geospatial analysis for everyone. Remote Sens. Environ. 202, 18-27. https://doi.org/10.1016/j.rse.2017.06.031.

Ha, T.V., Amichev, B.Y., Belcher, K.W., Bentham, M.J., Kulshreshtha, S.N., Laroque, C.P., Van Rees, K.C., 2019. Shelterbelt agroforestry systems inventory and removal analyzed by object-based classification of satellite data in Saskatchewan, Canada. Can. J. Remote. Sens. 45, 246-263. https://doi.org/10.1080/07038992.2018.1540297.

Hansen, M.C., Potapov, P.V., Moore, R., Hancher, M., Turubanova, S.A., Tyukavina, A., Thau, D., Stehman, S., Goetz, S.J., Loveland, T.R., 2013. High-resolution global maps of 21st-century forest cover change. Science 342, 850-853. https://doi.org/10.1126/science.1244693.

Hubau, W., De Mil, T., Van den Bulcke, J., Phillips, O.L., Ilondea, B.A., Van Acker, J., Sullivan, M.J., Nsenga, L., Toirambe, B., Couralet, C., Banin, L.F., 2019. The persistence of carbon in the African forest understory. Nat. Plants. 5, 133-140. https://doi.org/10.1038/s41477-018-0316-5.

Jin, Z.N., Azzari, G., You, C., Di Tommaso, S., Aston, S., Burke, M., Lobell, D.B., 2019. Smallholder maize area and yield mapping at national scales with Google Earth Engine. Remote Sens. Environ. 228, 115-128. https://doi.org/10.1016/j.rse.2019.04.016.

Jose, S., 2009. Agroforestry for ecosystem services and environmental benefits: an overview. Agrofor. Syst. 76, 1-10. https://doi.org/10.1007/s10457-009-9229-7.

Kort, J., Turnock, R., 1998. Carbon reservoir and biomass in Canadian prairie shelterbelts. Agrofor. Syst. 44, 175-186. https://doi.org/10.1023/A:1006226006785.

Kröbel, R., Moore, J., Ni, Y.Z., McPherson, A., Poppy, L., Soolanayakanahally, R.Y., Amichev, B.Y., Ward, T., Laroque, C.P., Van Rees, K.C., 2020. Demonstration and testing of the improved shelterbelt component in the Holos model. Front. Environ. Sci. https://doi.org/10.3389/fenvs.2020.00149.

Lim, S.S., Baah-Acheamfour, M., Choi, W.J., Arshad, M.A., Fatemi, F., Banerjee, S., Carlyle, C.N., Bork, E.W., Park, H.J., Chang, S.X., 2018. Soil organic carbon stocks in three Canadian agroforestry systems: From surface organic to deeper mineral soils. For. Ecol. Manag. 417, 103-109. https://doi.org/10.1016/j.foreco.2018.02.050.

Liu, L., Xiao, X.M., Qin, Y.W., Wang, J., Xu, X.L., Hu, Y.M., Qiao, Z., 2020. Mapping cropping intensity in China using time series Landsat and Sentinel-2 images and Google Earth Engine. Remote Sens. Environ. 239, 111624. https://doi.org/10.1016/j.rse.2019.111624.

Ma, Z.L., Chen, H.Y., Bork, E.W., Carlyle, C.N., Chang, S.X., 2020. Carbon accumulation in agroforestry systems is affected by tree species diversity, age and regional climate: A global meta-analysis. Glob. Ecol. Biogeogr. 29, 1817-1828. https://doi.org/10.1111/geb.13145.

Mildrexler, D.J., Berner, L.T., Law, B.E., Birdsey, R.A., Moomaw, W.R., 2020. Large Trees Dominate Carbon Storage in Forests East of the Cascade Crest in the United States Pacific Northwest. Front. for. glob. change 3, 127. https://doi.org/10.3389/ffgc.2020.594274.

Oelbermann, M., Voroney, R.P., Gordon, A.M., 2004. Carbon sequestration in tropical and temperate agroforestry systems: a review with examples from Costa Rica and southern Canada. Agric. Ecosyst. Environ. 104, 359-377. https://doi.org/10.1016/j.agee.2004.04.001.

Pankiw, J. and Piwowar, J., 2010. Seasonality of imagery: the impact on object-based classification accuracy of shelterbelts. Prairie Perspectives: Geographical Essays 13, 39-48.

Piwowar, J.M., Amichev, B.Y., Van Rees, K.C., 2016. The Saskatchewan shelterbelt inventory. Can. J. Soil Sci. 97, 433-438. ttps://doi.org/10.1139/cjss-2016-0098.

QGIS Development Team, 2018. QGIS (Version 3.2.1-București). Open Source Geospatial Foundation Project. http://qgis.osgeo.org.

Ravanelli, R., Nascetti, A., Cirigliano, R.V., Di Rico, C., Leuzzi, G., Monti, P., Crespi, M., 2018. Monitoring the impact of land cover change on surface urban heat island through Google Earth Engine: Proposal of a global methodology, first applications and problems. Remote Sens. 10, 1488. https://doi.org/10.3390/rs10091488.

Rempel, C.J., 2013. Costs, benefits, and barriers to the adoption and retention of shelterbelts in prairie agriculture as identified by Saskatchewan producers. Master's Thesis, University of Saskatchewan, Saskatoon, SK, Canada.

Rempel, J., Kulshreshtha, S., Van Rees, K., Amichev, B., 2014. Factors that Influence Shelterbelt Retention and Removal in Prairie Agriculture as Identified by Saskatchewan Producers. In Proceedings of the Soil and Science Workshop, Saskatoon, SK, Canada, 11 March 2014.

Rudd, L., Kulshreshtha, S., Belcher, K., Amichev, B., 2021. Carbon life cycle assessment of shelterbelts in Saskatchewan, Canada. J. Environ. Manage. 297, 113400. https://doi.org/10.1016/j.jenvman.2021.113400.

Soil Classification Working Group, 1998. The Canadian System of Soil Classification. NRC Research Press, Ottawa, Canada, 187 pp.

Stavi, I. and Lal, R., 2013. Agroforestry and biochar to offset climate change: a review. Agron. Sustain. Dev. 33, 81-96. https://doi.org/10.1007/s13593-012-0081-1.

Statistics Canada, 2014. Human activity and the environment: agriculture in Canada. http://www.statcan.gc.ca/pub/16-201-x/16-201-x2014000-eng.htm (accessed 12 December 2020).

Van Noordwijk, M., 2020. Agroforestry as nexus of sustainable development goals, IOP Conf. Ser.: Earth Environ. Sci. IOP Publishing, 012001 pp.

Wiseman, G., Kort, J., Walker, D., 2009. Quantification of shelterbelt characteristics using high-resolution imagery. Agric. Ecosyst. Environ. 131, 111-117. https://doi.org/10.1016/j.agee.2008.10.018.

Chapter 6. Conclusions and implications for future research

1. Overview of the study objectives

Climate change has caused serious issues to human beings. With increasing greenhouse gas (GHG) emissions, the influence of climate change may be intensified. Thus, there is great urgency to conduct climate change mitigation strategies to reduce the negative impact on human beings. Studies have shown that agroforestry systems such as hedgerow, shelterbelt and silvopasture systems are critical media for increasing C sequestration and achieving climate change mitigation (Baah-Acheamfour et al., 2014; Amichev et al., 2016; Lim et al., 2018). The province of Alberta has the second largest agricultural land area in Canada (Statistics Canada, 2014) and has many types of agroforestry systems (Baah-Acheamfour et al., 2017). Therefore, the agricultural land area has a high potential for climate mitigation by adopting agroforestry systems. Even though there have been quite a few studies on C stocks in those agroforestry systems (e.g., Takimoto et al., 2008; Lim et al., 2018; Shi et al., 2018), only a few have studied the stability of SOC that is sequestered in agroforestry systems (e.g., Baah-Acheamfour et al., 2014), which hinders our understanding of SOC dynamics within agroforestry systems. Meanwhile, with the increasing occurrence of climate extremes (Bush and Lemmen, 2019; Perkins et al., 2012; Perkins and Alexander, 2013), Canada is expected to have more frequent heat wave events in the summer (The Climate Atlas of Canada, 2019), which may negate the role of agroforestry systems in C sequestration, while such specific knowledge is lacking. In addition, regional C stocks and their associated economic value of sequestered C in typical agroforestry

systems in central Alberta have not been studied. Such knowledge gaps will restrain the development of agroforestry systems in Alberta.

This thesis research combined field study, laboratory incubation and geographic information system-based methods to investigate the influence of agroforestry systems, their component land-uses and soil depths on different aspects of SOC stability, the impact of heat wave events and their frequency on GHG emissions and soil labile C, and regional C stocks and their associated economic values. This thesis research aims to answer the following questions: 1) How is the stability of SOC affected by incorporating trees to form agroforestry systems and soil depth? 2) What is the difference in the effect of hedgerow and shelterbelt systems on SOC stability? 3) What is the influence of the heat wave event and its frequency on GHG emissions and soil labile C dynamics in agroforestry systems? And 4) What is the past C loss, current C stocks and future C increment due to agroforestry expansion, as well as the associated economic value of the current C stock and of typical agroforestry systems?

2. Research result summary and implications to management

Our results in Chapter 2 showed that SOC in forest soils had higher quality but not structural and thermal stabilities, and although forests did enhance SOC stocks (e.g., Lim et al., 2018) and SOC quality (Xu et al., 2020), the sequestered C was not characterized with high stability (Xu et al., 2020). Finally, SOC stability (both thermal and biological) increased with soil depth. This study only included soils from the 0-30 cm depth, and future research should include deeper layers which were typically neglected in studies about SOC (Gross and Harrison, 2019).

In Chapter 3, the thermal stability of SOC was influenced by land-use type, agroforestry system and the interaction of agroforestry system by land-use. However, the hedgerow system had a higher SOC biological stability than the shelterbelt system, which may result from the different tree characteristics in those two systems, highlighting the need for further understanding of the influence of tree characteristics on SOC pool size and stability, as well as the importance of maintaining the current hedgerow to increase the stability of SOC.

In Chapter 4, both cropland and forest soils from the hedgerow system had significantly higher CO_2 and N_2O emissions under heat wave treatment. The more frequently the heat wave events, the higher the CO_2 and N_2O emissions. These results indicate that extreme heat wave events may change agroforestry systems from GHG sinks to GHG sources. More attention should be paid to offset the impact of heat wave events on agroforestry systems, and the results should inspire researchers to pay more attention to the influence of climate extremes (e.g., duration, frequency and timing) on SOC dynamics; the impact of heat wave events on agroforestry systems has been overlooked compared with gradual change of the climate.

In central Alberta, cropland has the largest C stock, while cropland takes up close to half of the agricultural land area of the region. The C stored in the three typical agroforestry forests is substantial at the regional scale. The total C stock of the three agroforestry forests was estimated to be 699.9 Mt for the central Alberta region, highlighting the importance of agroforestry systems in C sequestration. While C stocks of both silvopasture forests and hedgerow forests decreased annually, and the C stock loss was summed to be 6.9 and 1.6 Mt C for silvopasture forests and hedgerow forests from 2001 to 2020 in central Alberta, respectively. Results also showed that the estimated potential increase in C stock expanding on shelterbelt establishment was 2.3 times the C stock currently found in shelterbelt forests. These results showed a high

potential of increasing C sequestration by implementing shelterbelt systems in the cropland and along road margins. Meanwhile, the silvopasture and hedgerow forests should be conserved, and the shelterbelt forests should be promoted for C sequestration purposes. Based on the current C credit (40 Canadian dollars per ton of CO_2 equivalent) (Energy Rates, 2021), the incremental C value of shelterbelt, hedgerow and silvopasture forests was estimated to be $0.9, $2.9 and $45.1 billion, highlighting the substantial economic value of these agroforestry systems.

It should be noted that even though incorporating trees to form agroforestry systems reduced the stability of SOC, the amount of stabilized C was higher in the forest than in the cropland (Baah-Acheamfour et al., 2014). The higher SOC stability in croplands arises from a net decline in SOC relative to adjacent forests, and this is the 'effect' of the loss of more labile SOC, which may have a strong negative influence on soil health, eventually lowering C storage in cropland than in the forest land-use. Hence, implementing agroforestry systems is beneficial for C sequestration and climate change mitigation.

3. Recommendations and future research needs

The stability of SOC was evaluated by solid-state NMR, thermal analysis and laboratory incubation for bulk soils. Since quantitative information (e.g., proportion) of different SOC pools (i.e., the labile C and recalcitrant C) is lacking, future studies need to investigate such information in agroforestry systems for a better understanding of the influence of agroforestry systems on SOC composition. Meanwhile, tree characteristics can have a major influence on the stability of SOC that has been sequestrated; understanding the influence of different tree species,

tree age, and tree species composition on SOC stability is needed to select appropriate tree species for greater C sequestration.

Further research is needed to expand our understanding of how extreme heat wave events affect soil processes in other agroforestry systems, especially under field conditions. Even though this study investigated the effect of the heat wave and its frequency on labile soil C and GHG emissions, as this was a laboratory incubation experiment, soil moisture content was maintained constant, which may not reflect the situation in the field. Moreover, in 2021, historical heat wave events (higher temperature and durations longer than previously recorded) took place in late June in western Canada, which may substantially change C sequestration and GHG mitigation in this region. Thus, more studies should be conducted on the effect of the duration, frequency, and timing of heat wave events and on the diurnal and nocturnal differences.

While this thesis research quantified the C stocks of three typical agroforestry forests, including the component croplands and grasslands of the agroforestry systems, the amount of C lost in the past, and the potential for C stock to increase by the expansion of agroforestry systems on a regional scale, information on the rate of afforestation in the region was not studied in this thesis due to lack of such data. Future research shall collect information on forest gains, which can provide a bigger picture of C dynamics at the regional scale. In addition, even though the economic value of these agroforestry systems was estimated to be very large, the monetary value of this ecosystem service was not publicly known. Policymakers should publicize the value of agroforestry systems to better promote the development of agroforestry systems.

References

Amichev, B.Y., Bentham, M.J., Kulshreshtha, S.N., Laroque, C.P., Piwowar, J.M., Van Rees, K.C., 2016. Carbon sequestration and growth of six common tree and shrub shelterbelts in Saskatchewan, Canada. Can. J. Soil Sci. 97, 368-381. https://doi.org/10.1139/cjss-2016-0107.

Baah-Acheamfour, M., Carlyle, C.N., Bork, E.W., Chang, S.X., 2014. Trees increase soil carbon and its stability in three agroforestry systems in central Alberta, Canada. For. Ecol. Manag. 328, 131-139. https://doi.org/10.1016/j.foreco.2014.05.031.

Baah-Acheamfour, M., Chang, S.X., Bork, E.W., Carlyle, C.N., 2017. The potential of agroforestry to reduce atmospheric greenhouse gases in Canada: Insight from pairwise comparisons with traditional agriculture, data gaps and future research. For. Chron. 93, 180-189. https://doi.org/10.5558/tfc2017-024.

Bush, E. and Lemmen, D.S., 2019. Canada's Changing Climate Report; Government of Canada, Ottawa, ON. 444 pp.

Energy Rates, 2021. Alberta Carbon Tax and Rebates. Government of Alberta https://energyrates.ca/alberta/alberta-carbon-levy-rebates/ (accessed on 10 Aug 2021).

Gross, C.D. and Harrison, R.B., 2019. The case for digging deeper: soil organic carbon storage, dynamics, and controls in our changing world. Soil Syst. 3, 28. https://doi.org/10.3390/soilsystems3020028.

Lim, S.S., Baah-Acheamfour, M., Choi, W.J., Arshad, M.A., Fatemi, F., Banerjee, S., Carlyle, C.N., Bork, E.W., Park, H.J., Chang, S.X., 2018. Soil organic carbon stocks in three Canadian agroforestry systems: From surface organic to deeper mineral soils. For. Ecol.

Manag. 417, 103-109. https://doi.org/10.1016/j.foreco.2018.02.050.Perkins, S., Alexander, L., Nairn, J., 2012. Increasing frequency, intensity and duration of observed global heatwaves and warm spells. Geophys. Res. Lett. 39. https://doi.org/10.1029/2012GL053361.

Perkins, S.E. and Alexander, L.V., 2013. On the measurement of heat waves. J. Clim. 26, 4500-4517. https://doi.org/10.1175/JCLI-D-12-00383.1.

Shi, L., Feng, W., Xu, J., Kuzyakov, Y., 2018. Agroforestry systems: Meta-analysis of soil carbon stocks, sequestration processes, and future potentials. Land Degrad. Dev. 29, 3886-3897. https://doi.org/10.1002/ldr.3136.

Statistics Canada, 2014. Human activity and the environment: agriculture in Canada. http://www.statcan.gc.ca/pub/16-201-x/16-201-x2014000-eng.htm (accessed 12 December 2020).

Takimoto, A., Nair, P.R., Nair, V.D., 2008. Carbon stock and sequestration potential of traditional and improved agroforestry systems in the West African Sahel. Agric. Ecosyst. Environ. 125, 159-166. https://doi.org/10.1016/j.agee.2007.12.010.

The Climate Atlas of Canada, 2019. Climate Atlas of Canada, version 2, using BCCAQv2 climate model data.

Xu, H., Qu, Q., Wang, M., Li, P., Li, Y., Xue, S., Liu, G., 2020. Soil organic carbon sequestration and its stability after vegetation restoration in the Loess Hilly Region, China. Land Degrad. Dev. 31, 568-580. https://doi.org/10.1002/ldr.3472.

Bibliography

Abbas, F., Hammad, H.M., Fahad, S., Cerdà, A., Rizwan, M., Farhad, W., Ehsan, S., Bakhat, H.F. 2017. Agroforestry: a sustainable environmental practice for carbon sequestration under the climate change scenarios - a review. Environ. Sci. Pollut. Res. 24, 11177-11191. https://doi.org/10.1007/s11356-017-8687-0.

Acosta-Martinez, V., Moore-Kucera, J., Cotton, J., Gardner, T. and Wester, D., 2014. Soil enzyme activities during the 2011 Texas record drought/heat wave and implications to biogeochemical cycling and organic matter dynamics. Appl. Soil Ecol. 75, 43-51. https://doi.org/10.1016/j.apsoil.2013.10.008.

Águas, A., Incerti, G., Saracino, A., Lanzotti, V., Silva, J.S., Rego, F.C., Mazzoleni, S., Bonanomi, G., 2018. Fire effects on litter chemistry and early development of Eucalyptus globulus. Plant Soil 422, 495-514. https://doi.org/10.1007/s11104-017-3419-2.

Alberta Agriculture and Forestry, 2016. Organic Matter Content of Cultivated Soils. Government of Alberta https://open.alberta.ca/dataset/4921c409-eb2c-4953-8755-af6652323e2c#detailed. (accessed 12 December 2020).

Alberta Agriculture and Forestry, 2018. Alberta Satellite Land Cover. Government of Alberta https://open.alberta.ca/dataset/c0511ea4-bee5-40f6-ab4d-59de37bbbe66#detailed (accessed on 12 Dec 2020).

Alberta Agriculture and Forestry, 2020. Interpolated Weather Data Since 1961 for Alberta Townships. Government of Alberta. https://acis.alberta.ca/township-data-viewer.jsp (accessed June 07, 2021).

Alberta Biodiversity Monitoring Institute, 2017. 3 × 7 km Sample-Based Human Footprint Data. http://abmi.ca/home/data-analytics/da-top/da-product-overview/GIS-Human-Footprint-Land-Cover-Data/Human-Footprint-Sample-Based-Inventory.html (accessed on 12 Dec 2020).

Alberta Biodiversity Monitoring Institute, 2018. Wall-to-Wall Human Footprint Inventory. https://www.abmi.ca/home/data-analytics/da-top/da-product-overview/Human-Footprint-Products/HF-inventory.html (accessed on 12 Dec 2020).

Amichev, B.Y., Bentham, M.J., Cerkowniak, D., Kort, J., Kulshreshtha, S., Laroque, C.P., Piwowar, J.M., Van Rees, K.C., 2015. Mapping and quantification of planted tree and shrub shelterbelts in Saskatchewan, Canada. Agrofor. Syst. 89, 49-65. https://doi.org/10.1007/s10457-014-9741-2.

Amichev, B.Y., Bentham, M.J., Kulshreshtha, S.N., Laroque, C.P., Piwowar, J.M., Van Rees, K.C., 2016. Carbon sequestration and growth of six common tree and shrub shelterbelts in Saskatchewan, Canada. Can. J. Soil Sci. 97, 368-381. https://doi.org/10.1139/cjss-2016-0107.

Amichev, B.Y., Laroque, C.P., Van Rees, K.C., 2020. Shelterbelt removals in Saskatchewan, Canada: implications for long-term carbon sequestration. Agrofor. Syst. 1-16. https://doi.org/10.1007/s10457-020-00484-8.

An, Z.F., Bernard, G.M., Ma, Z.L., Plante, A.F., Michaelis, V.K., Bork, E.W., Carlyle, C.N., Baah-Acheamfour, M., Chang, S.X. 2021. Forest land-use increases soil organic carbon quality but not structural or thermal stability in a hedgerow system. Agric. Ecosyst. Environ. 321, 107617. https://doi.org/10.1016/j.agee.2021.107617.

Angst, G., Mueller, K.E., Eissenstat, D.M., Trumbore, S., Freeman, K.H., Hobbie, S.E., Chorover, J., Oleksyn, J., Reich, P.B., Mueller, C.W. 2019. Soil organic carbon stability in forests: distinct effects of tree species identity and traits. Glob. Change Biol. 25, 1529-1546. https://doi.org/10.1111/gcb.14548.

Anjileli, H., Huning, L.S., Moftakhari, H., Ashraf, S., Asanjan, A.A., Norouzi, H., AghaKouchak, A., 2021. Extreme heat events heighten soil respiration. Sci. Rep. 11, 1-9. https://doi.org/10.1038/s41598-021-85764-8.

Baah-Acheamfour, M., Carlyle, C.N., Bork, E.W., Chang, S.X. 2020. Forest and perennial herbland cover reduce microbial respiration but increase root respiration in agroforestry systems. Agric. For. Meteorol. 280, 107790. https://doi.org/10.1016/j.agrformet.2019.107790.

Baah-Acheamfour, M., Carlyle, C.N., Bork, E.W., Chang, S.X., 2014. Trees increase soil carbon and its stability in three agroforestry systems in central Alberta, Canada. For. Ecol. Manag. 328, 131-139. https://doi.org/10.1016/j.foreco.2014.05.031.

Baah-Acheamfour, M., Carlyle, C.N., Lim, S.S., Bork, E.W., Chang, S.X. 2016. Forest and grassland cover types reduce net greenhouse gas emissions from agricultural soils. Sci. Total Environ. 571, 1115-1127. https://doi.org/10.1016/j.scitotenv.2016.07.106.

Baah-Acheamfour, M., Chang, S.X., Bork, E.W., Carlyle, C.N., 2017. The potential of agroforestry to reduce atmospheric greenhouse gases in Canada: Insight from pairwise comparisons with traditional agriculture, data gaps and future research. For. Chron. 93, 180-189. https://doi.org/10.5558/tfc2017-024.

Baah-Acheamfour, M., Chang, S.X., Carlyle, C.N. and Bork, E.W., 2015. Carbon pool size and stability are affected by trees and grassland cover types within agroforestry systems of

western Canada. Agric. Ecosyst. Environ. 213, 105-113. https://doi.org/10.1016/j.agee.2015.07.016.

Bailey, A.W., Wroe, R.A., 1974. Aspen invasion in a portion of the Alberta parklands. Rangel Ecol. Manag. 27, 263-266. https://doi.org/10.2307/3896819.

Baldock, J.A., Oades, J.M., Nelson, P.N., Skene, T.M., Golchin, A., Clarke, P., 1997. Assessing the extent of decomposition of natural organic materials using solid-state ^{13}C NMR spectroscopy. Soil Res. 35, 1061-1084. https://doi.org/10.1071/S97004.

Banerjee, S., Baah-Acheamfour, M., Carlyle, C.N., Bissett, A., Richardson, A.E., Siddique, T., Bork, E.W., Chang, S.X. 2016. Determinants of bacterial communities in Canadian agroforestry systems. Environ. Microbiol. 18, 1805-1816. https://doi.org/10.1111/1462-2920.12986.

Barré, P., Plante, A.F., Cécillon, L., Lutfalla, S., Baudin, F., Bernard, S., Christensen, B.T., Eglin, T., Fernandez, J.M., Houot, S., Kätterer, T., 2016. The energetic and chemical signatures of persistent soil organic matter. Biogeochemistry 130, 1-12. https://doi.org/10.1007/s10533-016-0246-0.

Barré, P., Plante, A.F., Cécillon, L., Lutfalla, S., Baudin, F., Bernard, S., Christensen, B.T., Eglin, T., Fernandez, J.M., Houot, S. 2016. The energetic and chemical signatures of persistent soil organic matter. Biogeochemistry 130, 1-12. https://doi.org/10.1007/s10533-016-0246-0.

Batjes, N.H., 1996. Total carbon and nitrogen in the soils of the world. Eur. J. Soil Sci. 47, 151-163. https://doi.org/10.1111/j.1365-2389.1996.tb01386.x

Benbi, D.K., Brar, K., Toor, A.S. and Singh, P., 2015. Total and labile pools of soil organic carbon in cultivated and undisturbed soils in northern India. Geoderma 237, 149-158. https://doi.org/10.1016/j.geoderma.2014.09.002.

Beule, L., Corre, M.D., Schmidt, M., Göbel, L., Veldkamp, E., Karlovsky, P., 2019. Conversion of monoculture cropland and open grassland to agroforestry alters the abundance of soil bacteria, fungi and soil-N-cycling genes. PloS One 14, e0218779. https://doi.org/10.1371/journal.pone.0220713.

Blum, W.E., de Baerdemaeker, J., Finkl, C.W., Horn, R., Pachepsky, Y., Shein, E.V., Konstankiewicz, K., Grundas, S., 2011. Encyclopedia of Agrophysics. Berlin, Germany, Springer. 378-382 pp.

Borden, K.A., Thomas, S.C., Isaac, M.E., 2020. Variation in fine root traits reveals nutrient-specific acquisition strategies in agroforestry systems. Plant Soil, 453, 139-151. https://doi.org/10.1007/s11104-019-04003-2.

Bork, E.W., Osko, T.J., Frerichs, L., Naeth, M.A., 2021. Low soil disturbance during boreal forest well site development enhances vegetation recovery after 10 years. For. Ecol. Manag. 482, 118849. https://doi.org/10.1016/j.foreco.2020.118849.

Bosatta, E. and Ågren, G.I. 1999. Soil organic matter quality interpreted thermodynamically. Soil Biol. Biochem. 31, 1889-1891. https://doi.org/10.1016/S0038-0717(99)00105-4.

Brown, J.R., Blankinship, J.C., Niboyet, A., van Groenigen, K.J., Dijkstra, P., Le Roux, X., Leadley, P.W. and Hungate, B.A., 2012. Effects of multiple global change treatments on soil N_2O fluxes. Biogeochemistry 109, 85-100. https://doi.org/10.1007/s10533-011-9655-2.

Bush, E. and Lemmen, D.S., 2019. Canada's Changing Climate Report; Government of Canada, Ottawa, ON. 444 pp.

Butterbach-Bahl, K., Baggs, E.M., Dannenmann, M., Kiese, R. and Zechmeister-Boltenstern, S., 2013. Nitrous oxide emissions from soils: how well do we understand the processes and their controls? Philos. Trans. R. Soc. Lond. B Biol. Sci. 368, 20130122. https://doi.org/10.1098/rstb.2013.0122.

Calzadilla, A., Rehdanz, K., Betts, R., Falloon, P., Wiltshire, A., Tol, R.S., 2013. Climate change impacts on global agriculture. Clim. Change 120, 357-374. https://doi.org/10.1007/s10584-013-0822-4.

Capriel, P., 1997. Hydrophobicity of organic matter in arable soils: influence of management. Eur. J. Soil Sci. 48, 457-462. https://doi.org/10.1111/j.1365-2389.1997.tb00211.x.

Cécillon, L., Baudin, F., Chenu, C., Houot, S., Jolivet, R., Kätterer, T., Lutfalla, S., Macdonald, A., Oort, F.v., Plante, A.F., 2018. A model based on Rock-Eval thermal analysis to quantify the size of the centennially persistent organic carbon pool in temperate soils. Biogeosciences 15, 2835-2849. https://doi.org/10.5194/bg-15-2835-2018.

Cepáková, Š., Tošner, Z., Frouz, J., 2016. The effect of tree species on seasonal fluctuations in water-soluble and hot water-extractable organic matter at post-mining sites. Geoderma 275, 19-27. https://doi.org/10.1016/j.geoderma.2016.04.006.

Christensen, B.T., 1996. Carbon in primary and secondary organomineral complexes. In: Carter, M.R., Stewart, B. A. (Eds), Structure and organic matter storage in agricultural soils. CRC Lewis Publishers, New York, 97-165 pp.

Ciais, P., Reichstein, M., Viovy, N., Granier, A., Ogée, J., Allard, V., Aubinet, M., Buchmann, N., Bernhofer, C., Carrara, A., 2005. Europe-wide reduction in primary productivity caused by the heat and drought in 2003. Nature 437, 529-533. https://doi.org/10.1038/nature03972.

Coleman, D., Elliot, E., 1988. Let the soil work for us. Ecol Bull 39, 23-32.

Culman, S.W., Snapp, S.S., Freeman, M.A., Schipanski, M.E., Beniston, J., Lal, R., Drinkwater, L.E., Franzluebbers, A.J., Glover, J.D., Grandy, A.S., 2012. Permanganate oxidizable carbon reflects a processed soil fraction that is sensitive to management. Soil Sci. Soc. Am. J. 76, 494-504. https://doi.org/10.2136/sssaj2011.0286.

De Mendiburu F., 2019. Agricolae: Statistical procedures for agricultural research. R Package Version 1.2-4.

De Stefano, A., Jacobson, M.G. 2018. Soil carbon sequestration in agroforestry systems: a meta-analysis. Agrofor. Syst. 92, 285-299. https://doi.org/10.1007/s10457-017-0147-9.

Dhillon, G.S. and Van Rees, K.C., 2017. Soil organic carbon sequestration by shelterbelt agroforestry systems in Saskatchewan. Can. J. Soil Sci. 97, 394-409. https://doi.org/10.1139/cjss-2016-0094.

Duarte, R.M., Fernández-Getino, A.P., Duarte, A.C., 2013. Humic acids as proxies for assessing different Mediterranean forest soils signatures using solid-state CPMAS ^{13}C NMR spectroscopy. Chemosphere 91, 1556-1565. https://doi.org/10.1016/j.chemosphere.2012.12.043.

Eisenhauer, N., Lanoue, A., Strecker, T., Scheu, S., Steinauer, K., Thakur, M.P., Mommer, L., 2017. Root biomass and exudates link plant diversity with soil bacterial and fungal biomass. Sci. Rep. 7, 1-8. https://doi.org/10.1038/srep44641.

Elbl, J., Vaverková, M., Adamcová, D., Plosek, L., Kintl, A., Losak, T., Hynst, J., Kotovicová, J., 2014. Influence of fertilization on microbial activities, soil hydrophobicity and mineral nitrogen leaching. Ecol. Chem. Eng. 21, 661. https://doi.org/10.1515/eces-2014-0048.

Energy Rates, 2021. Alberta Carbon Tax and Rebates. Government of Alberta https://energyrates.ca/alberta/alberta-carbon-levy-rebates/ (accessed on 10 Aug 2021).

Environment and Parks, 2006. Natural regions and subregions of Alberta. Government of Alberta https://open.alberta.ca/publications/0778545725#detailed (accessed on 12 Dec 2020).

Environment and Parks, 2012. Central Parkland Vegetation Inventory (CPVI) Polygons. Government of Alberta https://open.alberta.ca/opendata/gda-351dd940-9110-4218-9cc9-cb159a9ac20a (accessed on 12 Dec 2020).

Environment Canada, 2020. Alberta weather condition. Government of Alberta https://weather.gc.ca/forecast/canada/index_e.html?id=AB (accessed in 12 December 2020).

Environment Canada, 2021. Canadian Climate Normal 1981–2010. Government of Canada. https://climate.weather.gc.ca/climate_normals/(accessed June 08, 2021).

Environment Canada, 2021. Weather Information. https://weather.gc.ca (accessed July 01, 2021).

Esri Inc, 2020. ArcGIS Pro (Version 2.7). Esri Inc. https://www.esri.com/en-us/arcgis/products/arcgis-pro/overview.

Felton, A.J., Knapp, A.K. and Smith, M.D., 2019. Carbon exchange responses of a mesic grassland to an extreme gradient of precipitation. Oecologia 189, 565-576. https://doi.org/10.1007/s00442-018-4284-2.

Fissore, C., Giardina, C.P., Kolka, R.K., Trettin, C.C., King, G.M., Jurgensen, M.F., Barton, C.D., McDowell, S.D. 2008. Temperature and vegetation effects on soil organic carbon quality along a forested mean annual temperature gradient in North America. Glob. Change Biol. 14, 193-205. https://doi.org/10.1111/j.1365-2486.2007.01478.x.

Fontaine, S., Barot, S., Barré, P., Bdioui, N., Mary, B., Rumpel, C., 2007. Stability of organic carbon in deep soil layers controlled by fresh carbon supply. Nature 450, 277-280. https://doi.org/10.1038/nature06275.

Frank, D., Reichstein, M., Bahn, M., Thonicke, K., Frank, D., Mahecha, M.D., Smith, P., Van der Velde, M., Vicca, S., Babst, F., 2015. Effects of climate extremes on the terrestrial carbon cycle: concepts, processes and potential future impacts. Glob. Chang. Biol. 21, 2861-2880. https://doi.org/10.1111/gcb.12916.

Frank, D., Reichstein, M., Bahn, M., Thonicke, K., Frank, D., Mahecha, M.D., Smith, P., Van der Velde, M., Vicca, S. and Babst, F., 2015. Effects of climate extremes on the terrestrial carbon cycle: concepts, processes and potential future impacts. Glob. Chang. Biol. 21, 2861-2880. https://doi.org/10.1111/gcb.12916.

Ghani, A., Dexter, M. and Perrott, K., 2003. Hot-water extractable carbon in soils: a sensitive measurement for determining impacts of fertilisation, grazing and cultivation. Soil Biol. Biochem. 35, 1231-1243. https://doi.org/10.1016/S0038-0717(03)00186-X.

Gordon, A. M., Thevathasan, N., Nair, P. K. R., 2009. An agroecological foundation for temperate agroforestry. In “Temperate Agroforestry: Science and Practice” (H. E. Garrett and R. F. Fisher, Eds.), 25–44. American Society of Agronomy, Madison, WI.

Gorelick, N., Hancher, M., Dixon, M., Ilyushchenko, S., Thau, D., Moore, R., 2017. Google Earth Engine: Planetary-scale geospatial analysis for everyone. Remote Sens. Environ. 202, 18-27. https://doi.org/10.1016/j.rse.2017.06.031.

Griebel, A., Bennett, L.T., Metzen, D., Pendall, E., Lane, P.N. and Arndt, S.K., 2019. Trading water for carbon: Sustained photosynthesis at the cost of increased water loss during high

temperatures in a temperate forest. J. Geophys. Res. Biogeosci. 125. https://doi.org/10.1029/2019JG005239.

Griscom, B.W., Adams, J., Ellis, P.W., Houghton, R.A., Lomax, G., Miteva, D.A., Schlesinger, W.H., Shoch, D., Siikamäki, J.V., Smith, P., 2017. Natural climate solutions. PNAS 114, 11645-11650. https://doi.org/10.1073/pnas.1710465114.

Gross, C.D. and Harrison, R.B., 2019. The case for digging deeper: soil organic carbon storage, dynamics, and controls in our changing world. Soil Syst. 3, 28. https://doi.org/10.3390/soilsystems3020028.

Gross, C.D., Bork, E.W., Carlyle, C.N., Chang, S.X., 2021 Biochar and its manure-based feedstock have divergent effects on soil organic carbon and greenhouse gas emissions in croplands. Sci. Total Environ. (Under review).

Gu, L., Post, W.M. and King, A.W., 2004. Fast labile carbon turnover obscures sensitivity of heterotrophic respiration from soil to temperature: a model analysis. Glob. Biogeochem. Cycles 18. https://doi.org/10.1029/2003GB002119.

Gupta, N., Kukal, S., Bawa, S., Dhaliwal, G. 2009. Soil organic carbon and aggregation under poplar based agroforestry system in relation to tree age and soil type. Agrofor. Syst. 76, 27-35. https://doi.org/10.1007/s10457-009-9219-9.

Ha, T.V., Amichev, B.Y., Belcher, K.W., Bentham, M.J., Kulshreshtha, S.N., Laroque, C.P., Van Rees, K.C., 2019. Shelterbelt agroforestry systems inventory and removal analyzed by object-based classification of satellite data in Saskatchewan, Canada. Can. J. Remote. Sens. 45, 246-263. https://doi.org/10.1080/07038992.2018.1540297.

Hagedorn, F., Martin, M., Rixen, C., Rusch, S., Bebi, P., Zürcher, A., Siegwolf, R.T., Wipf, S., Escape, C., Roy, J., 2010. Short-term responses of ecosystem carbon fluxes to experimental

soil warming at the Swiss alpine treeline. Biogeochemistry 97, 7-19. https://doi.org/10.1007/s10533-009-9297-9.

Hansen, M.C., Potapov, P.V., Moore, R., Hancher, M., Turubanova, S.A., Tyukavina, A., Thau, D., Stehman, S., Goetz, S.J., Loveland, T.R., 2013. High-resolution global maps of 21st-century forest cover change. Science 342, 850-853. https://doi.org/10.1126/science.1244693.

Harvey, O.R., Myers-Pigg, A.N., Kuo, L.J., Singh, B.P., Kuehn, K.A., Louchouarn, P. 2016. Discrimination in degradability of soil pyrogenic organic matter follows a return-on-energy-investment principle. Environ. Sci. Technol. 50, 8578-8585. https://doi.org/10.1021/acs.est.6b01010.

He, Y., Chen, C.R., Xu, Z.H., William, D., Xu, J.M., 2009. Assessing management impacts on soil organic matter quality in subtropical Australian forests using physical and chemical fractionation as well as ^{13}C NMR spectroscopy. Soil Biol. Biochem. 41, 640-650. https://doi.org/10.1016/j.soilbio.2009.01.008.

Hoover, D., Knapp, A. and Smith, M., 2017. Photosynthetic responses of a dominant C4 grass to an experimental heat wave are mediated by soil moisture. Oecologia 183, 303-313. https://doi.org/10.1007/s00442-016-3755-6.

Hoover, D.L., Knapp, A.K. and Smith, M.D., 2016. The immediate and prolonged effects of climate extremes on soil respiration in a mesic grassland. J. Geophys. Res. Biogeosci. 121, 1034-1044. https://doi.org/10.1002/2015JG003256.

Hoover, D.L., Knapp, A.K., Smith, M.D., 2014. Resistance and resilience of a grassland ecosystem to climate extremes. Ecology 95, 2646-2656. https://doi.org/10.1890/13-2186.1.

Hou, Y.H., Chen, Y., Chen, X. He, K.Y., Zhu, B., 2019. Changes in soil organic matter stability with depth in two alpine ecosystems on the Tibetan Plateau. Geoderma 351, 153-162. https://doi.org/10.1016/j.geoderma.2019.05.034.

Howlett, D.S., Mosquera-Losada, M.R., Nair, P.R., Nair, V.D., Rigueiro-Rodríguez, A., 2011. Soil carbon storage in silvopastoral systems and a treeless pasture in northwestern Spain. J. Environ. Qual. 40, 825-832. https://doi.org/10.2134/jeq2010.0145.

Hubau, W., De Mil, T., Van den Bulcke, J., Phillips, O.L., Ilondea, B.A., Van Acker, J., Sullivan, M.J., Nsenga, L., Toirambe, B., Couralet, C., Banin, L.F., 2019. The persistence of carbon in the African forest understory. Nat. Plants. 5, 133-140. https://doi.org/10.1038/s41477-018-0316-5.

Incerti, G., Cartenì, F., Cesarano, G., Sarker, T.C., El-Gawad, A., Ahmed, M., D'Ascoli, R., Bonanomi, G., Giannino, F., 2018. Faster N release, but not C loss, from leaf litter of invasives compared to native species in Mediterranean ecosystems. Front. Plant Sci. 9, 534. https://doi.org/10.3389/fpls.2018.00534.

IPCC, 2007. Climate change 2007: The Physical Science Basis. Contribution of Working Group I to the Fourth Assessment Report of the Intergovernmental Panel on Climate Change. Geneva: IPCC.

Jarvi, M.P. and Burton, A.J., 2020. Root respiration and biomass responses to experimental soil warming vary with root diameter and soil depth. Plant Soil, 451, 435-446. https://doi.org/10.1007/s11104-020-04540-1.

Jeong, D.I., Sushama, L., Diro, G.T., Khaliq, M.N., Beltrami, H., Caya, D., 2016. Projected changes to high temperature events for Canada based on a regional climate model ensemble. Clim. Dyn. 46, 3163-3180. https://doi.org/10.1007/s00382-015-2759-y.

Jia, Z.J., Yakov, K., Myrold, D., Tiedje, J. 2017. Soil organic carbon in a changing world. Pedosphere 27, 789-791. https://doi.org/10.1016/S1002-0160(17)60489-2.

Jílková, V., Jandová, K., Cajthaml, T., Devetter, M., Kukla, J., Starý, J. and Vacířová, A., 2020. Organic matter decomposition and carbon content in soil fractions as affected by a gradient of labile carbon input to a temperate forest soil. Biol. Fertil. Soils 56, 411-421. https://doi.org/10.1007/s00374-020-01433-4.

Jin, Z.N., Azzari, G., You, C., Di Tommaso, S., Aston, S., Burke, M., Lobell, D.B., 2019. Smallholder maize area and yield mapping at national scales with Google Earth Engine. Remote Sens. Environ. 228, 115-128. https://doi.org/10.1016/j.rse.2019.04.016.

Jobbágy, E.G. and Jackson, R.B. 2000. The vertical distribution of soil organic carbon and its relation to climate and vegetation. Ecol. Appl. 10, 423-436. https://doi.org/10.1890/1051-0761(2000)010[0423:TVDOSO]2.0.CO;2.

Joergensen, R.G., 1996. The fumigation-extraction method to estimate soil microbial biomass: calibration of the kEC value. Soil Biol. Biochem. 28, 25-31. https://doi.org/10.1016/0038-0717(95)00102-6.

Jolliffe, I.T. and Cadima, J., 2016. Principal component analysis: a review and recent developments. Philos. Trans. A. Math. Phys. Eng. Sci. 374(2065), 20150202. https://doi.org/10.1098/rsta.2015.0202.

Jose, S., 2009. Agroforestry for ecosystem services and environmental benefits: an overview. Agrofor. Syst. 76, 1-10. https://doi.org/10.1007/s10457-009-9229-7.

Jose, S., Bardhan, S. 2012. Agroforestry for biomass production and carbon sequestration: an overview. Agrofor. Syst. 86, 105-111. https://doi.org/10.1007/s10457-012-9573-x.

Karhu, K., Auffret, M.D., Dungait, J.A., Hopkins, D.W., Prosser, J.I., Singh, B.K., Subke, J.A., Wookey, P.A., Ågren, G.I., Sebastia, M.T., 2014. Temperature sensitivity of soil respiration rates enhanced by microbial community response. Nature 513, 81-84. https://doi.org/10.1038/nature13604.

Kim, D.G., Kirschbaum, M.U., Beedy, T.L. 2016. Carbon sequestration and net emissions of CH_4 and N_2O under agroforestry: Synthesizing available data and suggestions for future studies. Agric. Ecosyst. Environ. 226, 65-78. https://doi.org/10.1016/j.agee.2016.04.011.

Knorr, W., Prentice, I.C., House, J., Holland, E., 2005. Long-term sensitivity of soil carbon turnover to warming. Nature 433, 298-301. https://doi.org/10.1038/s41467-020-17790-5.

Kort, J., Turnock, R., 1998. Carbon reservoir and biomass in Canadian prairie shelterbelts. Agrofor. Syst. 44, 175-186. https://doi.org/10.1023/A:1006226006785.

Kröbel, R., Moore, J., Ni, Y.Z., McPherson, A., Poppy, L., Soolanayakanahally, R.Y., Amichev, B.Y., Ward, T., Laroque, C.P., Van Rees, K.C., 2020. Demonstration and testing of the improved shelterbelt component in the Holos model. Front. Environ. Sci. https://doi.org/10.3389/fenvs.2020.00149.

Kwak, J.H., Lim, S.S., Baah-Acheamfour, M., Choi, W.J., Fatemi, F., Carlyle, C.N., Bork, E.W., Chang, S.X. 2019. Introducing trees to agricultural lands increases greenhouse gas emission during spring thaw in Canadian agroforestry systems. Sci. Total Environ. 652, 800-809. https://doi.org/10.1016/j.scitotenv.2018.10.241.

Lal, R. 2003. Global potential of soil carbon sequestration to mitigate the greenhouse effect. Crit. Rev. Plant Sci. 22, 151-184. https://doi.org/10.1080/713610854.

Lal, R. 2004. Soil carbon sequestration impacts on global climate change and food security. Science 304, 1623-1627. https://doi.org/10.1126/science.1097396.

Lal, R. 2007. Carbon management in agricultural soils. Mitig. Adapt. Strateg. Glob. Chang. 12, 303-322. https://doi.org/10.1007/s11027-006-9036-7.

Lenth, R. and Lenth, M.R., 2018. Package 'lsmeans'. Am. Stat. 34, 216-221.

Lenth, R.V. 2016. Least-squares means: the R package lsmeans. J. Stat. Softw. 69, 1-33.

Li, L.F., Qian, R.Y., Wang, W.J., Kang, X.M., Ran, Q.W., Zheng, Z.Z., Zhang, B., Xu, C., Che, R.X., Dong, J.F., 2020. The intra-and inter-annual responses of soil respiration to climate extremes in a semiarid grassland. Geoderma 378, 114629. https://doi.org/10.1016/j.geoderma.2020.114629.

Li, Y., Bruelheide, H., Scholten, T., Schmid, B., Sun, Z.K., Zhang, N.L., Bu, W.S., Liu, X.J., Ma, K.P. 2019. Early positive effects of tree species richness on soil organic carbon accumulation in a large-scale forest biodiversity experiment. J. Plant Ecol. 12, 882-893. https://doi.org/10.1093/jpe/rtz026.

Li, Y.F., Zhang, J.J., Chang, S.X., Jiang, P.K., Zhou, G.M., Shen, Z.M., Wu, J.S., Lin, L., Wang, Z.H., Shen, M.C., 2014. Converting native shrub forests to Chinese chestnut plantations and subsequent intensive management affected soil C and N pools. For. Ecol. Manag. 312, 161-169. https://doi.org/10.1016/j.foreco.2013.10.008.

Liang, Q., Wang, C., Zhang, K.X., Shi, S.W., Guo, J.X., Gao, F., Liu, J., Wang, J.X., Liu, Y. 2021. The influence of tree species on soil organic carbon stability under three temperate forests in the Baihua Mountain Reserve, China. Glob. Ecol. Conserv. 26, e01454. https://doi.org/10.1016/j.gecco.2021.e01454.

Lim, S.S., Baah-Acheamfour, M., Choi, W.J., Arshad, M.A., Fatemi, F., Banerjee, S., Carlyle, C.N., Bork, E.W., Park, H.-J., Chang, S.X., 2018. Soil organic carbon stocks in three

Canadian agroforestry systems: From surface organic to deeper mineral soils. For. Ecol. Manag. 417, 103-109. https://doi.org/10.1016/j.foreco.2018.02.050.

Perkins, S., Alexander, L., Nairn, J., 2012. Increasing frequency, intensity and duration of observed global heatwaves and warm spells. Geophys. Res. Lett. 39. https://doi.org/10.1029/2012GL053361.

Liu, L., Xiao, X.M., Qin, Y.W., Wang, J., Xu, X.L., Hu, Y.M., Qiao, Z., 2020. Mapping cropping intensity in China using time series Landsat and Sentinel-2 images and Google Earth Engine. Remote Sens. Environ. 239, 111624. https://doi.org/10.1016/j.rse.2019.111624.

Liu, R., Hayden, H.L., Suter, H., Hu, H.W., Lam, S.K., He, J.Z., Mele, P.M., Chen, D.L., 2017. The effect of temperature and moisture on the source of N_2O and contributions from ammonia oxidizers in an agricultural soil. Biol. Fertil. Soils 53, 141-152. https://doi.org/10.1007/s00374-016-1167-8.

Lopez-Capel, E., Sohi, S.P., Gaunt, J.L., Manning, D.A., 2005. Use of thermogravimetry–differential scanning calorimetry to characterize modelable soil organic matter fractions. Soil Sci. Soc. Am. J. 69, 136-140. https://doi.org/10.2136/sssaj2005.0136a.

Lu, M., Zhou, X.H., Yang, Q., Li, H., Luo, Y.Q., Fang, C.M., Chen, J.K., Yang, X., Li, B., 2013. Responses of ecosystem carbon cycle to experimental warming: a meta-analysis. Ecology 94, 726-738. https://doi.org/10.1890/12-0279.1.

Ma, Z.L., Chen, H.Y., Bork, E.W., Carlyle, C.N., Chang, S.X., 2020. Carbon accumulation in agroforestry systems is affected by tree species diversity, age and regional climate: A global meta-analysis. Glob. Ecol. Biogeogr. 29, 1817-1828. https://doi.org/10.1111/geb.13145.

Mathers, N.J., Xu, Z., Berners-Price, S.J., Perera, M.S., Saffigna, P.G., 2002. Hydrofluoric acid pretreatment for improving ^{13}C CPMAS NMR spectral quality of forest soils in south-east Queensland, Australia. Soil Res. 40, 665-674. https://doi.org/10.1071/SR01073.

Meyer, L. and Pachauri, R., 2014. The Fifth assessment report of the intergovernmental panel on climate change. Geneva: IPCC Secretariat.

Miao, S.J., Qiao, Y.F., You, M.Y., Zhang, F.T. 2016. Thermal stability of soil organic matter was affected by 23-yr maize and soybean continuous cultivation in northeast of China. J. Therm. 123, 2045-2051. https://doi.org/10.1007/s10973-015-4709-7.

Mildrexler, D.J., Berner, L.T., Law, B.E., Birdsey, R.A., Moomaw, W.R., 2020. Large Trees Dominate Carbon Storage in Forests East of the Cascade Crest in the United States Pacific Northwest. Front. for. glob. change 3, 127. https://doi.org/10.3389/ffgc.2020.594274.

Monda, H., Cozzolino, V., Vinci, G., Drosos, M., Savy, D., Piccolo, A., 2018. Molecular composition of the Humeome extracted from different green composts and their biostimulation on early growth of maize. Plant Soil 429, 407-424. https://doi.org/10.1007/s11104-018-3642-5.

Monda, H., Cozzolino, V., Vinci, G., Spaccini, R., Piccolo, A., 2017. Molecular characteristics of water-extractable organic matter from different composted biomasses and their effects on seed germination and early growth of maize. Sci. Total Environ. 590, 40-49. https://doi.org/10.1016/j.scitotenv.2017.03.026.

Muschler, R.G., 2016. Agroforestry: essential for sustainable and climate-smart land use, in: Pancel, L., Köhl, M. (Eds.), Tropical forestry handbook. Springer, pp. 2013-2116.

Nagele, P., 2003. Misuse of standard error of the mean (SEM) when reporting variability of a sample. A critical evaluation of four anaesthesia journals. Br. J. Anaesth. 90, 514-516. https://doi.org/10.1093/bja/aeg087.

Nair, P., Kumar, B., Nair, V.D., 2009. Agroforestry as a strategy for carbon sequestration. J. Plant. Nutr. Soil Sci. 172, 10-23. https://doi.org/10.1002/jpln.200800030.

Nair, P.R., 1993. An introduction to agroforestry. Springer Science & Business Media, Netherlands.

Nair, P.R., 2011. Agroforestry systems and environmental quality: introduction. J. Environ. Qual. 40, 784-790. https://doi.org/10.2134/jeq2011.0076.

Nair, P.R., Nair, V.D., Kumar, B.M., Haile, S.G., 2009. Soil carbon sequestration in tropical agroforestry systems: a feasibility appraisal. Environ. Sci. Policy. 12, 1099-1111. https://doi.org/10.1016/j.envsci.2009.01.010.

Näthe, K., Levia, D.F., Steffens, M., Michalzik, B., 2017. Solid-state ^{13}C NMR characterization of surface fire effects on the composition of organic matter in both soil and soil solution from a coniferous forest. Geoderma 305, 394-406. https://doi.org/10.1016/j.geoderma.2017.06.030.

Nie, X.D., Li, Z.W., Huang, J.Q. Liu, L., Xiao, H.B., Liu, C., Zeng, G.M., 2018. Thermal stability of organic carbon in soil aggregates as affected by soil erosion and deposition. Soil Tillage Res. 175, 82-90. https://doi.org/10.1016/j.still.2017.08.010.

Oelbermann, M., Voroney, R.P., Gordon, A.M. 2004. Carbon sequestration in tropical and temperate agroforestry systems: a review with examples from Costa Rica and southern Canada. Agric. Ecosyst. Environ. 104, 359-377. https://doi.org/10.1016/j.agee.2004.04.001.

Ogle, S.M., Breidt, F.J., Paustian, K. 2005. Agricultural management impacts on soil organic carbon storage under moist and dry climatic conditions of temperate and tropical regions. Biogeochemistry 72, 87-121. https://doi.org/10.1007/s10533-004-0360-2.

Ohno, T., Heckman, K.A., Plante, A.F., Fernandez, I.J., Parr, T.B., 2017. 14C mean residence time and its relationship with thermal stability and molecular composition of soil organic matter: A case study of deciduous and coniferous forest types. Geoderma 308, 1-8. https://doi.org/10.1016/j.geoderma.2017.08.023.

Pankiw, J. and Piwowar, J., 2010. Seasonality of imagery: the impact on object-based classification accuracy of shelterbelts. Prairie Perspectives: Geographical Essays 13, 39-48.

Paustian, K., Lehmann, J., Ogle, S., Reay, D., Robertson, G.P., Smith, P., 2016. Climate-smart soils. Nature 532, 49-57. https://doi.org/10.1038/nature17174.

Peltre, C., Fernández, J.M., Craine, J.M., Plante, A.F., 2013. Relationships between biological and thermal indices of soil organic matter stability differ with soil organic carbon level. Soil Sci. Soc. Am. J. 77, 2020-2028. https://doi.org/10.2136/sssaj2013.02.0081.

Pennock, D., Yates, T., and Braidek, J. 2008. Soil sampling designs. In M.R. Carter, Ed. Soil Sampling and Methods of Analysis, Canadian Society of Soil Science, Lewis Publishers, CRC Press, Boca Raton, 25-37 pp.

Perkins, S.E. and Alexander, L.V., 2013. On the measurement of heat waves. J. Clim. 26, 4500-4517. https://doi.org/10.1175/JCLI-D-12-00383.1.

Piccolo, A. and Mbagwu, J.S., 1999. Role of hydrophobic components of soil organic matter in soil aggregate stability. Soil Sci. Soc. Am. J. 63, 1801-1810. https://doi.org/10.2136/sssaj1999.6361801x.

Piccolo, A., Spaccini, R., Haberhauer, G., Gerzabek, M.H., 1999. Increased sequestration of organic carbon in soil by hydrophobic protection. Naturwissenschaften, 86(10), 496-499.

Pietri, J.A. and Brookes, P.C., 2008. Relationships between soil pH and microbial properties in a UK arable soil. Soil Biol. Biochem. 40, 1856-1861. https://doi.org/10.1016/j.soilbio.2008.03.020.

Piwowar, J.M., Amichev, B.Y., Van Rees, K.C., 2016. The Saskatchewan shelterbelt inventory. Can. J. Soil Sci. 97, 433-438. ttps://doi.org/10.1139/cjss-2016-0098.

Plante, A.F., Fernández, J.M., Haddix, M.L., Steinweg, J.M., Conant, R.T., 2011. Biological, chemical and thermal indices of soil organic matter stability in four grassland soils. Soil Biol. Biochem. 43, 1051-1058. https://doi.org/10.1016/j.soilbio.2011.01.024.

QGIS Development Team, 2018. QGIS (Version 3.2.1-București). Open Source Geospatial Foundation Project. http://qgis.osgeo.org.

R Core Team, 2018. R: A language and environment for statistical computing. R Foundation for Statistical Computing. Austria: Vienna.

Ravanelli, R., Nascetti, A., Cirigliano, R.V., Di Rico, C., Leuzzi, G., Monti, P., Crespi, M., 2018. Monitoring the impact of land cover change on surface urban heat island through Google Earth Engine: Proposal of a global methodology, first applications and problems. Remote Sens. 10, 1488. https://doi.org/10.3390/rs10091488.

Reichstein, M., Bahn, M., Ciais, P., Frank, D., Mahecha, M.D., Seneviratne, S.I., Zscheischler, J., Beer, C., Buchmann, N., Frank, D.C., 2013. Climate extremes and the carbon cycle. Nature 500, 287-295. https://doi.org/10.1038/nature12350.

Rempel, C.J., Costs, benefits, and barriers to the adoption and retention of shelterbelts in prairie agriculture as identified by Saskatchewan producers. Master's Thesis, University of Saskatchewan, Saskatoon, SK, Canada, 2013.

Rempel, J., Kulshreshtha, S., Van Rees, K., Amichev, B., Factors that Influence Shelterbelt Retention and Removal in Prairie Agriculture as Identified by Saskatchewan Producers. In Proceedings of the Soil and Science Workshop, Saskatoon, SK, Canada, 11 March 2014.

Rovira, P., Kurz-Besson, C., Coûteaux, M.M., Vallejo, V.R., 2008. Changes in litter properties during decomposition: a study by differential thermogravimetry and scanning calorimetry. Soil Biol. Biochem. 40, 172-185. https://doi.org/10.1016/j.soilbio.2007.07.021.

Rudd, L., Kulshreshtha, S., Belcher, K., Amichev, B., 2021. Carbon life cycle assessment of shelterbelts in Saskatchewan, Canada. J. Environ. Manage. 297, 113400. https://doi.org/10.1016/j.jenvman.2021.113400.

Salome, C., Nunan, N., Pouteau, V., Lerch, T.Z., Chenu, C., 2010. Carbon dynamics in topsoil and in subsoil may be controlled by different regulatory mechanisms. Glob. Change Biol. 16, 416-426. https://doi.org/10.1111/j.1365-2486.2009.01884.x.

Sarker, T.C., Incerti, G., Spaccini, R., Piccolo, A., Mazzoleni, S., Bonanomi, G., 2018. Linking organic matter chemistry with soil aggregate stability: insight from ^{13}C NMR spectroscopy. Soil Biol. Biochem. 117, 175-184. https://doi.org/10.1016/j.soilbio.2017.11.011.

Schädel, C., Beem-Miller, J., Aziz Rad, M., Crow, S.E., Hicks Pries, C.E., Ernakovich, J., Hoyt, A.M., Plante, A., Stoner, S., Treat, C.C., 2020. Decomposability of soil organic matter over time: the Soil Incubation Database (SIDb, version 1.0) and guidance for incubation procedures. Earth Syst. Sci. Data 12, 1511-1524. https://doi.org/10.5194/essd-12-1511-2020.

Schoeneberger, M., Bentrup, G., De Gooijer, H., Soolanayakanahally, R., Sauer, T., Brandle, J., Zhou, X.H., Current, D., 2012. Branching out: Agroforestry as a climate change mitigation and adaptation tool for agriculture. J. Soil Water Conserv. 67, 128A-136A. https://doi.org/10.2489/jswc.67.5.128A.

Shi, L., Feng, W., Xu, J., Kuzyakov, Y., 2018. Agroforestry systems: Meta-analysis of soil carbon stocks, sequestration processes, and future potentials. Land Degrad. Dev. 29, 3886-3897. https://doi.org/10.1002/ldr.3136.

Shrestha, B.M., Bork, E.W., Chang, S.X., Carlyle, C.N., Ma, Z., Döbert, T.F., Kaliaskar, D., Boyce, M.S., 2020. Adaptive Multi-Paddock Grazing Lowers Soil Greenhouse Gas Emission Potential by Altering Extracellular Enzyme Activity. Agronomy 10, p.1781. https://doi.org/10.3390/agronomy10111781.

Simpson, A.J., McNally, D.J., Simpson, M.J., 2011. NMR spectroscopy in environmental research: from molecular interactions to global processes. Prog. Nucl. Magn. Reson. Spectrosc. 3, 97-175. https://doi.org/10.1016/j.pnmrs.2010.09.001.

Singh, M., Sarkar, B., Sarkar, S., Churchman, J., Bolan, N., Mandal, S., Menon, M., Purakayastha, T.J., Beerling, D.J., 2018. Stabilization of soil organic carbon as influenced by clay mineralogy. Adv. Agron. 148, 33-84. https://doi.org/10.1016/bs.agron.2017.11.001.

Six, J., Bossuyt, H., Degryze, S., Denef, K., 2004. A history of research on the link between (micro) aggregates, soil biota, and soil organic matter dynamics. Soil Tillage Res. 79, 7-31. https://doi.org/10.1016/j.still.2004.03.008.

Šmejkalová, D., Spaccini, R., Piccolo, A., 2008. Multivariate analysis of CPMAS ^{13}C-NMR spectra of soils and humic matter as a tool to evaluate organic carbon quality in natural systems. Eur. J. Soil Sci. 59, 496-504. https://doi.org/10.1111/j.1365-2389.2007.01005.x.

Smith, M.D., 2011. An ecological perspective on extreme climatic events: a synthetic definition and framework to guide future research. J. Ecol. 99, 656-663. https://doi.org/10.1111/j.1365-2745.2011.01798.x.

Smith, P., Martino, D., Cai, Z.C., Gwary, D., Janzen, H., Kumar, P., McCarl, B., Ogle, S., O'Mara, F., Rice, C., 2008. Greenhouse gas mitigation in agriculture. Philos. Trans. R. Soc. B, Biol. Sci. 363, 789-813. https://doi.org/10.1098/rstb.2007.2184.

Smoyer-Tomic, K.E., Kuhn, R., Hudson, A., 2003. Heat wave hazards: an overview of heat wave impacts in Canada. Nat. Hazards 28, 465-486. https://doi.org/10.1023/A:1022946528157.

Soil Classification Working Group, 1998. The Canadian System of Soil Classification. NRC Research Press, Ottawa, Canada, 187 pp.

Sollins, P., Homann, P., Caldwell, B.A., 1996. Stabilization and destabilization of soil organic matter: mechanisms and controls. Geoderma, 74, 65-105. https://doi.org/10.1016/S0016-7061(96)00036-5.

Soucémarianadin, L.N., Cécillon, L., Guenet, B., Chenu, C., Baudin, F., Nicolas, M., Girardin, C., Barré, P., 2018. Environmental factors controlling soil organic carbon stability in French forest soils. Plant Soil 426, 267-286. https://doi.org/10.1007/s11104-018-3613-x.

Soucémarianadin, L.N., Quideau, S.A., MacKenzie, M.D., Bernard, G.M., Wasylishen, R.E., 2013. Laboratory charring conditions affect black carbon properties: a case study from Quebec black spruce forests. Org. Geochem. 62, 46-55. https://doi.org/10.1016/j.orggeochem.2013.07.005.

Statistics Canada, 2014. Human activity and the environment: agriculture in Canada. http://www.statcan.gc.ca/pub/16-201-x/16-201-x2014000-eng.htm (accessed 12 December 2020).

Stavi, I. and Lal, R., 2013. Agroforestry and biochar to offset climate change: a review. Agron. Sustain. Dev. 33, 81-96. https://doi.org/10.1007/s13593-012-0081-1.

Stone, M.M. and Plante, A.F. 2015. Relating the biological stability of soil organic matter to energy availability in deep tropical soil profiles. Soil Biol. Biochem. 89, 162-171. https://doi.org/10.1016/j.soilbio.2015.07.008.

Sun, S.H., Liu, J.J., Li, Y.F., Jiang, P.K., Chang, S.X., 2013. Similar quality and quantity of dissolved organic carbon under different land use systems in two Canadian and Chinese soils. J. Soils Sediments. 13, 34-42. https://doi.org/10.1007/s11368-012-0604-z.

Takimoto, A., Nair, P.R., Nair, V.D., 2008. Carbon stock and sequestration potential of traditional and improved agroforestry systems in the West African Sahel. Agric. Ecosyst. Environ. 125, 159-166. https://doi.org/10.1016/j.agee.2007.12.010.

Tatarinov, F., Rotenberg, E., Maseyk, K., Ogée, J., Klein, T. and Yakir, D., 2016. Resilience to seasonal heat wave episodes in a Mediterranean pine forest. New Phytol. 210, 485-496. https://doi.org/10.1111/nph.13791.

Teskey, R., Wertin, T., Bauweraerts, I., Ameye, M., McGuire, M.A., Steppe, K., 2015. Responses of tree species to heat waves and extreme heat events. Plant Cell Environ. 38, 1699-1712. https://doi.org/10.1111/pce.12417.

Teuling, A.J., Seneviratne, S.I., Stöckli, R., Reichstein, M., Moors, E., Ciais, P., Luyssaert, S., Van Den Hurk, B., Ammann, C., Bernhofer, C., 2010. Contrasting response of European forest and grassland energy exchange to heatwaves. Nat. Geosci. 3, 722-727. https://doi.org/10.1038/NGEO950.

Teuling, A.J., Seneviratne, S.I., Stöckli, R., Reichstein, M., Moors, E., Ciais, P., Luyssaert, S., Van Den Hurk, B., Ammann, C., Bernhofer, C., 2010. Contrasting response of European

forest and grassland energy exchange to heatwaves. Nat. Geosci. 3, 722-727. https://doi.org/10.1038/NGEO950.

The Climate Atlas of Canada, 2019. Climate Atlas of Canada, version 2, using BCCAQv2 climate model data. https://climateatlas.ca/climate-atlas-version-2.

Thevathasan, N., Gordon, A. 2004. Ecology of tree intercropping systems in the North temperate region: Experiences from southern Ontario, Canada. New Vistas in Agroforestry. Springer, 257-268 pp.

Trasar-Cepeda, C., Leirós, M., Gil-Sotres, F. 2008. Hydrolytic enzyme activities in agricultural and forest soils. Some implications for their use as indicators of soil quality. Soil Biol. Biochem. 40, 2146-2155. https://doi.org/10.1016/j.soilbio.2008.03.015.

Van Noordwijk, M., 2020. Agroforestry as nexus of sustainable development goals, IOP Conf. Ser.: Earth Environ. Sci. IOP Publishing, 012001 pp.

Vance, E.D., Brookes, P.C., Jenkinson, D.S., 1987. An extraction method for measuring soil microbial biomass C. Soil Biol. Biochem. 19, 703-707. https://doi.org/10.1016/0038-0717(87)90052-6.

Vesterdal, L., Clarke, N., Sigurdsson, B.D., Gundersen, P. 2013. Do tree species influence soil carbon stocks in temperate and boreal forests? For. Ecol. Manag. 309, 4-18. https://doi.org/10.1016/j.foreco.2013.01.017.

von Lützow, M. and Kögel-Knabner, I., 2009. Temperature sensitivity of soil organic matter decomposition—what do we know? Biol. Fertil. Soils 46, 1-15. https://doi.org//10.1007/s00374-009-0413-8.

von Lützow, M., Kögel-Knabner, I., Ekschmitt, K., Flessa, H., Guggenberger, G., Matzner, E., Marschner, B., 2007. SOM fractionation methods: relevance to functional pools and to

stabilization mechanisms. Soil Biol. Biochem. 39, 2183-2207. https://doi.org/10.1016/j.soilbio.2007.03.007.

Wang, H., Liu, S.R., Wang, J.X., Shi, Z.M., Lu, L.H., Zeng, J., Ming, A.G., Tang, J.X., Yu, H.L. 2013. Effects of tree species mixture on soil organic carbon stocks and greenhouse gas fluxes in subtropical plantations in China. Forest Ecol. Manag. 300, 4-13. https://doi.org/10.1016/j.foreco.2012.04.005.

Wang, S.J., Wang, H., Li, J.H. 2016. Does tree species composition affect soil CO_2 emission and soil organic carbon storage in plantations? Trees 30, 2071-2080. https://doi.org/10.1007/s00468-016-1434-1.

Watson, R.T., Zinyowera, M.C., Moss, R.H., Dokken, D.J., 1998. The regional impacts of climate change. IPCC, Geneva.

Weil, R.R., Islam, K.R., Stine, M.A., Gruver, J.B. and Samson-Liebig, S.E., 2003. Estimating active carbon for soil quality assessment: A simplified method for laboratory and field use. Am. J. Alternative Agr., 3-17.

Williams, E.K., Fogel, M.L., Berhe, A.A., Plante, A.F., 2018. Distinct bioenergetic signatures in particulate versus mineral-associated soil organic matter. Geoderma 330, 107-116. https://doi.org/10.1016/j.geoderma.2018.05.024.

Williams, E.K. and Plante, A.F. 2018. A bioenergetic framework for assessing soil organic matter persistence. Front. Earth Sci. 6: 143. https://doi.org/10.3389/feart.2018.00143.

Williams, E.K., Rosenheim, B.E., McNichol, A.P., Masiello, C.A. 2014. Charring and non-additive chemical reactions during ramped pyrolysis: Applications to the characterization of sedimentary and soil organic material. Org. Geochem. 77, 106-114. https://doi.org/10.1016/j.orggeochem.2014.10.006.

Wiseman, G., Kort, J., Walker, D., 2009. Quantification of shelterbelt characteristics using high-resolution imagery. Agric. Ecosyst. Environ. 131, 111-117. https://doi.org/10.1016/j.agee.2008.10.018.

Xia, S.P., Song, Z.L., Wang, Y.D., Wang, W.Q., Fu, X.L., Singh, B.P., Kuzyakov, Y., Wang, H.L., 2021. Soil organic matter turnover depending on land use change: Coupling C/N ratios, $\delta^{13}C$, and lignin biomarkers. Land Degrad. Dev. 32, 1591-1605. https://doi.org/10.1002/ldr.3720.

Xu, H., Qu, Q., Wang, M., Li, P., Li, Y., Xue, S., Liu, G., 2020. Soil organic carbon sequestration and its stability after vegetation restoration in the Loess Hilly Region, China. Land Degrad. Dev. 31, 568-580. https://doi.org/10.1002/ldr.3472.

Xu, X., Cheng, X., Zhou, Y., Luo, Y., Ruan, H., Wang, J., 2010. Variation of soil labile organic carbon pools along an elevational gradient in the Wuyi Mountains, China. J. Res. Ecol. 1, 368-374. https://doi.org/10.3969/j.issn.1674-764x.2010.04.010.

Xu, X., Thornton, P.E., Post, W.M., 2013. A global analysis of soil microbial biomass carbon, nitrogen and phosphorus in terrestrial ecosystems. Glob. Ecol. Biogeogr. 22, 737-749. https://doi.org/10.1111/geb.12029.

Yang, L., Pan, J., Shao, Y., Chen, J.M., Ju, W.M., Shi, X., Yuan, S., 2007. Soil organic carbon decomposition and carbon pools in temperate and sub-tropical forests in China. J. Environ. Manage. 85, 690-695. https://doi.org/10.1016/j.jenvman.2006.09.011.

Yuan, W.P., Cai, W.W., Chen, Y., Liu, S.G., Dong, W.J., Zhang, H.C., Yu, G.R., Chen, Z.Q., He, H.L. and Guo, W.D., 2016. Severe summer heatwave and drought strongly reduced carbon uptake in Southern China. Sci. Rep. 6, 1-12. https://doi.org/10.1038/srep18813.

Zhang, F.W. and Cao, G.M., 2017. Resilience of Energy and CO 2 Exchange to a Summer Heatwave in an Alpine Humid Grassland on the Qinghai-Tibetan Plateau. Pol. J. Environ. Stud. 26. https://doi.org/10.15244/pjoes/64912.

Zhang, K., Dang, H., Tan, S., Cheng, X., Zhang, Q., 2010. Change in soil organic carbon following the 'Grain-for-Green' programme in China. Land Degrad. Dev. 21, 13–23. https://doi.org/10.1002/ldr.954.

Zhang, X., Liu, S.R., Huang, Y.T., Fu, S.L., Wang, J.X., Ming, A.G., Li, X.Z., Yao, M.J., Li, H. 2018. Tree species mixture inhibits soil organic carbon mineralization accompanied by decreased r-selected bacteria. Plant Soil 431, 203-216. https://doi.org/10.1007/s11104-018-3755-x.

Zhuang, S.Y., Sun, X., Liu, G.Q., Wong, M.H., Cao, Z.H., 2011. Carbon sequestration in bamboo plantation soil with heavy winter organic mulching management. Bot. Rev. 77(3), 252. https://doi.org/10.1007/s12229-011-9081-0.

Zibilske, L. 1994. Carbon mineralization. Methods of Soil Analysis: Part 2 Microbiological and Biochemical Properties 5, 835-863. https://doi.org/10.2136/sssabookser5.2.c38.

Appendices

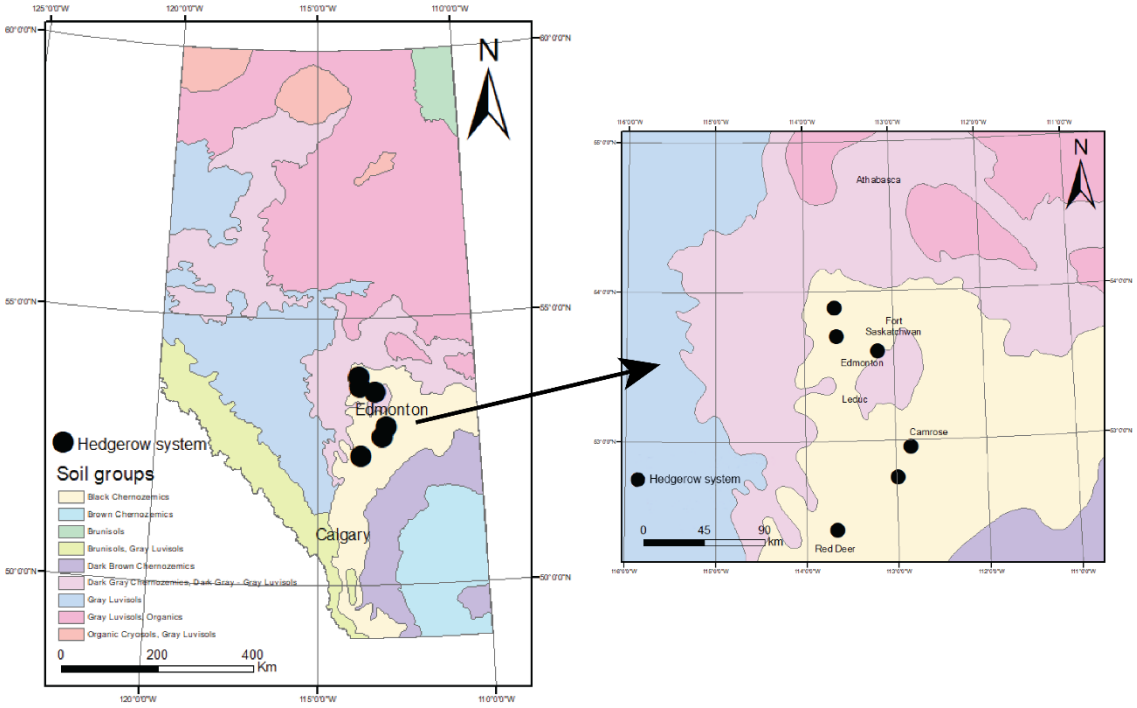

Appendix 2-1. Locations of the six hedgerow sites sampled for this study in Alberta, Canada.

Appendix 2-2. Select soil properties (mean ± standard deviation) for the paired cropland and forested land-uses examined within the hedgerow agroforestry system (based on data in Baah-Acheamfour et al., 2014).

Land-use	Depth (cm)	pH	Carbon (C) (%)	Nitrogen (N) (%)	Bulk density (g cm^{-3})
Cropland	0-10	5.31±1.09	5.12±1.67	0.48±0.17	1.27±0.12
	10-30	6.37±0.74	2.81±1.69	0.25±0.17	1.36±0.10
Forest	0-10	5.47±0.49	8.46±1.98	0.73±0.21	0.94±0.15
	10-30	5.76±0.98	5.98±2.15	0.50±0.18	1.11±0.26

Appendix 2-3. Pearson correlation coefficients of basic soil properties, soil organic carbon structural and thermal indices (n=6).

Properties	Carbon	Nitrogen	Bulk density	pH	HB/HI	A/OA	ARM	LigR	DSC-T_{50}	CO_2-T_{50}	TG-T_{50}	Energy density
Nitrogen	0.98***	1.00										
Bulk density	-0.60**	-0.65***	1.00									
pH	-0.44*	-0.43*	0.10	1.00								
HB/HI	-0.65***	-0.59**	0.43*	0.43*	1.00							
A/OA	-0.76***	-0.71***	0.46*	0.55**	0.81***	1.00						
ARM	-0.46*	-0.38	0.23	0.13	0.80***	0.54**	1.00					
LigR	0.56**	0.54**	-0.32	0.03	-0.67***	-0.51*	-0.85***	1				
DSC-T_{50}	0.27	0.35	-0.46*	0.20	0.12	-0.00	0.19	0.14	1.00			
CO_2-T_{50}	0.13	0.24	-0.31	0.35	0.43*	0.29	0.38	-0.04	0.84***	1		
TG-T_{50}	-0.38	-0.40	0.43*	0.56**	0.60**	0.48*	0.23	-0.14	-0.15	0.19	1.00	
Energy density	0.32	0.36	-0.51*	-0.22	-0.38	-0.37	-0.14	0.28	0.53**	0.12	-0.77***	1.00
Energy content	0.65***	0.69***	-0.85***	-0.20	-0.52**	-0.54**	-0.25	0.35	0.56**	0.32	-0.56**	0.64***

Note: Table content and the font size were customized by removing non-significant correlations in rows and columns and reducing the font size, especially to fit the page; *, ** and *** represent significance at the 0.05, 0.01 and 0.001probability levels, respectively. HB/HI, hydrophobicity index; A/OA, alkyl index; ARM, aromaticity index; LigR, lignin ratio. TG-T_{50}, the temperature that 50% of the

exothermic mass is lost; DSC-T_{50}, the temperature that 50% of the exothermic energy is released; CO_2-T_{50}, the temperature that 50% of the CO_2 is produced.

Appendix 2-4. Pearson correlation coefficients of soil texture (sand clay and silt), soil organic carbon structural and thermal indices (n=6)

Properties	HB/HI	A/OA	ARM	LigR	DSC-T_{50}	CO_2-T_{50}	TG-T_{50}	Energy density	Energy content
Sand %	-0.32	-0.21	-0.28	0.27	0.45	0.19	-0.60*	0.68*	0.31
Clay %	0.31	0.22	0.23	0.04	-0.05	0.17	0.57	-0.35	-0.17
Silt %	0.09	0.03	0.14	-0.47	-0.67*	-0.54	0.22	-0.65*	-0.30

Note: Soil texture data is only available in 0-10 cm soils; *, ** and *** represent significance at the 0.05, 0.01 and 0.001 probability levels, respectively. HB/HI, hydrophobicity index; A/OA, alkyl index; ARM, aromaticity index; LigR, lignin ratio. TG-T_{50}, the temperature that 50% of the exothermic mass is lost; DSC-T_{50}, the temperature that 50% of the exothermic energy is released; CO_2-T_{50}, the temperature that 50% of the CO_2 is produced.

Appendix 3-1. Soil organic carbon, total N, microbial biomass carbon (MBC) and nitrogen (MBN) (mean ± standard error, n=12) in the 0–10 cm soil layer as affected by agroforestry system and land-use in central Alberta, Canada (Banerjee et al., 2016; Baah-Acheamfour et al., 2020).

Description	Hedgerow cropland	Hedgerow Forest	Shelterbelt cropland	Shelterbelt forest
MBC (g kg^{-1})	307.49±36.47	587.19±107.13	460.28±89.97	994.53±132.51
MBN (g kg^{-1})	58.84±8.75	85.51±18.44	68.94±12.25	150.83±22.35
SOC (g kg^{-1})	38.22±3.95	63.92±6.87	50.13±5.22	52.34±5.45
Total N (g kg^{-1})	3.47±0.37	4.95±0.54	4.67±0.44	4.48±0.44
DOC (g kg^{-1})	1.70±0.14	4.29±0.54	2.05±0.17	5.31±1.17
DON (g kg^{-1})	0.73±0.11	0.64±0.13	0.85±0.08	0.86±0.24
pH	6.28±0.32	6.71±0.25	5.57±0.24	6.02±0.19
Bulk density (g cm^{-3})	1.38±0.03	1.02±0.04	1.28±0.04	0.99±0.03
Sand (%)	34.69±5.81	31.06±2.70	27.13±3.39	26.55±1.72
Clay (%)	21.51±2.13	26.72±1.48	28.36±2.23	26.15±1.78
Silt (%)	43.80±4.41	42.22±2.40	44.51±2.89	47.30±1.93

Note: DOC and DON represent soil dissolved organic carbon and nitrogen, respectively.

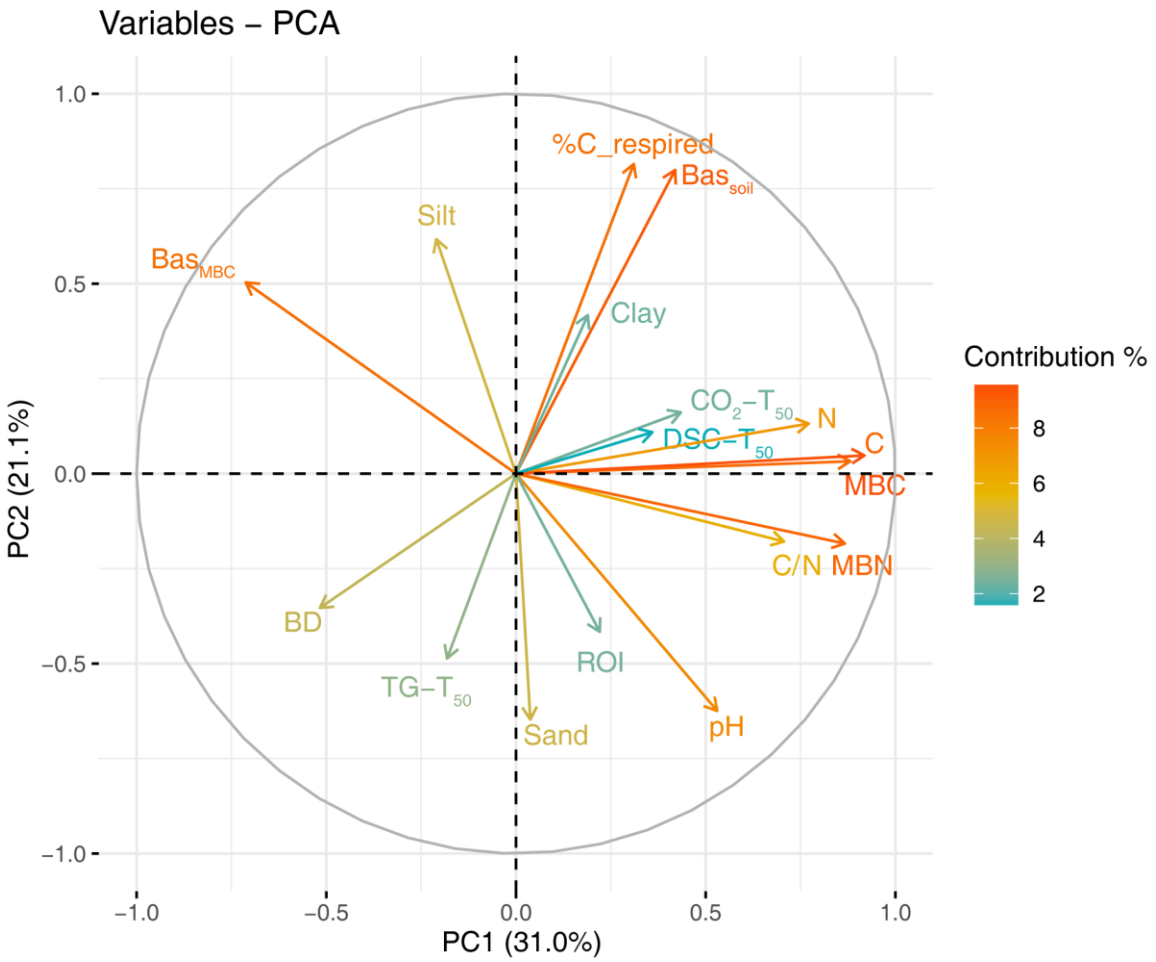

Appendix 3-2. Percentage contribution of select variables to the C stability profile.

Note: Ea, activation energy; BD, bulk density; Bas, basal respiration rate; Ed, energy density, Cum, cumulative respiration; %C_respired, the proportion of C respired; TG-T_{50}, the temperature that 50% of the exothermic mass is lost; DSC-T_{50}, the temperature that 50% of the exothermic energy is released; CO_2-T_{50}, the temperature that 50% of the CO_2 is produced; ROI, return on energy investment.

Appendix 3-3. Pearson correlation coefficients of basic soil properties, soil organic carbon biological and thermal indices (n=12).

Description	Bas_{soil}	Bas_{MBC}	%C respired	C	N	C/N	pH	MBC	MBN	Sand	Clay	Silt	CO_2-T_{50}
%C_respired	0.97***	0.30*	1										
C	0.35*	-0.52***	0.27	1									
N	0.36*	-0.42**	0.30*	0.95***	1								
C/N	0.2	-0.48***	0.12	0.59***	0.34*	1							
pH	-0.26	-0.71***	-0.34*	0.36*	0.23	0.47***	1						
MBC	0.45**	-0.78***	0.34*	0.70***	0.61***	0.57***	0.48***	1					
MBN	0.23	-0.85***	0.12	0.65***	0.55***	0.52***	0.69***	0.92***	1				
Sand	-0.29*	-0.14	-0.26	-0.01	-0.12	0.22	0.26	-0.06	0.02	1			
Clay	0.31*	-0.04	0.25	0.18	0.26	-0.13	-0.15	0.23	0.13	-0.56***	1		
Silt	0.23	0.29*	0.25	-0.17	-0.08	-0.26	-0.29*	-0.12	-0.15	-0.81***	0.1	1	
BD	-0.49***	0.22	-0.42**	-0.31*	-0.26	-0.40**	-0.09	-0.51***	-0.30*	0.1	-0.32*	0.01	
TG-T_{50}	-0.43**	-0.13	-0.42**	-0.21	-0.2	-0.19	0.44**	-0.15	0.03	0.11	0	-0.14	
CO_2-T_{50}	0.26	-0.09	0.18	0.39**	0.32*	0.30*	0.09	0.25	0.22	0.05	-0.1	0.03	1
DSC-T_{50}	0.17	-0.06	0.11	0.31*	0.26	0.21	0.1	0.17	0.2	0.06	-0.06	-0.01	0.85***
ROI	-0.25	-0.22	-0.29*	0.38**	0.33*	0.30*	0.12	0.04	0.09	0.29*	0.05	-0.46**	-0.12

Note: Table content and the font size were customized by removing non-significant correlations in rows and columns and reducing the font size, especially to fit the page; *, ** and *** represent significance at the 0.05, 0.01 and 0.001 probability levels, respectively. Bas, basal respiration rate; %C_respired, the proportion of C respired; MBC, microbial biomass C; MBN, microbial biomass N; BD, bulk density; TG-T_{50}, the temperature that 50% of the exothermic mass is lost; DSC-T_{50}, the temperature that 50% of the exothermic energy is released; CO_2-T_{50}, the temperature that 50% of the CO_2 is produced; ROI, return on energy investment.

Appendix 4-1. Basic soil properties of the studied hedgerow system sites [mean ±standard error].

Properties	pH	Clay	Silt	Sand	Total C	Total N
		%	%	%	%	%
Cropland	5.8±0.3	24.1±3.4	48.8 ±1.5	27.0±3.9	3.8±0.9	0.3±0.1
Forest	7.1±1.1	21.9±0.9	21.9±0.9	30.6±2.6	7.1±1.1	0.5±0.1

Note: The texture (clay, silt and sand) information was adapted from Baah-Acheamfour et al. (2015).

Appendix 4-2. Average daily soil CO_2 and N_2O emissions in the five-day long heat wave period under control and heat wave treatments in both forest and cropland soils.

Description	Daily CO_2 emissions mg C kg^{-1} soil		Daily N_2O emissions mg N kg^{-1} soil	
	Forest	Cropland	Forest	Cropland
Five day heat wave period	43.07	28.62	15.77	4.19
Five day period in control	11.96	7.70	0.44	0.42

Appendix 4-3. Spearman correlation coefficients of basic soil properties, soil labile C and soil CO_2 and N_2O emissions (n=4).

Properties	Sand	Clay	Silt	N	C	C/N	pH	Cu_CO_2	Cu_N_2O	HWEOC	POXC	MBC	Ba_CO_2
Clay	-0.83***	1											
Silt	-0.68***	0.15	1										
N	0.06	0.09	-0.22	1									
C	0.32	-0.19	-0.32	0.94***	1								
C/N	0.3	-0.38	-0.04	0.68***	0.83***	1							
pH	0.62**	-0.55**	-0.38	0.56**	0.75***	0.72***	1						
Cu_CO_2	0.05	0.08	-0.19	0.26	0.15	0.06	-0.28	1					
Cu_N_2O	0.1	-0.12	-0.01	0.31	0.32	0.34	0.08	0.59**	1				
HWEOC	0.23	0.02	-0.44*	0.88***	0.88***	0.68***	0.65***	0.21	0.3	1			
POXC	0.17	0.06	-0.39	0.88***	0.88***	0.67***	0.62**	0.19	0.15	0.80***	1		
MBC	0.47*	-0.16	-0.61**	0.79***	0.81***	0.59**	0.61**	0.39	0.32	0.90***	0.70***	1	
Ba_CO_2	-0.09	0.26	-0.18	0.17	0	-0.18	-0.45*	0.77***	0.08	0.08	0.08	0.31	1
Ba_N_2O	0.2	-0.12	-0.2	-0.04	-0.03	-0.02	-0.12	0.46*	0.4	-0.06	-0.02	0.14	0.33

Note: Table content and the font size were customized by removing non-significant correlations in rows and columns and reducing the font size, especially to fit the page; *, ** and *** represent significance at the 0.05, 0.01 and 0.001probability levels, respectively. Ba_CO_2 and Ba_N_2O, Basal CO_2 and N_2O rate; Cu_CO_2 and Cu_N_2O, cumulative CO_2 and N_2O emissions; C, soil total carbon; N, soil total nitrogen; C/N, carbon to nitrogen ratio; POXC, permanganate oxidable carbon; MBC, microbial biomass carbon; HWEOC, hot-water extractable organic carbon.